DISCLAIMER:

This document does not meet the
current format guidelines of
the Graduate School at
The University of Texas at Austin.

It has been published for
informational use only.

The Dissertation Committee for Catrina Ann Chitjian Certifies that this is the approved version of the following dissertation:

Regulation of Elongation Factor 2 Kinase (eEF-2K) by Acidity

Committee:

Kevin N. Dalby, Supervisor

Walter L. Fast

Jennifer S. Brodbelt

Seongmin Lee

Edward Mills

Regulation of Elongation Factor 2 Kinase (eEF-2K) by Acidity

by

Catrina Ann Chitjian

Dissertation

Presented to the Faculty of the Graduate School of

The University of Texas at Austin

in Partial Fulfillment

of the Requirements

for the Degree of

Doctor of Philosophy

The University of Texas at Austin

August 2018

Dedication

To all those

dear in my heart

who have provided unconditional love and support

through these crazy years.

And to my mama

whom I love

more than snickerdoodles.

Acknowledgements

First I'd like to acknowledge my mentor and supervisor Dr. Kevin Dalby for all of the patience and support he demonstrated through the ups and the downs of the past six years. I believe there are few who would have acted as you did; you are truly astounding.

I also extend my thanks to the other members of my dissertation committee, Dr. Ted Mills, Dr. Jennifer Brodbelt, Dr. Walter Fast and Dr. Seongmin Lee for all their advice, guidance and being among the sets of eyes to look upon this dissertation.

Thank you to Clint Tavares, without whom I would surely be lost. You patiently trained me and it was your mentorship and camaraderie that led me to join the lab. Thanks to Juliana Taliaferro for proposing to me with a light up ring and all of the conversations of commiseration, especially those of what it means to be a woman in science. I also appreciate the time shared with the previous and present members of Dalby Lab (especially those who were just as continually baffled, surprised and frustrated by eEF-2K as I was): Rachel Sammons, David Giles, Tamer Kaoud, Scarlett Ferguson, Gabriel Stancu and Ashwini Devkota.

Additionally, I'd like to thank our various collaborators for the work contributed to understanding this unique kinase: Dr. Ranajeet Ghose (City College of New York); and Dr. Karen Browning (Department of Molecular Biosciences, UT Austin).

I would like to acknowledge the Institute for Cellular and Molecular Biology and the College of Pharmacy, University of Texas at Austin, as well as NIH and CPRIT for grants awarded to Dr. Kevin Dalby, which provided me with the financial coverage that allowed me to pursue my studies.

A most sincere thank you to Luisa Moretto; my lelliephant you were always there to amoeba and understand. I hope we will continue talking about science and nonsense

and creativity for ages to come. Emily Chadbourne, your sincerity and optimism never ceases to amaze me. I cannot thank you for all of the love and support you have shown me, the extrovertedness you have brought upon me, or the gentle ways of communication you have taught me. Bethany Jones, you are as comforting and reliable as the moon above. Thank you for your friendship and wordless understandings that I hope we will continue to share always. Thanks to John Jennings, you got me through some real rough spots. Most importantly, you opened my eyes and heart to the idea of walking with faith, which will affect the rest of my life. A sincere thank you to Steven Schelling- your empathy, compassion, strength and support have meant so much to me in the final months leading up to defending.

Jaquelyn Yeh, you have been with me through every step of this since the day we went to see Hannah Montana in theatres. You are the reason I unashamedly write "Hannah Montana" in my PhD dissertation, and without you I would have surely lost my sanity. I am constantly floored by how anyone can be as kind, generous and reliable as you. As far as best friends go, I know I've got the best one. And thanks to Zachariah Skinner for always believing in me, even when I couldn't. I'm still betting on you.

Thanks to the wonderful strong ladies at Celebrate Recovery, and a special mention for Mollie Axtell and my spiritual sponsor Courtney. You have taught me so many things about loving the Lord, forgiveness, struggle and recovery. You helped me step out of the darkest dark and into the brightest light.

Mommy, I love you more than anything and you know me in a way no one can ever compare to. Thank you for always being ready to come to my rescue. Finally, the most heartfelt gratitude and praise goes to God for giving me the strength and wisdom to finish graduate school, that really was a close call.

Regulation of Elongation Factor 2 Kinase (eEF-2K) by Acidity

Catrina Ann Chitjian, Ph.D.

The University of Texas at Austin, 2018

Supervisor: Kevin N. Dalby

Eukaryotic elongation factor 2 kinase (eEF-2K) is a calmodulin (CaM)/calcium regulated kinase whose activity disrupts translation elongation resulting in the global decrease of protein synthesis[1]. Translation is one of the most energy intensive processes in a cell; eEF-2K is critical in maintaining cellular homeostasis. The dysregulation of eEF-2K is associated with an assortment of diseases including several types of cancer[2], depression[3,4], and Alzheimer's disease[5], which has prompted closer examination across multiple studies of the enzyme in recent decades. Notably, the kinetic mechanism of eEF-2K has been detailed as a two-step process: 1) The binding of Ca^{2+}-CaM enables the autophosphorylation of Thr-348 and 2) The resulting conformational change enables eEF-2K to bind and phosphorylate its substrate. We have uncovered many surprising layers of eEF-2K regulation in past years, from kinetic mechanism to upstream affecters to models of CaM binding. This study focuses on the role of pH in regulating eEF-2K.

pH homeostasis is also vital for cellular function. Even a slight disruption between the intra- and extracellular pH ratio can affect an array of processes such as ATP synthesis, enzyme function, as well as the proliferation, migration, and invasion of tumor

cells[6]. Acidosis is a common effect of high intensity exercise, diabetic ketoacidosis, ischemia, and solid tumors[7–9]. It has been demonstrated that eEF-2K activity is increased and protein translation decreased in cells under acidic conditions, suggesting the enzyme's potential cytoprotective effects[10–12].

This work reports the following: 1) A novel mechanism where H^+ instead of Ca^{2+} activates eEF-2K; 2) A novel mechanism where H^+ can replace Ca^{2+} in promoting eEF-2K substrate phosphorylation; 3) H^+ promotes the binding of CaM to eEF-2K in a Ca^{2+}-independent manner; 4) There are five histidine residues on eEF-2K that may contribute to the stabilized activity of eEF-2K under acidic conditions.

Table of Contents

List of Tables

List of Figures

List of Illustrations

Chapter 1: Introduction

1.1. Overview

There are approximately 518 genes in the human genome, roughly 2% of all human genes, corresponding to protein kinases[13]. These enzymes stabilize the transfer of phosphate from a high-energy molecule, such as ATP or GTP, to their corresponding protein substrates. Typically this covalent modification occurs on amino acids with a free hydroxyl group, most commonly serine, threonine, tyrosine, and less commonly histidine[14,15]. 478 protein kinases are classified into seven main groups based on the sequence similarity of their catalytic domains. eEF-2K (EC: 2.7.11.20) is included with the 40 remaining enzymes in the 8th group, 'atypical' kinases, which have do not share sequence homology with their counterparts[13,16,17].

Up to 30% of human proteins are predicted to be phosphorylated by kinases[18]. Phosphatases are enzymes that remove covalent phosphorylation which makes this post-translational modification reversible, a characteristic that is useful in the context of protein regulation. Indeed, kinases are known to play important roles in cellular processes including proliferation, cellular differentiation, morphogenesis, survival, transcription, metabolism and more[1,3,19].

1.2. Physical characterization of Elongation Factor-2 Kinase

In order to begin to understand and characterize eEF-2K, it is critical to have a reliable and consistent enzyme form. In 1985 when eEF-2K was a novel protein and

before its sequence was mapped and reported, the kinase was isolated from rat pancreas and rabbit reticulocytes for study[20,21]. Because it was purified from living tissue, the multisite regulatory phosphorylations weren't homogenous, yields were low and as we now know had comparatively low activity[22,23]. Still, this form was sufficient to provide initial kinetic analysis and to begin identifying upstream regulators[24–28]. The 1996 sequencing and cloning of rat muscle eEF-2K cDNA was the start of understanding eEF-2K structure, and the 1999 bacterial expression and purification of GST-tagged eEF-2K was the standard for studying eEF-2K until our 2011 tagless human recombinant enzyme purification[29–31]. The main drawbacks of pre-2011, or studies still using GST-tagged eEF-2K is this form tends to oligomerize, skewing experimental results, and is significantly less active than our optimized purification[30–32]. Our purification strategy was novel in that we coexpressed with λ-phosphatase in order to homogenize the phosphorylation state, we used a specialized bacterial strain (Rosetta-gami (DE3)) to accommodate the high proportion of rare codons, our purification involved three column purifications in sequence (initial Ni-NTA affinity, anion-exchange to further clean, and gel filtration size exclusion to remove any dimers) and we yielded milligram amounts of enzyme per purification batch (2-6L)[31].

There is still yet to be a successful report of a three-dimensional eEF-2K structure as it has been notoriously difficult enzyme to obtain a crystal structure or NMR analysis for, likely in part due to the ~150 amino acid loop located in the middle of the enzyme[33]. Over the years, however, a compilation of many studies has led to a model for the structure and organization of eEF-2K.

1.2.1. Homology Studies of eEF-2K

eEF-2K was initially identified by its substrate eEF-2 (then known as a 100,000kDa protein) and was reported as Ca^{2+}/CaM-dependent protein kinase III (CaMK-III) as the study reported it requiring both Ca^{2+} and CaM to be active[20,34–36]. While there is a Ca^{2+}/CaM-dependent kinase (CAMK) family of protein kinases, eEF-2K does not share sequence similarity with them.

Modern kinases are classified into 11 groups, 134 families and 196 subfamilies primarily based on kinase domain similarity and also additional domain similarities, evolutionary conservation and function similarity[13,37,38]. Traditionally, kinases can be separated 90% into the superfamily eukaryotic protein kinase (ePK) and the remaining 10% into ty protein kinases (APK) which represent the protein kinases that lack of sequence homology to ePKs[16,17,39]. More recently the APK group has been split to accommodate new protein sequences. eEF-2K, upon its initial sequencing, was classified as atypical protein kinase but now belongs to the PKL group, characterized by a protein kinase like fold and similar catalytic mechanisms[40,41]. The PKL family known as alpha kinases are unique to eukaryotes as they appeared relatively recently in evolution; eEF-2K is actually classified as an alpha protein kinase, the only CaM/Ca^{2+} dependent kinase in this family. Subfamilies of alpha kinases have very different domain structures but are defined by a catalytic domain homology to the myosin heavy chain kinases (MHCK)[16,17,42]. The alpha kinases are so named as many target substrate residues within an alpha-helix conformation[43,44].

Apart from the MHCK proteins, a well-studied alpha kinase is TRPM7 kinase of the TRP ion channel family [48, 49]. The solved crystal structure of the TRPM7 kinase domain in 2001 greatly helped shape our understanding of alpha kinases; despite the lack of sequence homology the final structure has similarities to the conventional protein kinase (CPK). The similarities to CPKs that TRPM7 demonstrated include: 1) a β-sheet N-terminal lobe containing a phosphate-binding loop; 2) an ATP-binding inter-lobe catalytic cleft; 3) a propensity to contain C-terminal α-helices and an activation loop. Differences include: 1) differences in C-terminal structures; 2) binding mode of ATP; 3) location of the glycine-rich motif ; and 4) presence of a zinc-finger in the C-terminus of alpha-kinases[16,45]. These homology studies laid the groundwork to our current understanding of eEF-2K domain and structure[45–47].

1.2.2. eEF-2K Domain Organization

The current proposed domain organization of eEF-2K is summarized in Scheme 1.1. The studies defining this primarily used primary sequence alignment, mutational studies, and homology studies of alpha-kinase crystal structures MHCK and TRPM7[30,48]. Reviewing the structure starting at the N-terminus: there is an aspartic acid-heavy DXDXDG motif at amino acids 24-29 that is a potential Ca^{2+} binding domain (CRD) whose role is currently unknown[49]. This is shortly followed by a inhibiting regulatory phosphorylation site, Ser-78, and residues 79-96 contain a calmodulin (CaM) binding domain (CBD) that is critical for activation. Specifically, residue Trp-85 is suggested to be a critical part of CaM binding and kinase activity, perhaps as a result of the former[50].

The atypical α-kinase catalytic kinase domain (KD) of eEF-2K spans from residues 116-326, which is located more towards the N-terminus compared to other atypical kinases[30,48]. In the kinase domain there are four conserved residues critical for kinase activity; the corresponding residues in TRMP7 function for the coordination of a Zn^{2+} ion[51] which suggests the possibility of a Zn^{2+} ion to be necessary for eEF-2K catalytic activity. There are several other elements involved in the catalytic domain and ATP coordination: 1) Between residues 296-301 is a glycine rich loop GXGXXG which is involved in ATP localization[16]; 2) Lys-170 interacts with the α- and β-phosphates of ATP to stabilize its binding; 3) Asp-284 is part of the conventional DFG (DPQ in eEF-2K) motif and is involved in chelating the Mg^{2+} ion that helps orient and coordinate ATP; 4) Glu-299 and Thr-283 form a hydrophobic pocket for ATP; 5) Asp-274 acts as a catalytic base; and 6) Lys-205, Arg-252, and Thr-254 form a phosphate binding pocket which binds autophosphorylated Thr-348 and promotes for allosteric activation of eEF-2K[16,52,53].

The linker region of eEF-2K, residues 327-477, form a regulatory loop (R-loop) that carries four of the main regulatory phosphorylation sites (Thr-348, Ser-359, Ser-366, and Ser-398) as well as a ^{440}DSGXXS^{445} degron motif (DM). The diphosphorylation of the serine residues in this motif is involved in the recognition of eEF-2K by the $SCF^{\beta TrCP}$ ubiquitin ligase. This event prompts degradation of eEF-2K and adds another layer of eEF-2K regulation and translational control[54–56]. Autophosphorylation of Thr-348 and its subsequent binding to the abovementioned phosphate binding pocket in the kinase domain is a prerequisite for kinase activity[54,57].

After the linker region there is the C-terminal lobe, residues 478-725 that is comprised of three helical SEL1-type domains (SHR), which are typically known to be involved in protein-protein interactions, and a C-terminal tail that interact with the KD. This region is necessary for substrate phosphorylation but not intrinsic activity which implicates a role in substrate interaction although it has been suggested that the extreme C-terminal domain of eEF-2K is not a primary eEF-2 docking site on its own[33,58]. Knowing all of this information about eEF-2K domain organization is important understanding its various physiological contexts.

1.3. PHYSIOLOGICAL CONTEXT OF EUKARYOTIC ELONGATION FACTOR-2 KINASE

Eukaryotic elongation factor 2 kinase (eEF-2K) is a calmodulin (CaM)/calcium regulated kinase whose activity disrupts translation elongation resulting in the global decrease of protein synthesis[1]. Translation is one of the most energy intensive processes in a cell; eEF-2K is critical in maintaining cellular homeostasis. The dysregulation of eEF-2K is associated with an assortment of diseases including several types of cancer[2], depression[59], and Alzheimer's disease[5].

1.3.1 Translational Control and Energy Regulation

The translation of mRNA into amino acids is a highly regulated process that occurs in three steps of initiation, elongation, and termination. It was first believed that initiation was the primary point of regulation however the 1980's discovery of eEF-2K

led to the studies suggesting elongation is a critical point of protein synthesis[1]. There are three elongation factors that assist the tRNA and growing polypeptide chain through the A, P and E sites of the ribosome (Scheme 1.1). Elongation factor-1 alpha (eEF-1a) is responsible for recruiting aminoacyl-tRNA (aa-tRNA) molecules to the A site of the ribosome. Upon a successful codon-anticodon match eEF-1a catalyzes GTP hydrolysis finalizing the binding of the aa-tRNA to the ribosome[60]. Elongation factor 2 (eEF-2) is responsible for the translocation of the tRNA from the A site to the P site after the newest peptide bond has formed; this translocation is also a GTP-dependent step[61]. Elongation factor 3 (eEF-3) is not present in all eukaryotes but associates with the E site of the ribosome and has various suggested functions including the catalysis of the ATP-dependent release of the tRNA from the ribosome and the assistance of eEF-1a in aa-tRNA recruitment[62]. In this way each protein requires a minimum of two ATP/GTP per amino acid to be synthesized, which is why translation is so energy intensive. Many of the translation factors' activities are modulated via phosphorylation, allowing for precise control over protein synthesis rate and related energy expenditures[63].

In particular, the only known substrate of eEF-2K (82kDa) is eEF-2 (100kDa). eEF-2K phosphorylates eEF-2 at Thr-56 thereby inhibiting its activity; it has been suggested that a decreased affinity to the ribosome is the cause behind this inhibition[34,64–66]. There are a number of factors that can alter the rate or protein synthesis utilizing this schematic alone including: amount of active vs. inactive eEF-2K, amount of ribosome-bound eEF-2 (which is protected from phosphorylation)[67], as well as post-translational modifications on both eEF-2K (which alter its activity) and eEF-2 (which alter the rate

and amount of Thr-56 phosphorylation). Examples include cyclin A-CDK2 which recruits eEF-2K by phosphorylating eEF-2 at Ser-535 and protein phosphatase 2A (PP2A) which is associated with eEF-2 dephosphorylation[68]. Post-translational modifications affecting eEF-2K activity will be discussed in the next section with the contexts in which they occur.

With this in mind, there is already a flexible and complex balance between eEF-2K and eEF-2 activity and all of their regulators. eEF-2K adds a further layer of delicate orchestration as it is known to induce translation of select transcripts[69–71], despite its typical effect of global downregulation of protein synthesis.

1.3.2 eEF-2K in the Cell Cycle

In every actively replicating cell type it is vital to control the progression, and protein synthesis along with it, through the cell cycle. During the G1 phase, protein synthesis is important to build up and essentially double the size of the cell; eEF-2K must be inactivated for this to happen. This occurs through the inactivating phosphorylations on Ser-359 and Ser-366, which are downstream of cdc2 kinase (a cyclin-dependent cell cycle regulator) and the growth factor and nutrient activated mitogen-activated protein kinase kinase/extracellular signal-regulated kinases (MKK/ERK), mammalian target of rapamycin/S6 kinase 1 (mTOR/S6K1) pathways (Scheme 1.2)[72–74]. As the cell cycle progresses, this inhibition of eEF-2K must be alleviated to halt protein translation so the cell may progress into the DNA synthesis S phase and proofreading/cell division G2/M phase. This is likely accomplished by 1) an eEF-2K-activiting rise in cAMP, thereby

activating PKA which targets the activating phosphorylation site Ser-500 on eEF-2K, 2) Ca^{2+} levels, which stimulate CaM binding to eEF-2K, as well as 3) phosphatase-removal of inactivating phosphorylations[75,76]. The current model of mechanism behind the activating Ser-500 phosphorylation is in part the generation of Ca^{2+} independent activity of eEF-2K; CaM is still required for this activity. Phospho-Ser-500 has been also been shown to increase eEF-2K affinity for Ca^{2+}-bound CaM and apo-CaM and is associated with increased catalytic activity against the eEF-2K peptide-substrate[36,53,77]. *In vitro* studies have also shown that PKA can phosphorylate Ser-366 on eEF-2K but this site was not significant in *in vivo* studies.

Additionally, eEF-2K is known to be phosphorylated at Ser-78 by transient receptor potential cation channel, subfamily M, member 7 (TRPM7), a channel-kinase that regulates Mg^{2+} homeostasis (a process tied to cell growth)[78,79]. Ser-78 is generally known to be an inhibiting site of phosphorylation; the mechanism behind its effect on eEF-2K activity requires further study[80]. This phenomenon also goes to speak to the intricate web that is regulation by eEF-2K multi-site phosphorylation.

1.3.3. eEF-2K and Cell Stress

eEF-2K has been implicated in several types of cell stress, including hypoxia, autophagy, nutrient deprivation and endoplasmic reticulum (ER) stress[81–87]. The activation of eEF-2K and global downregulation of the energy-consuming protein synthesis allows the cell a chance to reestablish homeostasis.

Hypoxia: Hypoxic stress occurs for a variety of cellular processes and diseases including embryogenesis, would repair, high intensity exercise, heart disease, stroke, diabetes and cancer[88]. Under hypoxic conditions, cells cannot undergo oxidative phosphorylation to produce ATP and so are in a state of energy shortage and conservation. Hypoxia is known to lead to inhibition of protein synthesis by activating eEF-2K in a number of ways: a) Activation of the energy sensing protein AMP-activated kinase (AMPK) which activates eEF-2K by inhibiting its inhibitors; AMPK downregulates both ribosome-associated kinase $p70^{S6K}$ and mammalian target of rapamycin (mTOR) which phosphorylate and inhibit eEF-2K on Ser-366[89]. mTOR is additionally known to phosphorylate and inhibit eEF-2K on Ser-78 and Ser-359[74,90,91]. *In vivo* AMPK activity has also been correlated to a rise in phosphorylated Ser-398 on eEF-2K in cells, a site that was proposed to potentially increase activity by increasing the affinity of eEF-2K to CaM[90]. The mechanisms behind this and the Ser-359 and Ser-366 inhibitory phosphorylations are still unclear and require further validation, although it is hypothesized that based on location the Ser-78 phosphorylation may act in affecting CaM binding[90]. b) Activation of the hypoxia inducible factors HIF-1α/β which leads to the inactivation of mTOR, once again alleviating this source of eEF-2K inhibition[92].

Nutrient Deprivation: Metabolic stress occurs in situations of nutrient deprivation such as inadequate blood circulation and solid tumors. This puts the cell in a state of high energy demand and conservation similar to hypoxia. eEF-2K is also activated under similar mechanisms; 1) AMPK responds to a drop in the ratio of ATP:ADP, activating eEF-2K via mTOR inhibition and potentially the activating Ser-398

phosphorylation[5,90,93,94]. 2) mTOR is directly regulated by ATP and amino acid availability- its inacivation is in part through AMPK and ultimately leads to higher eEF-2K activity[5,92]. 3) [95,96].

Endoplasmic Reticulum Stress: ER stress is a collection of issues such as ischemia, ER Ca^{2+} depletion, hypoxia, and oxidative stress. Together the result is an accumulation of unfolded or misfolded proteins which initiates the cell's unfolded protein response (UPR) which results in either regained homeostasis or initiation of apoptosis[97]. eEF-2K is activated under ER stress to slow down the synthesis of new proteins and decrease the load on the ER [98]. AMPK is a prominant pathway activated during ER stress, and it is likely that this is the mechanism through which eEF-2K is regulated[89,97].

Other Stress: eEF-2K has been shown to be downstream of the stress-activated protein kinase 4 (SAPK4), also known as the mitogen-activated protein kinase p38δ (MAPK13)[99]. This protein serves as a stress response to stimuli such as inflammatory cytokines, ultra-violet radiation, growth factors, endotoxins and osmotic shock. SAPK4/p38δ activity has been correlated with eEF-2K phosphorylation on Ser-359, an inhibitory site of regulation, and Ser-396 which in combination decrease eEF-2K activity by 80%[74,100]. It is interesting that SAPK4/p38δ responds to both stress conditions that could be expected to increase eEF-2K activity as well as growth factors where it is logical to increase eEF-2 activity and is ultimately correlated with inhibitory phosphorylations on eEF-2K. This is an example of why and how eEF-2K must orchestrate its myriad of regulatory phosphorylations into a coherent output of activity level that is ultimately beneficial to the current cellular state.

Autophagy: When a cell is overwhelmed by an accumulation of stressors that are too much to process, the balance of singalling processes tip towards cell death rather than striving towards homeostasis. Autophagy often includes a variety of cell stresses we have discussed up until this point, and reports have shown that eEF-2K is required to mediate autophagy through these pathways and mechanisms[85,87,101,102].

1.4. IMPLICATIONS OF EEF-2K IN DISEASE

1.4.1. Significance in Cancer

We have discussed the involvement of eEF-2K in stress responses involving hypoxia, autophagy, ER stress and nutrient deprivation. These are all hallmarks of tumor cells, and so it makes sense that dysregulation of eEF-2K during these processes has been tied to cancer. Since 1999 eEF-2K has been implicated in having various supportive roles in several types of cancer including breast cancer, pancreatic cancer and glioblastoma[87,101,103]. Upregulated activity of the enzyme has been correlated to cytoprotection, increased survival, as well as enhanced proliferation and invasion of tumors[104–107]. Even before eEF-2K was specifically implicated, Rosenwald et al. demonstrated transient inhibition of protein translation induced the expression of proto-oncogenes and stimulation of cells into an active mitotic state[108]. Elevated levels of eEF-2K have been associated with poor prognosis for hepatocellular cancer, medulloblastoma and glioblastoma[109,110].

Studies on eEF-2K and breast cancers have demonstrated its overexpression in several breast cancer cell lines and that siRNA knockdown of the enzyme inhibits

proliferation and invasive properties while inducing apoptosis[109]. A similar *in vivo* study confirmed that an eEF-2K knockdown in an orthotopic xenograft of human breast cancer in a mouse model results in decreased growth and increased anti-cancer drug sensitivity[111].

Its relationship to various cancers provides a compelling platform for the study of eEF-2K and has resulted in novel mechanism discoveries. Still, there is much more to study and investigate regarding its potential therapeutic inhibition and underlying mechanisms in promoting tumor health.

1.4.2. Significance in Neuronal Processes and Diseases

Neurons are known for the speed of their communication and their vast signaling network. They accomplish this by with propagated electric pulses and ion gradients that are initiated by neurotransmitters. Different types of neurotransmitters elicit different types of signals/electric pulses that can vary in frequency and amplitude. Ca^{2+} is a widely used ion in the generation of these signals, which is how eEF-2K became implicated in neuronal processes such as synaptic plasticity, learning and memory[112–114]. eEF-2K must interpret and integrate calcium oscillations into its activity output and control of protein translation[115]. Synaptic plasticity refers to the ability of synapses to strengthen (quickly transmit signals) or weaken over time as a response to how often they're utilized, and is believed to be the mechanism behind learning and memory[113,116–118].

Studies involving eEF-2K in neurons have demonstrated that while eEF-2K downregulates global protein synthesis, select transcripts are upregulated in dendrites.

Upregulated transcripts are all proteins implicated in the modification of synapses and include the alpha subunit of Ca^{2+}/CaM-dependent protein kinase II (αCaMK-II)[117], microtubule-associated protein 1B (MAP1B)[119], activity-regulated cytoskeletal-associated protein (Arc)[71], brain-derived neurotrophic factor (BDNF)[69], and AMPA receptors[120]. Such a phenomenon had not been previously observed and the mechanism behind this location-specific translation is unknown.

Due to the involvement of eEF-2K in neuronal processes it follows logically that its dysregulation can impact neuronal diseases. Indeed, eEF-2K has been implicated in depression, as studies have shown that eEF-2K is a critical mediator of the antidepressant effect of the rapid-acting drug ketamine, and Alzheimer's, where reports show increased eEF-2 phosphorylation[4,98,121–125]. Unfortunately these effects of eEF-2K in neuronal disease are not widely studied and remain poorly understood.

1.5. Regulation of Elongation Factor-2 Kinase by Calcium and Calmodulin

1.5.1. Intro to Calcium and Calmodulin

Calcium ions are universally utilized in various signaling events, usually involving rapid oscillations and spikes in concentration and requiring highly efficient ion channels and stores[126]. Resting cytoplasm Ca^{2+} concentrations are maintained around 100nM, 20,000-100,000 times lower than the extracellular or organelle concentration[127]. Cells are capable of releasing, maintaining, and retracting varying times and concentrations of Ca^{2+} spikes. During a calcium signal, cytoplasmic Ca^{2+} can rapidly rise

utilizing concentration gradients; time and location of this signal can be tightly controlled with Ca^{2+}-binding proteins and Ca^{2+} pumps that return ions to the extracellular matrix or organelle stores[128–131].

Calmodulin (CaM) is the primary protein used to interpret these various Ca^{2+} signals, and is specialized to eukaryotes[128]. CaM structure is well studied; it is a 16kDa protein, typically dumbbell shaped. The two lobes of the dumbbell are each composed of two EF-hands which cooperatively bind a Ca^{2+} ion albeit with varying affinity. The C-terminal Ca^{2+} binding sites have an affinity (K_d) towards Ca^{2+} that range from 500nM to 5μM, which is 3-5 times higher than the N-terminal sites[128]. The lobes are separated by a flexible linker that is critical in conveying allosteric changes with each ion binding[132].

CaM is such a central and critical protein to cellular function that it has been suggested to make up 0.1% of total proteins in the cell, with cytoplasmic concentrations ranging from 2-25μM[128,133]. Furthermore CaM binds many proteins, over 100 distinct targets, with varying specificity and effects- with each Ca^{2+} ion bound it has a different conformation and therefore each state has a different affinity for its many substrates. CaM has been known to bind irreversibly independent of Ca^{2+} concentrations, it has been known to change affinity on the same complex based on Ca^{2+} levels and there are examples of CaM both inhibiting and activating kinases[126,128]. An additional perspective to consider is the free CaM concentration which can range from 10pM to 10μM because of the targets that CaM is binding to at any given point[128,134].

A study released in 2012 by our lab demonstrated that in the presence of saturating CaM (2μM), eEF-2K is barely active when free calcium concentrations are at

25nM and fully active at $[Ca^{2+}]_{free}$ = 3 μM; we calculated the K_d for free Ca^{2+} at 140nM[135]. We also did a study using phosphate-free enzyme in measuring CaM affinity as other reports used various forms of post-translationally modified eEF-2K which have varying affinities for CaM. Our lab reported a K_d for fluorescently labeled Ca^{2+}/CaM around 25nM[53]. These findings are in line with the idea that the enzyme responding to calcium signals and oscillations; at resting intracellular levels of calcium eEF-2K should have little activity which is enhanced by raised Ca^{2+} levels. It is important to note, however, that a study in cells reported that transient Ca^{2+} influxes are sufficient to induce eEF-2 phosphorylation but insufficient in affecting global translation[136].

Studies have confirmed that the roles of Ca^{2+} and CaM in regulating eEF-2K are promoting autophosphorylation of eEF-2K at Thr-348 and Ser-500, promoting efficient substrate phosphorylation, and (for CaM) ultimately allowing for continued activity of eEF-2K in the absence of Ca^{2+} [20,35,36,54,137,138]. Our data (chapters 2-3) have shown a novel mechanism for a calcium-independent mechanism of eEF-2K via acidic conditions, which would provide an additional layer of physiological regulation to help explain the *in vivo* functions of eEF-2K.

1.5.2 Binding Interaction between eEF-2K and Calmodulin

A full crystal structure for eEF-2K has not successfully been defined however recently a group has resolved the structural binding details of CaM with an eEF-2K truncation mutant. Given CaM's integral role in eEF-2K activation and activity, studying the nature of the interaction between CaM and eEF-2K can give us massive insight into

understanding the nature of regulation on eEF-2K by CaM. This study employed a number of methods, including mass spectrometry, small angle x-ray scattering, NMR and computational modeling, to gain insight to eEF-2K conformation and binding to CaM.

In other CaM regulated kinases, CaM binding causes a conformational rearrangement of a substrate-like-moiety away from the substrate recognition site in a method referred to as the release-of-inhibition mode of activation[53,139,140]. eEF-2K does not operate in this manner; instead the study demonstrated that with each step of CaM binding, i.e. during activation and substrate phosphorylation, there is a favorable change in conformation allowing for either autophosphorylation or substrate interaction[139]. In other words, the eEF-2K conformational change results in increased in intrinsic activity/ability to phosphorylate rather than an increase in substrate affinity, which does not significantly change upon CaM binding[53].

This study also unexpectedly reported that even in high calcium concentrations CaM binds eEF-2K with only two Ca^{2+} ions bound in the N-terminus. This Ca^{2+}-loaded region of CaM only forms sparse and weak interactions with eEF-2K on sites distinct from the calmodulin-binding domain (CBD)[126,141,142]. Furthermore it is the Ca^{2+}-free C-terminus of CaM that binds the CBD of eEF-2K; the conserved W85 residue on eEF-2K inserts deep into a hydrophobic cavity on CaM..

While CaM is required for eEF-2K activation and substrate phosphorylation, these events have been observed to occur under in its absence, though it is on the timescale of minutes to hours instead of seconds[54]. Apart from the CaM structure discussed earlier, it is important to note that it has been demonstrated that H^+ ions have

the capability of promoting a similar conformational change in CaM similar to Ca^{2+} binding[142,143]. Based on this study our hypothesis and working model suggests that protons supplement Ca^{2+} in favorably altering CaM concentration to bind eEF-2K- we confirm this in Chapter 4.

1.5.3. Autophosphorylation of eEF-2K by Calcium and Calmodulin

Thr-348: Upon its discovery eEF-2K was initially referred to as Ca^{2+}/CaM-dependent protein kinase 3 (CaMK-III) because it was identified as needing Ca^{2+}/CaM to exhibit activity[10,144,145]. It was later discovered that Ca^{2+}/CaM is necessary for initial autophosphorylation of Thr-348 which represents the first step in activation (Scheme 1.2) and although eEF-2K can exhibit Ca^{2+}-independent activity CaM remains constantly critical [36,52–54,135,146]. Under saturating conditions the rate of Thr-348 autophosphorylation is extremely rapid, occurring at a rate of 3 s^{-1} [54]. Truncation studies have revealed the mechanism of activation behind Thr-348: this site is located on the regulatory loop (R-loop) and its Ca^{2+}/CaM induces autophosphorylation by stabilizing the appropriate conformation. This autophosphorylated form of eEF-2K promotes binding to a conserved hydrophobic pocket, formed by Lys-205, Arg-252, and Thr-254, near the catalytic domain which in turn promotes substrate binding[54]. Phosho-Thr-348 also allosterically promotes the autophosphorylation of Ser-500[36,135].

Ser-500: Ser-500 is located in the SHR domain of eEF-2K (Scheme 1.1) and is a site of activating phosphorylation. It can be autophosphorylated after activation (Thr-348 autophosphorylation) and is also known to be phosphorylated externally via PKA and the

cAMP pathway[36,53]. The mechanism resulting in increased eEF-2K activity is increasing the enzyme's affinity for Ca^{2+} bound CaM as well as apo-CaM (Ca^{2+}-free form). This is significant because it was the first instance of Ca^{2+}-independent activity observed of eEF-2K, which could be an explanation of the location-specific activity of eEF-2K seen in neuronal cells[30,147]. Ser-500 phosphorylated enzyme also shows increase substrate phosphorylation, possibly as a result of increased CaM sensitivity[36,53,135].

1.6. Summary of the Multi-Site Phosphorylations of Elongation Factor-2 Kinase

We have discussed the various phosphorylation sites of eEF-2K in the context of the conditions where they occur, and here we accessibly summarize the various site and their possibilities (Scheme 1.1). The types of phosphorylations that can occur are activating, inhibiting and degradation-promoting and they can occur either by autophosphorylation or via upstream kinases. The many phosphorylation sites mentioned above provide a flexible and multi-input method for the cell to fine-tune eEF-2K activity, and mechanism behind the effect for many of them are believed to be associated with enhancing or diminishing the enzyme's affinity to CaM.

Activating phosphorylations of eEF-2K typically occur under situations of stress where it is helpful to conserve energy and direct resources towards establishing homeostasis. Examples of stress include hypoxia, nutrient deprivation and endoplasmic reticulum stress; upstream pathways that activate eEF-2K include elevated Ca^{2+} levels and the AMPK and PKA pathways. Activating phosphorylation sites include Thr-348,

Ser-500, and Ser-398. Thr-348 and Ser-500 are autophosphorylation sites and Ser-500 and Ser-398 are phosphorylated by other kinases.

Inhibiting phosphorylations of eEF-2K are typically promoted by situations of cell growth and proliferation where it's important to have full protein synthesis. Inhibition of eEF-2K can occur when Ca^{2+} levels are too low to facilitate CaM binding or with mTOR, MAPK (MEK/ERK), cdc2-cyclin B, p38δ, $p70^{S6K}$ and $p90^{RSK1}$ activities[74,80,95,100,148]. Inhibiting phosphorylation sites include Ser-78, Ser-359, Ser-366 and Ser-396; the first three can be autophosphorylated after Ca^{2+}/CaM stimulation and all four can be phosphorylated via the upstream pathways[80,149]. These autophosphorylations incorporate relatively slow compared to the activating autophosphorylations of Thr-348 and Ser-500[52,135]. It is hypothesized that Ser-78, Ser-359 and Ser-366 may function to inhibit CaM rebinding after it dissociates from eEF-2K although additional studies are required to validate these postulations[36,141,150].

Degradation-promoting phosphorylation sites are located at Ser-441 and Ser-445 in the degron motif ^{440}DSGXXS^{445} at the end of the R-loop on eEF-2K[55,151]. A study in 2005 was the first to report eEF-2K ubiquitination and regulation by degradation, later reported to be carried out via the ubiquitin ligase $SCF^{\beta TrCP}$[151,152]. There are several hypotheses of the mechanism behind when eEF-2K degradation is initiated: 1) eEF-2K has been reported to associate with the chaperone heat shock protein Hsp90, which protects eEF-2K from ubiquitination. eEF-2K synthesis and degradation may exist in a balance between Hsp90 stabilization of eEF-2K over time. 2) Several studies have suggested that Ser-398 and Ser-500 phosphorylation promote proteasome degradation of

eEF-2K. It is postulated that as these phosphorylations enhance CaM affinity and as degradation is decreased in the eEF-2K W85S mutant (has lower CaM affinity), CaM binding may cause a conformational change that promotes autophosphorylation of the degron motif[36,141,153].

1.7. Regulation of Elongation Factor-2 Kinase by Acidity

An additional form of eEF-2K regulation that has been proposed is pH[154]. Common physiological events involving intracellular pH fluctuations include gamete activation and fertilization, cell cycle, and stimulation by mitogens and growth factors[155,156]. Cytoplasm acidification has been correlated to global protein synthesis suppression and occurs under stress conditions such as ischemia, hypoxia, high intensity exercise, diabetic ketoacidosis, and solid tumors[7–9,81,157]. Tight control of pH homeostasis is vital to cellular function as many processes have evolved to operate at the narrow physiological range (typically 7.2-7.5) and movement outside of this range can cause dysregulation[158]. Several studies have demonstrated that acidic conditions are activating to the enzyme however there has been no in depth kinetic study to explain this effect[11,154,159]. Nairn et al[10] first connected eEF-2K activation to acidity, Xie et al[12] looked into this activation by various signaling pathways, and Dorovkov et al[11] demonstrated an *in vitro* increase in maximum rate at low pH. A more thorough kinetic evaluation is important for providing insight into how pH affects eEF-2K activity aside from upstream signaling, for example increased efficiency of activation, CaM binding or intrinsic activity.

Acidity has also been tied to calmodulin, which is necessary for eEF-2K activation and activity as described above. Calmodulin has four Ca^{2+} binding sites that trigger a conformational change that in turn regulates its binding properties and relays calcium signals to CaM-binding proteins[126,143]. Low pH has been demonstrated to affect CaM structure and binding similarly to calcium which would likely affect eEF-2K activation[143].

Here we report more definitive kinetic mechanisms where acidity appears to enhance increase the affinity of Ca^{2+}-CaM as well as apo-CaM, resulting in increased rate of autophosphorylation (activation) and substrate phosphorylation (intrinsic activity) that is particularly apparent in the absence of Ca^{2+} (Chapters 2-4). Because histidine residues are known to ionize in the pH 6 range we additionally use mutational studies to identify His-103, His-201, His-227, His-230 and His-288 as potential histidine residues that are critical for the partial mitigation of this activation via H^+ ion.

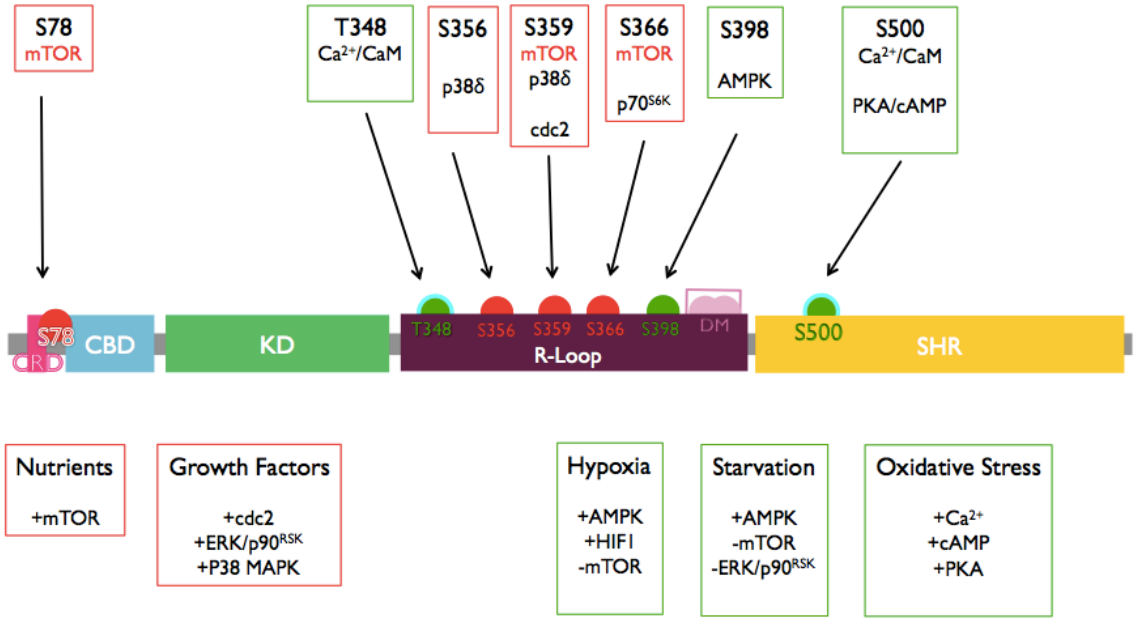

Scheme 1.1. Summary of eEF-2K domains and regulatory phosphorylation sites.

(Figure adapted from Chapter 4). Between CaM/Ca^{2+} control and the various possible phosphorylation states (colored circles; green for activating and red for inhibiting) it is clear that there are many layers to eEF-2K regulation that allow the complex integration of cellular signals. Current studies suggest that CaM binding acts as an on/off binary switch while the phosphorylation sites act in combination through various mechanisms to determining the level of activity[54]. Of the phosphorylation sites discussed here, T348 and S500 are autophosphorylated upon Ca^{2+}/CaM stimulation (light blue outline)[135], S398 is phosphorylated by AMPK under energy stress[90], and S500 can be additionally phosphorylated by cAMP-dependent protein kinase (PKA)[138]; these three sites are activating. On the other hand, mTOR, via downstream kinases, phosphorylates the three inhibitory sites: S78 which is thought to affect CaM binding[95], S359 which is specifically influenced by cdc2-cyclin B[59] and p38δ[160], and S366 which is influenced by p70 S6

kinase as well as Erk-activated $p90^{RSK1}$ [95]. It is not clear what prompts the diphosphorylation site in the degron motif (DM), but it is hypothesized to be, in part, through autophosphorylation[151]. Studies have also made progress into detailing the mechanisms by which these sites exert control over eEF-2K activity, especially in regards to T348 and S500. CaM/Ca^{2+} has been shown to increase the ability of eEF-2K to autophosphorylate T348, which can then bind to a basic allosteric binding pocket that is likely to cause a conformational change in the R-loop that allows for enhanced efficiency to phosphorylate substrate[54,135]. Additionally, phosphorylation of S500 has been implicated in imparting Ca^{2+} independent activity of eEF-2K[53] and because S500 can also be phosphorylated by PKA, under cellular conditions of elevated cAMP it could help maintain significant translational pause without calcium signaling[138]. In summary, there are many complex layers of eEF-2K regulation, some yet to be unraveled, to be considered when studying mechanism.

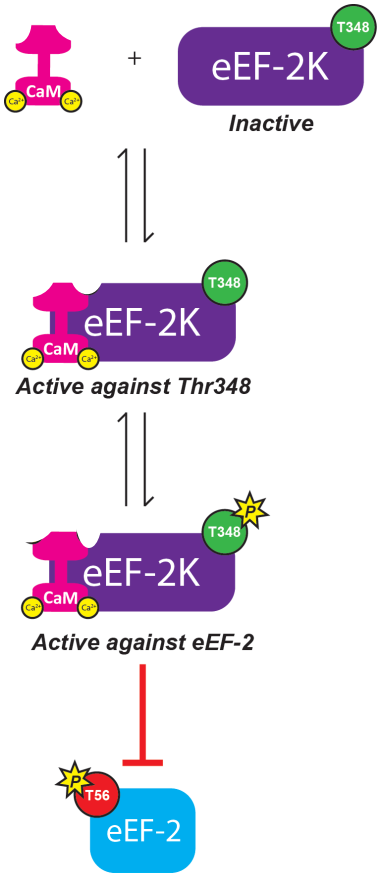

$$E + CaM \underset{k_{-1}}{\overset{k_{1\,[CaM]}}{\longleftrightarrow}} E\bullet CaM \xrightarrow{k_2^{auto}} E^p\bullet CaM$$

$$E^p + CaM + S \underset{k_{-3}}{\overset{k_3}{\longleftrightarrow}} E^p\bullet CaM\bullet S \xrightarrow{k_4^{phos}} E^p\bullet CaM\bullet P$$

Scheme 1.2. The activation and activity of eEF-2K.

(Scheme adapted from Chapters 2 and 4). The model consists of inactive eEF-2K (E) reversibly binding calmodulin (CaM) (k_1/k_{-1}) to form an E•CaM complex capable of phosphorylating eEF-2K on Thr-348 (E^P) (k_2^{auto}). This is the form of eEF-2K that is a prerequisite to phosphorylating substrate (S), but in order to do so E^p must reversibly bind CaM, S and ATP (k_3/k_{-3}) to form the Ep•CaM•S complex capable of phosphorylating S (k_4^{phos}).

Chapter 2: Effect of pH on eEF-2K Activation

2.1. ABSTRACT

Eukaryotic elongation factor 2 kinase (eEF-2K) regulates the global rate of protein synthesis by phosphorylating and inactivating its only known substrate, eukaryotic elongation factor 2 (eEF-2). This is physiologically significant in the context of controlling energy expenditure, as translation is a major consumer of cellular energy, and whenever it is desirable to control growth, such as during various phases of the cell cycle. It follows logically that a protein with such a significant and broad impact as eEF-2K would also be tightly regulated. Many studies have identified and confirmed that eEF-2K activity is affected by calcium (Ca^{2+}), calmodulin, autophosphorylations, and upstream pathway affecters. This myriad of regulatory inputs converges into a complex orchestration of eEF-2K activity that exists on a spectrum of more active to less active, rather than a binary switch of on *versus* off.

The recent (2011) purification of a robustly active human recombinant kinase has allowed for the characterization and biochemical analysis of eEF-2K. Studies have investigated and reported effects of autophosphorylations and various *in vitro* kinetic parameters, as well as a detailed kinetic mechanism. While the enzyme has been studied under standard *in vitro* conditions, there have been several reports of eEF-2K being affected by pH, which is an effect that remains uncharacterized. The goal of this study was to kinetically characterize how acidity modulates the enzyme's behavior. This is a

first step towards understanding an additional way by which eEF-2K adapts to its environment.

In order to achieve this goal, we looked at the eEF-2K mechanism piecewise. Inactive enzyme first binds Ca^{2+}-CaM, which promotes Thr-348 autophosphorylation. We refer to this first step as activation. At both this step and after eEF-2K integrates a variety of signals into a cohesive output we see as its kinetic activity. Here we report our findings of how acidity affects the first activation step of eEF-2K.

2.2. INTRODUCTION

Protein synthesis represents a large (up to 40%) expenditure of cellular energy. It is a process that involves three distinct phases: initiation, elongation and termination, each of which have their own regulating factors[63,161–163]. eEF-2 is one of the primary factors controlling elongation, its job being the translocation of the tRNA and growing polypeptide chain from the A site to the P site in the ribosome[164–166], and its activity is in turn controlled by eEF-2K. eEF-2 is the only known substrate of eEF-2K, that is to say eEF-2K activity is directly tied to the state of eEF-2 and therefore the progression of global protein translation. While eEF-2 has a binary mode of operation (unphosphorylated/able to bind the ribosome vs. phosphorylated on Thr-56/unable to bind the ribosome) the level of eEF-2K activity appears exists on a continuous spectrum[34,64,65,154,167,168].

In order for this to make sense, we must consider individual eEF-2K molecules, as well as the cumulative profile of all eEF-2K molecules in the cell. The activity of eEF-

2K is dependent on external factors, and here "activity" refers to the ability of eEF-2K to phosphorylate its substrate, as reflected by the average rate of phosphate incorporation. Ca^{2+}/CaM binding, autophosphorylation and multisite phosphorylation via upstream pathways are all external factors that must come together into a cohesive output of eEF-2K activity. If we consider an individual unphosphorylated eEF-2K molecule, it must bind Ca^{2+}/CaM, which stabilizes the conformation necessary for autophosphorylation of Thr-348, located on a regulatory loop (R-loop) and subsequent binding to a pocket in the kinase domain[22,35,54,65]. We refer to this step as activation (Figure 2.2). Ca^{2+}/CaM has also been shown to: 1) enhance peptide substrate phosphorylation via activated eEF-2K (already Thr-348 autophosphorylated) and 2) promote autophosphorylation of Ser-500 on the activated enzyme. Ser-500, once phosphorylated, promotes calcium-independent activity of eEF-2K. In summary, Ca^{2+}/CaM promotes activation of eEF-2K, is necessary for efficient substrate phosphorylation, and ultimately allows for continued activity of eEF-2K in the absence of Ca^{2+}[20,35,36,54,137,138].

At this point, we are considering an enzyme molecule that is activated via Thr-348 autophosphorylation, dependent on Ca^{2+}-CaM concentrations for substrate phosphorylation, but with activity still potentially independent of Ca^{2+} fluctuations due to Ser-500 phosphorylation. The complexity deepens when we take additional upstream effecters into account. The mTOR and MAPK (MEK/ERK) pathways, cAMP-dependent protein kinase (PKA) and AMP-activated protein kinase (AMPK) have all been implicated in activity-altering phosphorylations of eEF-2K– the former three activating and the latter two inhibiting[35,95,138,169]. As there are so many combinations of regulatory

phosphorylations that a single enzyme molecule can have, each one can and must have a cohesive output which we can see as the observed average efficiency of substrate phosphorylation.

Finally, an additional form of eEF-2K regulation that has been proposed is pH. Common situations accompanied by intracellular pH fluctuations include gamete activation and fertilization, cell cycle, and stimulation by mitogens and growth factors[155,156]; cytoplasm acidification has been correlated to global protein synthesis suppression and occurs under stress conditions such as ischemia, hypoxia, high intensity exercise, diabetic ketoacidosis, and solid tumors[7–9,81,157]. Precise pH homeostasis is vital to cellular function as many processes have evolved to operate at the narrow physiological range (typically 7.2-7.5[158]). Several studies have demonstrated that acidic conditions are activating to the enzyme however there has been no in depth kinetic study to explain this effect[11,154,159]. There are several potential mechanisms to mediate acidity-induced increase in eEF-2K activity, namely either making more active enzyme (i.e. the eEF-2K activation steps of CaM binding and T348 autophosphorylation) or making the enzyme more active (i.e. increasing intrinsic activity, summarized by an enzyme's catalytic efficiency). This study is the first to use a robustly active recombinant human eEF-2K to investigate how lowering pH affects the activating autophosphorylation of Thr-348. Detailing the mechanism behind the effect of low pH on eEF-2K could lead to a deeper understanding of the mediation of the cellular stress response.

2.3. MATERIALS AND METHODS

2.3.1. Reagents, Strains, Plasmids and Equipment

Yeast extract, tryptone and agar were purchased from USB Corporation (Cleveland, OH). Isopropyl β-D-1-thiogalactopyranoside (IPTG) and dithiothreitol (DTT) were obtained from US Biological (Swampscott, MA). Qiagen (Valencia, CA) supplied Ni-NTA Agarose, QIAprep Spin Miniprep Kit, QIAquick PCR Purification Kit and QIAquick Gel Extraction Kit. Restriction enzymes, PCR reagents and T4 DNA Ligase were obtained from either New England BioLabs (Ipswich, MA) or Invitrogen Corporation (Carlsbad, CA). Lambda Protein Phosphatase was from New England BioLabs (Ipswich, MA). BenchMark™ Protein Ladder was from Invitrogen Corporation. SIGMA*FAST*™ Protease inhibitor cocktail tablets for purification of His-tagged proteins, ultra-pure grade Tris-HCl, HEPES and calmodulin were from Sigma-Aldrich (St. Louis, MO). All other buffer components or chemicals were purchased from either Sigma-Aldrich or Fischer Scientific (Pittsburgh, PA). Amicon Ultrafiltration Stirred Cells, Ultracel Amicon Ultrafiltration Discs and Amicon Ultra Centrifugal Filter Units were from Millipore (Billerica, MA). MP Biomedicals (Solon, OH) supplied [γ-^{32}P]ATP.

Escherichia coli strain DH5α – for cloning – was obtained from Invitrogen Corporation, and BL21(DE3) and Rosetta-gami™ 2(DE3) – for recombinant protein expression – were from Novagen, EMD4Biosciences (Gibbstown, NJ). The pET-32α vector was obtained from Novagen.

The ÄKTA FPLC™ System, the HiPrep™ 26/60 Sephacryl™ S-200 HR gel filtration column and the HiLoad™ 16/60 Superdex™ 200 prep grade gel filtration column were obtained from Amersham Biosciences / GE Healthcare Life Sciences (Piscataway,

NJ). Absorbance readings were performed on a Cary 50 UV-Vis spectrophotometer. Radioactivity measurements were performed on either a Packard 1500 Lab TriCarb Liquid Scintillation Analyzer or a Wallac MicroBeta® TriLux Scintillation Counter from PerkinElmer (Waltham, MA). Proteins were resolved by Tris-glycine sodium dodecyl sulfate polyacrylamide gel electrophoresis (SDS-PAGE), under denaturing conditions on 10% gels, using the Mini-PROTEAN 3 vertical gel electrophoresis apparatus from Bio-Rad Laboratories (Hercules, CA). A Techne Genius Thermal Cycler purchased from Techne, Inc. (Burlington, NJ) was used for PCR.

2.3.2. Molecular Biology

p32TeEF-2K. The modified pET-32α vector (p32TeEF-2K) containing cDNA encoding human eEF-2K (GenBank entry NM_013302) was used for the expression of Trx-His6-tagged eEF-2K. This expression vector was originally chosen because of the thioredoxin tag (Trx-tag) for increased protein solubility and the hexa-histidine tag (His_6-tag) for nickel affinity chromatography purification. There was also an enterokinase protease recognition sequence site (DDDDK) that allows for cleavage of the tags, however this site had been modified to a Tobacco Etch Virus (TEV) protease recognition sequence site (ENLYFQGDI). The vector was modified by the previous graduate student Clint Tavares[31] using site directed mutagenesis between the *Kpn*I (underlined) and *Eco*RV (italicized) recognition sites (Figure 2.1.A). Additional plasmid DNA was obtained by transforming the modified construct into DH5α cells and purifying the DNA using the Qiagen QIAprep Miniprep Kit. The sequence then verified by sequencing at the

ICMB Core Facilities, UT Austin, using an Applied Biosystems automated DNA sequencer.

2.3.3. Expression and Purification of Proteins

Expression of eEF-2K. Recombinant human eEF-2K was expressed in the *E. coli* strain Rosetta-gami™ 2(DE3) (Novagen) using the p32TeEF-2K expression vector. The Rosetta-gami™ 2(DE3) cells were chosen because they carry the pRARE2 plasmid which supplies tRNAs for seven rare codons. eEF-2K contains 63 rare codons, an 8.7% of its 725 residues, so the aim with selecting these expression cells was to promote healthy and successful expression.

A single colony of freshly transformed cells was used to inoculate a starter culture of LB media containing 135 μM ampicillin, 300 μM chloramphenicol and 20 μM tetracycline, and grown overnight at 37 ˚C on a shaker (225 rpm). For co-expressions with lambda phosphatase (encoded in a pCDF-Duet (Novagen) expression vector), 70ng each of p32TeEF-2K and phosphatase DNA were transformed into the Rosetta-gami™ 2(DE3) cells and 20μM spectinomycin was added to all LB media. The culture was diluted 20-fold into LB media containing the same concentration of antibiotics and incubated at 37 ˚C on a shaker (225 rpm) for 3-4 h until it reached an OD_{600} of 0.6-0.8. To induce protein expression the temperature was reduced to 22 ˚C, 0.4 mM isopropyl β-D-1-thiogalactopyranoside (IPTG) was added and the cultures were incubated for 18h. The cells were harvested by centrifugation (7000*g* for 10 min at 4 ˚C), flash frozen in liquid nitrogen and stored at -80 ˚C.

Purification of eEF-2K. The purification step of eEF-2K was performed in three stages of chromatography (Figure 2.1.B): Ni-NTA, anion exchange and gel filtration. To start the bacterial pellet (typically 3.5g wet cells per 1 L of cultured LB) was thawed on ice and resuspended in 25mL of Buffer 2.A (20 mM tris-HCl (pH 8.0), 0.5 M NaCl, 5 mM imidazole, 5 mM $MgCl_2$, 1% triton X-100 (*v/v*), 0.03% brij 30 (*v/v*), 0.1% 2-mercaptoethanol (*v/v*), 1 mM benzamidine hydrochloride hydrate, 0.1 mM tosyl phenylalanyl chloromethyl ketone (TPCK), 0.1 mM phenylmethanesulfonyl fluoride (PMSF) and 7 μM lysozyme). The suspension was sonicated for 12 min (10s pulses) and the temperature was monitored and maintained between 4-6 ˚C. The lysate suspension was centrifuged (Sorvall – SS34 rotor) at 27,000*g* for 30 min at 4 ˚C. The supernatant was gently agitated with 600μL of Ni-NTA beads (Qiagen) per liter of culture for 1 h at 4 ˚C. Prior to agitation, the beads were equilibrated in a chromatography column with 50 mL of Buffer 2.A per liter of culture and after agitation the beads were washed with 100mL of Buffer 2.B (20 mM tris-HCl (pH 8.0), 0.25 M NaCl, 40 mM imidazole, 0.03% brij 30 (*v/v*), 0.1% 2-mercaptoethanol (*v/v*), 1 mM benzamidine hydrochloride hydrate, 0.1 mM TPCK and 0.1 mM PMSF) per liter of culture. The Trx-His_6-TEV-eEF-2K was eluted in four fractions of 10mL of Buffer 2.C (20 mM tris-HCl (pH 8.0), 0.25 M NaCl, 250 mM imidazole, 0.03% brij 30 (*v/v*), 0.1% 2-mercaptoethanol (*v/v*), 1 mM benzamidine hydrochloride hydrate, 0.1 mM TPCK and 0.1 mM PMSF) per liter of culture. The purification stages were monitored via SDS-PAGE: uninduced culture, induced culture, lysis suspension post sonication, centrifuged pellet, centrifuged

supernatant, chromatography column wash flow-through and the various elution fractions.

The eluted fractions containing Trx-His_6-tagged eEF-2K from the Ni-NTA purification were pooled and dialyzed against Buffer 2.D (20 mM tris-HCl (pH 8.0), 0.15 M NaCl, 5 mM $MgCl_2$ and 0.1% 2-mercaptoethanol (*v/v*)) for 16h at 4˚C in the presence of 1.5% TEV protease (*w/w*). The extent of cleavage was confirmed by SDS-PAGE.

After cleavage, the protein was filtered (0.35µm filter) and applied to a MonoQ HR 10/100 (column volume 8mL) anion exchange column pre-equilibrated with filtered Buffer 2.E (25 mM HEPES (pH 7.5), 0.15 MNaCl, 5 mMMgCl2, 0.03% brij 30 (v/v), and 0.1% 2-mercaptoethanol (v/v)). A salt gradient was applied to the column from 0.15–1.0 M NaCl in Buffer 2.E over 160 mL at a flow rate of 2 mL/min. The eluted fractions were collected and protein concentration was monitored with UV; eEF-2K elutes approximately 25% into the applied gradient.

An additional gel filtration step was performed to separate the eEF-2K monomers from the aggregates as advised by previous protocols[31]. Pooled fractions from the anion exchange step were concentrated to under 5mL using an Amicon Ultra-15 Centrifugal Filter Unit, MW cutoff of 35 kDa (Millipore) and applied to a HiPrep™ 26/60 Sephacryl™ S-200 HR gel filtration column pre-equilibrated with Buffer 2.D. The sample was eluted over one column volume (320 mL) at a flow rate of 1mL/min.

Fractions were collected and analyzed for purity using SDS–PAGE; the monomeric kinase eluted around 120mL. Select fractions were pooled and dialyzed against Buffer 2.F (25 mM HEPES (pH 7.5), 2 mM DTT, 50 mM KCl, 0.1 mM EGTA,

0.1 mM EDTA and 10% glycerol) for storage. The dialyzed protein was concentrated using a centrifugal filter unit to 5-10 μM, aliquoted, flash frozen in liquid nitrogen and stored at -80°C. The concentration of eEF-2K was calculated using its absorbance at 280nm and the extinction coefficient (A280) of 97150$cm^{-1}M^{-1}$. Enzyme purity was estimated during the chromatography steps by analyzing Coomassie stained, SDS-PAGE resolved samples (Figure 2.1.C). Final enzyme integrity was estimated by determining specific activity against a peptide substrate (see general kinetic assays).

Expression and purification of TEV protease. Tobacco Etch Virus protease was expressed from the pRK793 expression vector (gifted by Dr. John Tesmer, Life Sciences Institute, University of Michigan, Ann Arbor, MI). The construct was transformed into Rosetta-gami™ 2 (DE3) cells, protein expression was induced with 0.5 mM IPTG at 28 °C and the culture was incubated for 4h. The bacterial culture was centrifuged and the cells were harvested and purified according to protocols published earlier[170,171].

Expression and purification of calmodulin. The calmodulin (CaM) clone in the pET-23 expression vector was gift by Dr. Neal Waxham (Department of Neurobiology and Anatomy, University of Texas Medical School at Houston, Houston, TX). The construct was transformed into BL21 (DE3) cells (Novagen). 250 mL of LB media containing 150 μM ampicillin was inoculated with a single colony and grown overnight at 37°C on a shaker (225 rpm). The culture was diluted 20-fold into LB media with 150μM ampicillin and incubated at 37°C on a shaker (225 rpm) for about 3h until it reached an OD600 of 0.6. Protein expression was then induced with 0.5 mM IPTG for 6

h at 30°C. The cells were harvested by centrifugation (7000 g for 10 min at 4°C), flash frozen in liquid nitrogen and stored at -80°C.

The bacterial pellet was thawed on ice and resuspended in 25mL of Buffer C1 (50 mM Tris–HCl (pH 7.5), 10 mM EDTA, 0.1 TPCK, 0.1 mM PMSF and 1 mM benzamidine). The suspension was sonicated for 15' min (20s pulses) and the temperature was monitored and maintained between 4–6°C. The lysate was cleared by centrifugation (Sorvall –SS34 rotor) at 27,000 g for 30 min at 4°C and the supernatant brought to 2.5 M ammonium sulfate over 1h at room temperature. The solution was cleared by centrifugation (Sorvall –SS34 rotor) at 12,000g for 10 min at 4°C and the supernatant was saturated with ammonium sulfate (about 2.5-3 M) over 1 h. The solution was cleared once more by centrifugation (Sorvall –SS34 rotor) at 12,000 g for 10 min at 4°C, the supernatant was discarded and the pellet was resuspended in 50mL Buffer 2.G (50 mM Tris–HCl (pH 7.5), 1 mM EDTA, 200 mM ammonium sulfate, 0.1 TPCK, 0.1 mM PMSF and 1 mM benzamidine).

The resuspended pellet was filtered and applied to a HiPrep™ Phenyl (FF) 16/10 column pre-equilibrated with Buffer C2. 2.5 mM $CaCl_2$ and 200 mM ammonium sulfate were slowly added to the flow through while 50 mL Buffer 2.G was applied to the column and discarded. The flow through with added calcium was filtered and reapplied to the column pre-equilibrated with Buffer 2.H (50 mM Tris–HCl (pH 7.5), 2 mM $CaCl_2$, and 200 mM ammonium sulfate). The column was washed with an additional 50 mL of Buffer C3 and the sample was eluted over 100 mL of Buffer 2.I (50 mM Tris–HCl (pH

7.5), 1 M NaCl, and 2.5 mM EGTA). SDS-PAGE was used to identify fractions containing CaM, and the corresponding fractions were pooled.

Pooled fractions were concentrated using an Amicon Ultra-15 Centrifugal Filter Unit (Millipore) and applied to a 26/60 sephacryl S-200 prep grade gel filtration column pre-equilibrated with 50 mM Tris–HCl (pH 8). The sample was eluted over a column volumes (320 mL) at a flow rate of 2 mL/min. Fractions were collected and analyzed for purity using SDS–PAGE; select fractions were pooled and dialyzed against Buffer 2.J (25 mM HEPES (pH 7.5). The dialyzed protein was concentrated using a centrifugal filter unit, aliquoted, flash frozen in liquid nitrogen and stored at -20°C. The concentration of CaM was calculated using its absorbance at 280 nm and the extinction coefficient (A280) of 2980 $cm^{-1}M^{-1}$. Enzyme purity was estimated after each purification step by analyzing Coomassie stained, SDS-PAGE resolved samples. These methods were adapted from previous protocols[172,173].

2.3.4. Analytical Methods

General kinetic assays. eEF-2K was assayed at 30°C in Buffer A (25 mM buffer, 2 mM DTT, 10 μg/mL BSA, 50 mM KAcO, 10 mM $MgCl_2$, 100 μM EGTA, 150 μM pep-S) ±50 μM free calcium (added as $CaCl_2$) in a final reaction volume of 100 μL. 1 mM EGTA was added for assays performed in the absence of calcium. Changes in free calcium concentration over varied pH were accounted for using Stanford University's maxchelator calculator. 2 μM CaM was used in assays considered to be CaM saturated, varying concentrations (0-100 μM) of CaM were used for dose response curves. Assays

were performed using 2 nM eEF-2K (untreated/not expressed with λ-phosphatase) and 1mM [γ-^{32}P]ATP (100-1000 cpm/pmol). Either HEPES or Bis-Tris buffers were used for assays assessing pH dependence in their appropriate buffer range as calculated by The University of Liverpool's PFG buffer calculator. Samples were prepared on ice and all reactions and buffers were individually adjusted to the proper pH (range of pH5.8-7.5). 90 µL of Buffer A was incubated at 30°C for 2 min, 5 µL of enzyme was mixed in and heated for an additional 3min, and the reaction was initiated by the addition of 5 µL ATP. Samples were quenched at various time points (1-8min) by spotting 10 µL reaction on P81 paper and immediately immersing in 0.1 M phosphoric acid. Samples were thrice washed for 15minutes in phosphoric acid and once in acetone. Samples were dried and analyzed via the Perkin Elmer Tricarb 2910 TR Liquid Scintillation Analyzer. Each data point was performed in duplicate. The pH of the remaining reaction was confirmed to be consistent with the assay start. The amount of labeled peptide associated with each paper was determined by measuring the cpm on a liquid scintillation counter. Kinase activity was determined by calculating the rate of phosphorylation of eEF-2 (µM.s^{-1}), and the data were fitted to equation 2.1.

$$v = \frac{V_{\max}^{app}[S]}{K_M^{app} + [S]} \qquad \text{(Equation 2.1)}$$

The parameters are defined as follows: v, initial velocity; $V_{\max}^{app}$, apparent maximum velocity; [S], concentration of varied substrate; K_M^{app}, apparent substrate concentration required to achieve half maximal activity.

Autophosphorylation Assays*:* eEF-2K was assayed at 30°C in Buffer 2.L (25 mM buffer, 2 mM DTT, 10 μg/mL BSA, 50 mM KCl, 10 mM $MgCl_2$, 100 μM EGTA, 0.3 μM CaM) ±50 μM free calcium (added as $CaCl_2$, calculated as described in general kinetic assays) in a final reaction volume of 60 μL. Either HEPES or Bis-Tris buffers were used as previously described and the pH of individual reactions were adjusted accordingly (range of pH5.8-7.5). Samples were incubated at 30°C for 2 min, 200 nM eEF-2K (unphosphorylated; co-expressed with λ-phosphatase) was mixed in and incubated for an additional 3 min before the reaction was initiated with ATP (1mM final). 7 μL of each reaction were quenched in Buffer 2.M (final quench volume 25 μL, 115 ng enzyme, 0.1 M EDTA, 5% SDS loading buffer) at varying time points (0-2 h). SDS buffer is 250 mM TrisHCl (pH6.8), 10% SDS, 30% glycerol, 5% β-mercaptoethanol, and 0.02% bromophenol blue. Samples were then analyzed by Western blotting for the incorporation of phosphate at Thr-348 with specific antibodies; 50 ng enzyme was loaded into each lane. The pH of the remaining reaction was confirmed to be consistent with the assay start.

Western blot analysis and quantification of blots: Immobilon-FL PVDF Membrane (Millipore) was used for transfer. Membranes were processed with 25% Odyssey ® Blocking Buffer (LI-COR, Lincoln, NE) in TBS, primaries antibodies in 5% BSA or non-fat dry milk in TBST, and secondary antibodies in 25% Odyssey ® Blocking Buffer in TBST. Blots were scanned and processed on an Odyssey ® Sa Imaging System with Image Studio V.3.1 (LI-COR).

Antibodies: The following antibodies were purchased from: *a. LI-COR*: IRDye ® 680RD Goat anti-Mouse IgG (H+L) (#926-68170, 1:15000); IRDye 800CW Goat anti-Rabbit IgG (H+L) (#827-08365). *b. Epitomics (Burlingame, CA):* eEF-2K (C-terminal) (catalog no. 1754-1). *c. ECM Biosciences (Versailles, KY)*: eEF2K (Thr-348), phospho-specific (catalog no. EP4411). eEF2K (Ser-500), phospho-specific (catalog no. EP4451).

2.4. RESULTS

Nairn et al[10] were the first to demonstrate an increase in eEF-2K activity at low pH. This group successfully identified eEF-2 (then unnamed) as a substrate of eEF-2K. They used phosphorylation assays with cytosolic extracts at pH 7.4 and 6.2 and noted that the increase in eEF-2 phosphorylation, and thereby eEF-2K activity, was independent of additional CaM/Ca^{2+} in the assay at pH 6.2. More than a decade later Dorovkov et al[11] demonstrated that acidity induced an increase in eEF-2 phosphorylation and a decrease in protein translation in mice. This group also used purified recombinant GST-eEF-2K in radiometric phosphorylation assays with both rabbit eEF-2 and peptide to compare basic kinetic parameters of varying pH. This group reported relatively unchanged $K_{m,ATP}$ and $K_{m,substrate}$ but an increase in V_{max} of eEF-2K under low pH. This study also investigated the CaM/Ca^{2+} independence claimed by Nairn et al[10] and found that CaM was necessary for eEF-2K activity under all conditions. They did not, however, look at the calcium dependence and attributed the previous effects to trace CaM in cytosolic extracts. Finally, a recent study by Xie et al[12] primarily focused on the accompanying effects of associated signaling pathways and translation rate in cancer cells; their kinetic work was poorly

defined. In summary, in regards to eEF-2K and its relationship to acidity, previous studies have found: 1) There is an increased rate under low pH but substrate K_m values do not reflect an effect on substrate binding. 2) CaM is necessary for activity at all observed pH levels. 3) In vitro effects are seemingly translated into cellular observations and various histidine residues, which will be discussed in later chapters, may have underlying contribution to this effect by acidic conditions. To date no studies have used a tagless purified form of eEF-2K with comparable activity to its *in vivo* counterpart. This means we are lacking clearly defined kinetic parameters and a model for a kinetic mechanism to describe eEF-2K's relationship to pH.

This study analyzes the entire kinetic mechanism of eEF-2K under acidic conditions by first breaking it down to its individual parts. To start with, this section looks at activation, the first step of the eEF-2K mechanism. Later sections will look into CaM binding and substrate phosphorylation.

2.4.1. Assessment of the pH sensitivity of eEF-2K in the presence of calcium

The first step taken in the study was to confirm previous studies' observations of increased activity of our tagless recombinant eEF-2K under acidic conditions. The pH range used in this study generally stays within 6.2-7.5, which is typically the lowest observed physiological acidic value[158]. On occasion we tested down to pH 5.8 for extrapolation purposes.

We used two forms of eEF-2K in our studies; co-expressed with lambda-phosphatase and not. Even though bacteria do not express CaM, eEF-2K

autophosphorylates at very low rates under standard conditions in its absence. Lambda-phosphatase removes all existing phosphorylations so that the rate of autophosphorylation incorporation may be accurately measured. On the other hand, enzyme that is not co-expressed with the phosphatase is already activated (Thr-348 phosphorylated, not shown) and so the rate of activation does not interfere with intrinsic activity (substrate phosphorylation) readings.

To initially study the activity we used 2 nM eEF-2K (not co-expressed with λ-phosphatase) and 2 μM CaM incubated in reaction buffer (25 mM buffer, 2 mM DTT, 10 μg/mL BSA, 50 mM KAcO, 10 mM $MgCl_2$, 100 μM EGTA, 150 μM pep-S) with 10 μM free calcium (added as $CaCl_2$) in a final reaction volume of 100 μL. HEPES buffer was used for pH 7.5 and Bis-Tris was used for pH 6.2. Reactions were initiated with 1mM [γ-^{32}P]ATP (100-1000cpm/pmol) and samples were quenched at various time points (1, 2, 3, 4, 6 and 8 min) by spotting 10 μL reaction on P81 paper and immediately immersing in 0.1M phosphoric acid. The amount of labeled peptide associated with each paper was determined by measuring the counts per minute (CPM) on a liquid scintillation counter. The rate of phosphate incorporation on the eEF-2 peptide substrate was determined by calculating the slope of CPM over time. Contrary to previous reports[11,159], under standard conditions for the general kinetic assay (max concentrations of the variables: 2 μM CaM, 50 μM free calcium, 150 μM peptide) we initially saw a slight decrease in eEF-2K activity at lower pH (Figure 2.1; 28.2 ± 0.4 s^{-1} at pH 7.5 vs. 12.9 ± 0.2 s^{-1} at pH 6.2) which prompted further investigation.

2.4.2. Assessment of the pH sensitivity of eEF-2K in the absence of calcium

To further examine the activity of eEF-2K under low pH, we surveyed a matrix of varying CaM and calcium concentrations (Ca^{2+} concentrations were varied 0, 0.001, 0.01, 0.1 and 10 μM per assay and analyzed at CaM concentrations of 2000, 500, 50 and 5 nM at both pH 6.2 and 7.5). The highlights of this matrix are illustrated in Figure 2.2. The most striking pattern we noticed was how in the complete absence of calcium (in the presence of 1 mM excess chelating EGTA), the pH 6.2 assays retained activity (9.7 ± 0.2 s^{-1}) while the pH 7.5 assays did not (1.0 ± 0.03 s^{-1}).

These data support the notion that a moderate decrease in pH from pH 7.5 to 6.2 has a dramatic effect on the activity of eEF-2K, primarily in the absence of Ca^{2+}. In light of this observation, we continued the study prioritizing the comparison of the presence and absence of calcium.

2.4.3. Activation of eEF-2K at low pH in the presence of calcium

To begin the analysis of eEF-2K autophosphorylation, we used a phosphate-free form of the enzyme by co-expressing it with lambda phosphatase. This way the enzyme is homogenously at ground zero for examining activation. Examination of the rate of autophosphorylation was accomplished by incubating 200 nM enzyme, 0.3 μM CaM and 50 μM free Ca^{2+} at pH 6.2 in reaction buffer 2.L (25 mM Bis-Tris, 2 mM DTT, 10 μg/mL BSA, 50 mM KCl, 10 mM $MgCl_2$, 100 μM EGTA). Autophosphorylation reactions were initiated with 1 mM ATP and were quenched at the indicated timepoints with 0.1 M EDTA and 5% SDS loading buffer. Samples were analyzed with SDS-PAGE (50 ng

enzyme per well) and western blotting with a phospho-specific Thr-348 antibody to monitor autophosphorylation and total eEF-2K as a control. Potential differences that pH might make to assay component concentrations were taken into account, primarily total free calcium. To ensure the consistency of pH throughout the assay, minimal volume was used to initiate reactions and the pH was checked before and after the assay for each individual reaction.

We first assayed autophosphorylation in the presence of 50μM Ca^{2+} (Figure 2.2). Autophosphorylation at 0, 1, 2, 4, 10, 30 and 60min was analyzed at pH6.2 and 7.5. Under standard/saturating conditions (pH 7.5, 50μM free Ca^{2+}, 2μM CaM) autophosphorylation occurs on the scale of seconds (2.6±0.3/s)[54] so this experiment was primarily to compare whether eEF-2K could maintain the rate of autophosphorylation at pH6.2 comparable to pH7.5. At the aforementioned timepoints (as well as an additional 30s timepoint, not shown) autophosphorylation under both pH values was saturated and so there was no observable difference with this assay.

2.4.2. Activation of eEF-2K at low pH in the absence of calcium

To continue the study of pH and eEF-2K autophosphorylation, we repeated the assay as described above in the absence of calcium (excess EGTA; Figure 2.4). We were expecting the reactions to be slower so we looked at longer timepoints of 0, 2, 5, 30, 60, 120 and 240min. There was an initial observed difference at the 2min timepoint: autophosphorylation at pH7.5 is visibly slower. To look into the difference more closely, additional lower timepoints were tested: 5s and 30s for pH6.2 and slightly longer points

of 30s, 1m, and 4m for pH7.5 because of the initial slower observed rate. Autophosphorylation was saturated at 5 and 30s under pH6.2 and at pH7.5 the phosphate was just beginning to incorporate onto Thr-348. These results show that low pH accelerates the activation of eEF-2K in the absence of calcium.

2.5. DISCUSSION

This is the first study to study the *in vitro* effects of pH on a robustly active recombinant human eEF-2K and to break down the mechanism investigation piecewise. The only previous study to report kinetic values attributed the difference in eEF-2K behavior at low acidity to V_{max}; they reported a V_{max} of 4 nmol/min/mg at pH 6.6 and 0.4nmol/min/mg at pH 7.4[11]. Their reported K_m for ATP and substrate were not significantly different.

2.5.1. Effect of pH on maximal rate of substrate phosphorylation in the presence of calcium

When considering the study of activity using incorporation of phosphate on a peptide substrate, we must consider the enzymatic mechanism as a whole, including the binding of all substrates :

$$\boldsymbol{E^P + ATP + CaM + S + Ca^{2+} \leftrightharpoons E_{CaM}^{ATP \bullet S} \xrightarrow{k_{cat}} E \bullet CaM + P \bullet ADP} \qquad \text{(Equation 2.2)}$$

Where E^P is autophosphorylated/activated enzyme, S is the substrate to be phosphorylated, P is phosphorylated substrate, and $k_{cat} = \frac{V_{max}}{[E]}$.

Our kinetic assay measures the maximal rate of substrate phosphorylation within the E•CaM•S•ATP complex; under the conditions we use all substrates are expected to bind and form the enzyme complex so that we can measure k_{cat}. Our initial observations suggested that low pH does not increase this maximal rate of eEF-2K in the presence of saturating calcium and CaM. In fact, it appears to decrease it slightly in our assay. The observed rate constant under saturating CaM in the presence of calcium were 28.2±0.4 s^{-1} at pH 7.5 vs. 12.9±0.2 s^{-1} at pH 6.2. The differences in kinetic parameters between this and previous studies may be attributed to our enzyme preparation which is some 2000 times more active than the previous standard of GST-tagged eEF-2K.

2.5.2. Effect of pH on observed rate of substrate phosphorylation in the absence of calcium

The highlight from further exploration of Ca^{2+} and CaM concentrations under low pH was the retention of activity at pH 6.2 in the absence of calcium. The observed rate at pH6.2 (under saturating conditions including 2 μM CaM and 150 μM pep-S) is significantly higher than at pH 7.5 (1.0 ± 0.03 s^{-1} at pH 7.5 vs. 9.7 ± 0.2 s^{-1} at pH 6.2). This represents the first evidence of a pH-dependent calcium independent mechanism for eEF-2K.

Considering Eqn. 2.2, while we don't know with certainty that substrates bind to form the enzyme complex in the absence of calcium. Although there is no activity under pH 7.5, this is most likely because CaM has not bound rather than ATP or pep-S.

2.5.3. Effect of pH on eEF-2K autoactivation in the presence of calcium

This study reports for the first time the investigation into the impact of pH on eEF-2K activation. We used unphosphorylated eEF-2K, time-quench assays, and Western blotting to look at relative rates of Thr-348 phosphorylation.

In our first experiment we were looking to verify that there was no observable slowing of autophosphorylation at pH 6.2 in the presence of calcium. Under standard, saturating conditions (max CaM, Ca^{2+} at pH 7.5) we have previously reported an autophosphorylation rate of 2.8 s^{-1} [54]. Here, as expected we established that autophosphorylation is also fast at pH 6.2 with no observable difference compared to pH 7.5.

2.5.4. Effect of pH on autoactivation in the absence of calcium

We observed a difference of eEF-2K behavior under pH 6.2; in the absence of calcium, activity was maintained, whereas at pH 7.5 calcium is required to see activity. Under the first time course we did see slower autophosphorylation at the lowest timepoint of 2 min, though by 5 min both pH were showing saturating autophosphorylation. This prompted an examination into smaller timepoints which confirmed that low pH accelerates eEF-2K activation in the absence of calcium. We observed max autophosphorylation at pH 6.2 at 5 s, and though this is not a precise kinetic measurement it is within 2-fold of the 2.8/s rate reported for standard conditions.

It is important to take the entire autophosphorylation steps together:

$$E + CaM + ATP \overset{k_1}{\leftrightarrow} E \bullet CaM \bullet ATP \overset{k_2}{\rightarrow} E^P \bullet CaM \qquad \text{(Equation 2.3)}$$

Where E is eEF-2K, the first binding/complex formation is defined by the equilibrium between binding and dissociation ($k_1/k_{-1} = K_D^{CaM}$), the second step is a rate defined by k_2 and represents the autophosphorylation step where E^P is phospho-Thr-348-eEF-2K. Our autophosphorylation experiment does not measure the complex formation and autophosphorylation steps separately, that is we don't know if an effect we observe is due to a change in K_D^{CaM} or k_2.

2.6. CONCLUSION

In this chapter we establish that a) the V_{max} of eEF-2K does not appear to increase at lower pH in the presence of calcium, b) its activity does increase in the absence of Ca^{2+} when CaM is present and c) its intrinsic activity appears to be similar at pH 6.2 in the presence and absence of Ca^{2+}. Continuing on to study autophosphorylation in the presence and absence of Ca^{2+} we: 1) established that in the absence of Ca^{2+} autophosphorylation is fast at pH 6.2 (<5 s), 2) established that in the absence of Ca^{2+} the rate of activation is significantly slower at pH 7.5 compared to pH 6.2; and 3) established that in the presence of calcium the rate of activation is high at both pH 6.2 and 7.5.

Taken together these data suggest that eEF-2K and CaM interact differently, and perhaps more efficiently, at low pH. This is of significance because it establishes a new mechanism whereby CaM is able to robustly stimulate autophosphorylation in the absence of calcium, which is typically necessary. Furthermore, this stimulated autophosphorylation, that is normally catalyzed by Ca^{2+}, was catalyzed by just a 20-fold increase in H^+.

These studies set the foundation for a more detailed analysis of the mechanism of acid-catalyzed activation of eEF-2K in both the presence and absence of Ca^{2+} and Mg^{2+}, using pre-steady state rapid chemical quench and stopped-flow approaches, to define the number and order of steps for both CaM binding and autophosphorylation. Furthermore, they also provide the basis for investigating how post-translational modifications of eEF-2K may influence activation. In addition, these studies suggest that structural studies will be essential to determine the precise role of Ca^{2+} and H^{+} ions in the promotion of CaM-mediated eEF-2K activation.

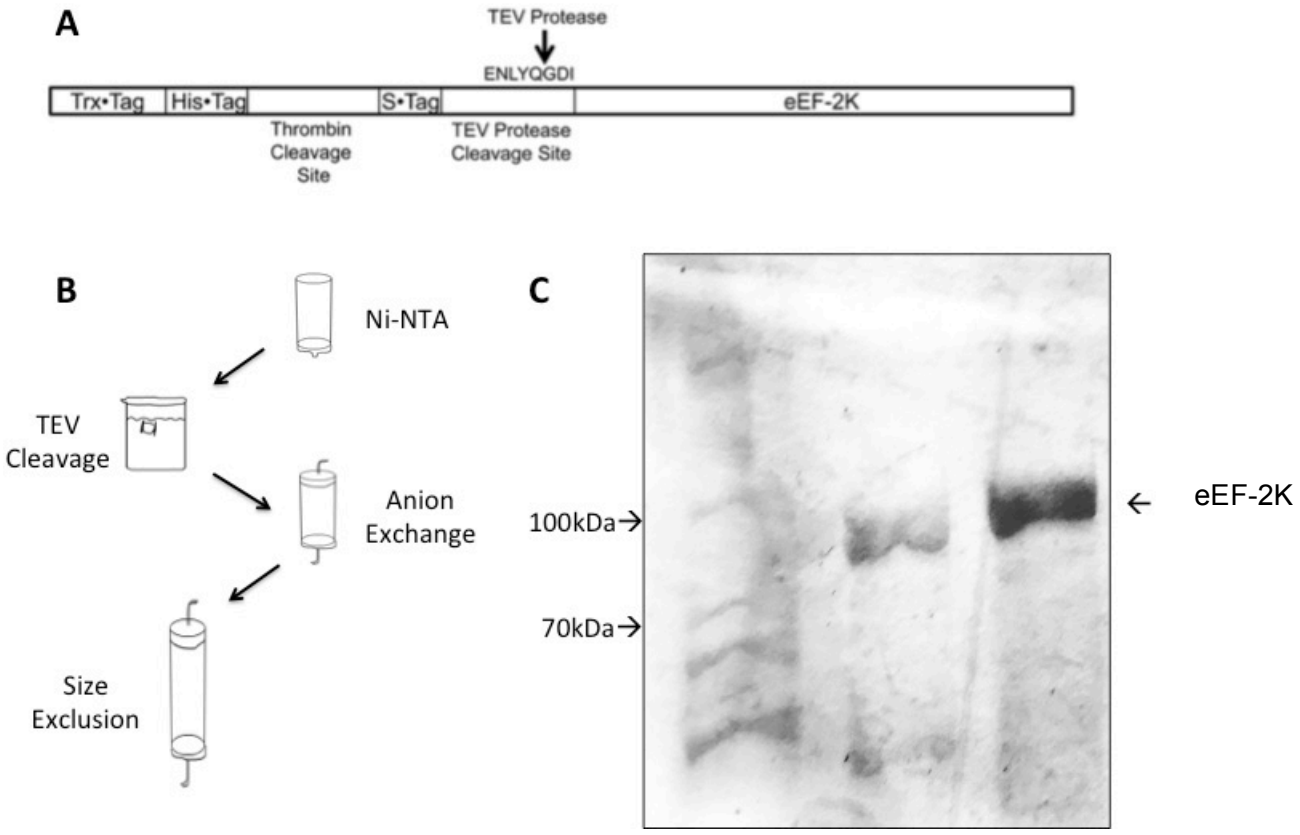

Scheme 2.1. Schematic representation of eEF-2K expression and purification.

(A) Illustrates the modified p32TeEF-2K vector, as designed and cloned previously[31]. From left to right, the thioredoxin tag increases protein solubility, the histidine tag allows for nickel affinity chromatography purification, the thrombin site is meant for cleavage of the previous two tags, the S-tag provides an alternative option for purification (unused here), and the TEV site (modified, originally an enterokinase cleavage site) was inserted to allow for fuller cleavage of the purification tags and a cleaner final protein product. **(B)** Schematic procession of eEF-2K purification: 1) Cleared bacterial lysate is run through a Ni-NTA chromatography column which has a strong affinity for the his-tag. 2) The extra

length of tags are cleaved during an overnight dialysis with TEV protease. 3) Anion exchange chromatography is used to increase protein purity and 4) Gel filtration is used to separate aggregates from monomers. **(C)** The final purity of two fractions of recombinant eEF-2K sample after gel filtration analyzed by Coomassie stained SDS-PAGE against BenchMark™ ladder.

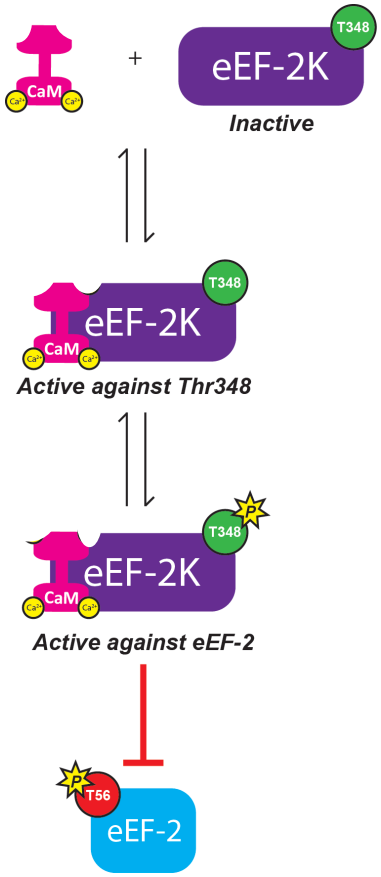

Scheme 2.2. Mechanism of Activation of eEF-2K.

Inactive eEF-2K binds CaM/Ca^{2+} which stabilizes a conformation that allows T348 autophosphorylation which in turn confers ability to phosphorylate substrate (eEF-2, on T56)[54].

A

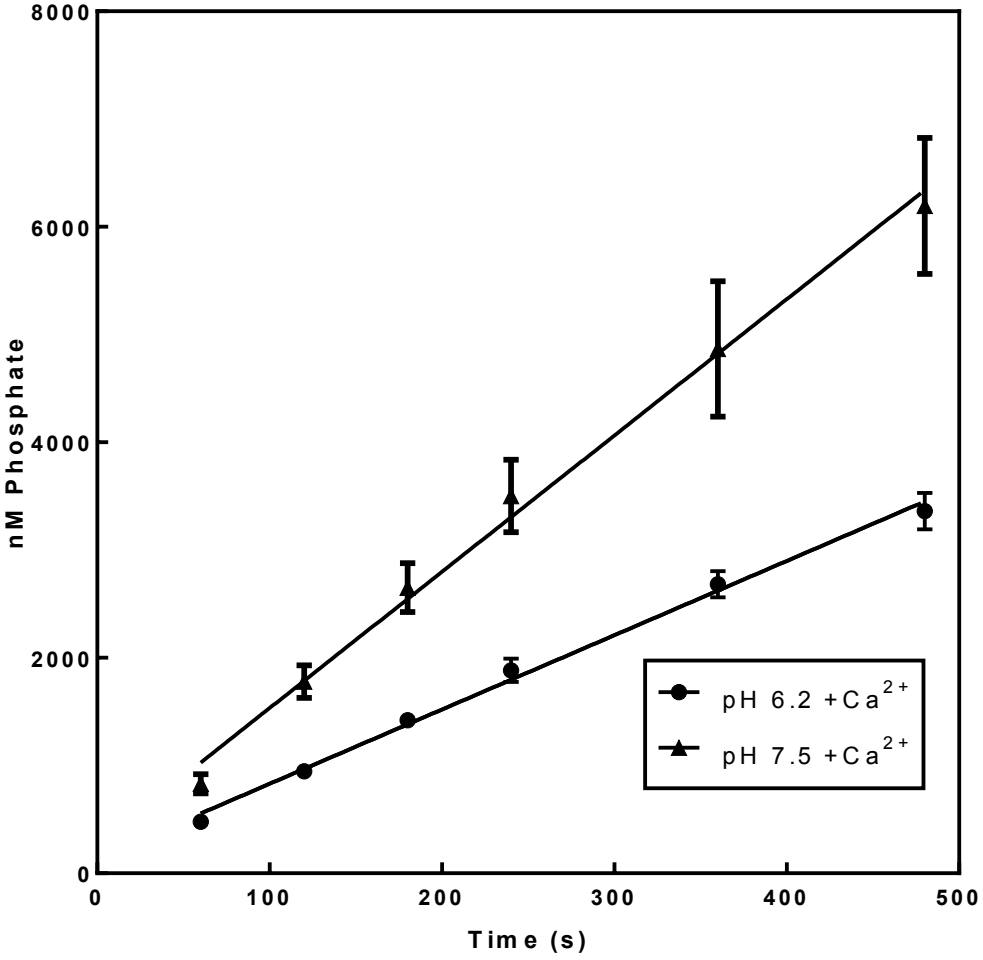

B

	10µM Ca^{2+}	
nM CaM	**pH 7.5 (s^{-1})**	**pH6.2 (s^{-1})**
2000	28.2±0.4	12.9±0.2
0	n/a	n/a

Figure 2.1. (See following page)

Figure 2.1. Low pH does not increase rate of eEF-2K activity.

(A) Our first step was to confirm reports that low pH promotes an increase in eEF-2K activity; we used general kinetic assays to address this. 2 nM eEF-2K (untreated/not expressed with λ-phosphatase) and 2 μM CaM was incubated in reaction buffer (25 mM buffer, 2 mM DTT, 10 μg/mL BSA, 50 mM KAcO, 10 mM $MgCl_2$, 100 μM EGTA, 150 μM pep-S) ±10 μM free calcium (added as $CaCl_2$) in a final reaction volume of 100μL. HEPES buffer was used for pH 7.5 and Bis-Tris was used for pH 6.2. 1 mM EGTA was added for the assays performed in the absence of calcium. Reactions were initiated with 1 mM [γ-^{32}P]ATP (100-1000cpm/pmol) and samples were quenched at various time points (1-8min) by spotting 10 μL reaction on P81 paper and immediately immersing in 0.1M phosphoric acid. The amount of labeled peptide associated with each paper was determined by measuring the counts per minute (CPM) on a liquid scintillation counter. The rate of phosphate incorporation (B) was determined by calculating the slope of CPM over time. The significant observation here is contrary to previous reports[11,159] the rate of substrate phosphorylation (eEF-2K intrinsic activity) does not increase under low pH. This was our first clue to look elsewhere for any effect of pH on eEF-2K.

A

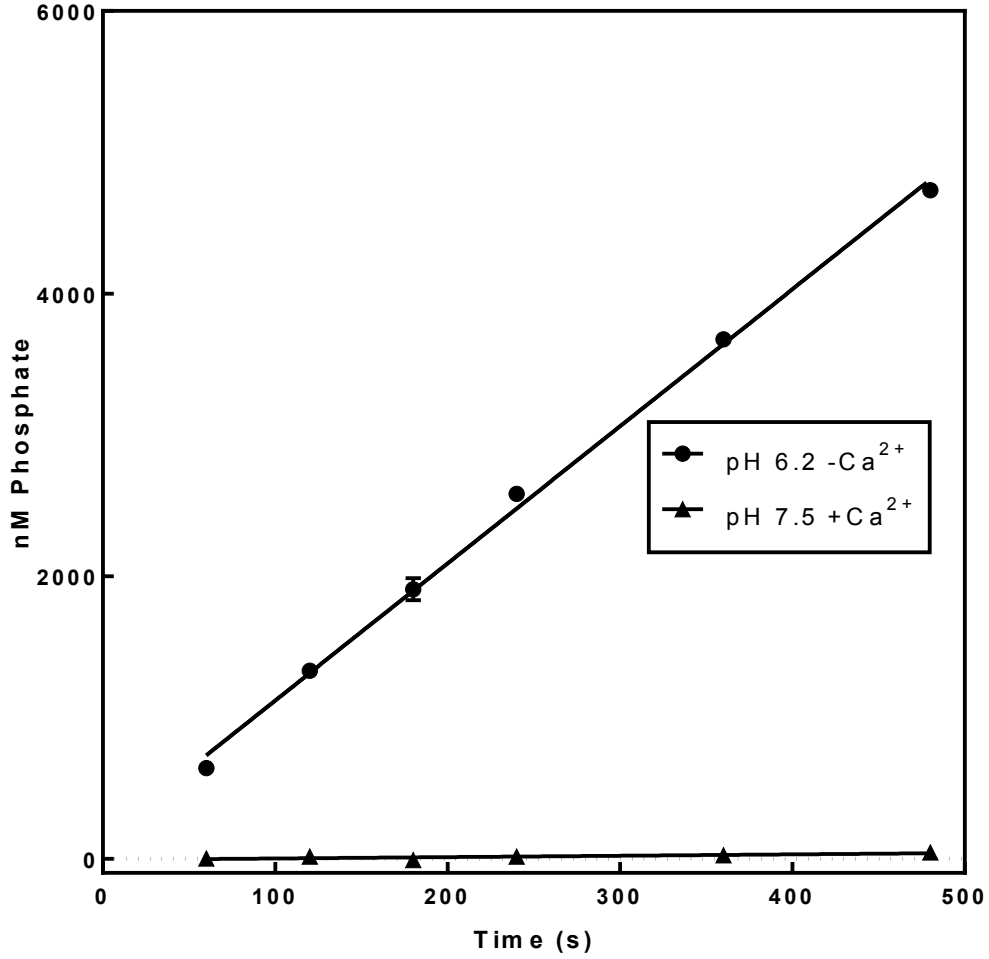

B

0nM Ca^{2+}		
nM CaM	**pH 7.5 (s^{-1})**	**pH6.2 (s^{-1})**
2000	<1.0±0.03	9.7±0.2
0	n/a	n/a

Figure 2.2. (See following page)

Figure 2.2. Low pH rescues eEF-2K activity in the absence of Ca^{2+}.

While performing general kinetic assay tests on eEF-2K involving calcium under high and low pH we discovered an interesting phenomenon (summarized in the table). We noticed that in the absence of calcium, which is typically required, acidic conditions rescued eEF-2K activity. That is, under saturating (2 μM) CaM in the absence of Ca^{2+}, eEF-2K did not have activity at pH 7.5, but did at pH 6.2. This effect is still CaM dependent as there was no observable rate in its absence. Experimental details are as follows: 2 nM eEF-2K (untreated/not expressed with λ-phosphatase) was incubated in reaction buffer (25mM buffer, 2mM DTT, 10μg/mL BSA, 50mM KAcO, 10mM $MgCl_2$, 100μM EGTA, 150μM pep-S) ±10μM free calcium (added as $CaCl_2$) in a final reaction volume of 100μL. HEPES buffer was used for pH 7.5 and Bis-Tris was used for pH 6.2. 1mM EGTA was added for the assays performed in the absence of calcium. Reactions were initiated with 1mM [γ-^{32}P]ATP (100-1000cpm/pmol) and samples were quenched at various time points (1-8min) by spotting 10μL reaction on P81 paper and immediately immersing in 0.1M phosphoric acid. The amount of labeled peptide associated with each paper was determined by measuring the counts per minute (CPM) on a liquid scintillation counter. The rate of phosphate incorporation (reported in the table) was determined by calculating the slope of CPM over time.

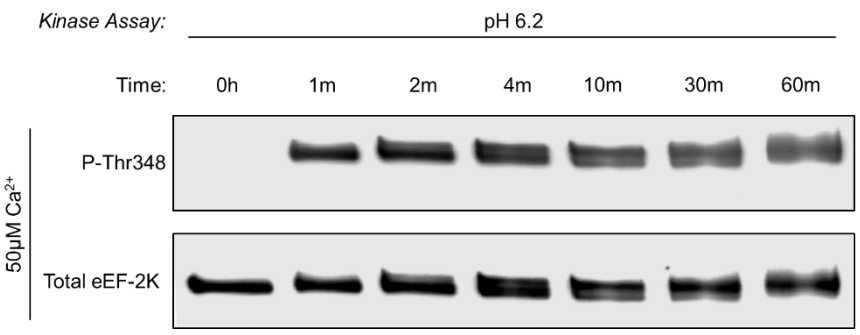

Figure 2.3. Thr-348 Autophosphorylation at pH 6.2 in the presence of Ca^{2+}.

Assays were carried out with 200 nM enzyme, 0.3 μM CaM and 50 μM free Ca^{2+} at pH 6.2 in reaction buffer 2.L (25 mM Bis-Tris, 2 mM DTT, 10 μg/mL BSA, 50 mM KCl, 10 mM $MgCl_2$, 100 μM EGTA). Autophosphorylation reactions were initiated with 1 mM ATP and were quenched at the indicated timepoints with 0.1 M EDTA and 5% SDS loading buffer. Samples were analyzed with SDS-PAGE (50 ng enzyme per well) and western blotting with a phospho-specific Thr-348 antibody to monitor autophosphorylation and total eEF-2K as a control. Here we can see there is no observable difference in either the loading control (total eEF-2K) or the activation of eEF-2K (Thr-348 autophosphorylation). As phospho-T348 incorporation typically occurs on the second timescale, we were expecting to see this saturation at the lowest (1 min) point. We were primarily looking to confirm this phenomenon to see that under acidic conditions the autophosphorylation wasn't observably slower.

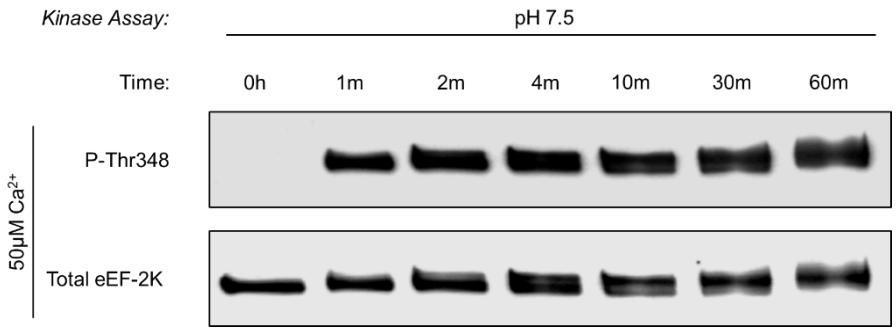

Figure 2.4. Thr-348 Autophosphorylation at pH 7.5 in the presence of Ca^{2+}.

Assays were carried out with 200 nM enzyme, 0.3 μM CaM and 50 μM free Ca^{2+} at pH 7.5 in reaction buffer 2.L (25 mM HEEPS, 2 mM DTT, 10 μg/mL BSA, 50 mM KCl, 10 mM $MgCl_2$, 100 μM EGTA). Autophosphorylation reactions were initiated with 1 mM ATP and were quenched at the indicated timepoints with 0.1 M EDTA and 5% SDS loading buffer. Samples were analyzed with SDS-PAGE (50 ng enzyme per well) and western blotting with a phospho-specific Thr-348 antibody to monitor autophosphorylation and total eEF-2K as a control. Here we can see there is no observable difference in either the loading control (total eEF-2K) or the activation of eEF-2K (Thr-348 autophosphorylation). As phospho-T348 incorporation typically occurs on the second timescale, we were expecting to see this saturation at the lowest (1 min) point. We were primarily looking to confirm this that under this timescale acidic and normal conditions are comparable.

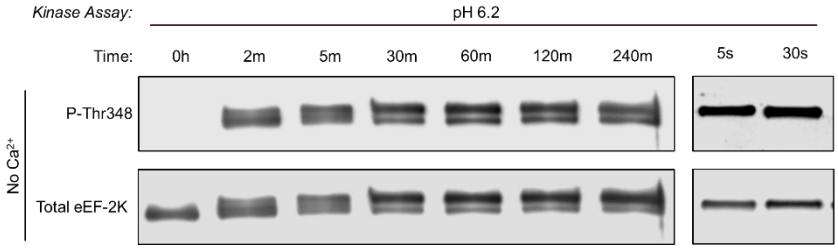

Figure 2.5. Thr-348 Autophosphorylation at pH 6.2 in the absence of Ca^{2+}.

Assays were carried out with 0μM free Ca^{2+} (1 mM EGTA), 200 nM enzyme, and 0.3 μM CaM at pH 6.2 in reaction buffer 2.L (25 mM Bis-Tris, 2 mM DTT, 10 μg/mL BSA, 50 mM KCl, 10 mM $MgCl_2$). Autophosphorylation reactions were initiated with 1 mM ATP and were quenched at the indicated timepoints with 0.1 M EDTA and 5% SDS loading buffer. Samples were analyzed with SDS-PAGE (50 ng enzyme per well) and western blotting with a phospho-specific Thr-348 antibody to monitor autophosphorylation and total eEF-2K as a control. Here we can see that under the 2 min timepoint the autophosphorylation was already saturated. We carried out lower time points of 5 s and 30 s in an additional experiment (0 min control not shown) and observed that even at 5 s autophosphorylation was saturated at pH 6.2.

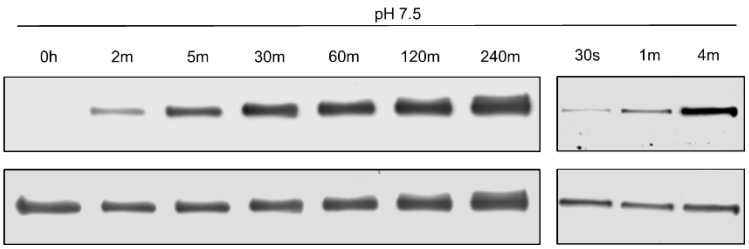

Figure 2.6. Thr-348 Autophosphorylation at high and low pH in the absence of Ca^{2+}. Assays were carried out with 0μM free Ca^{2+} (1 mM EGTA), 200 nM enzyme, and 0.3 μM CaM at pH 7.5 in reaction buffer 2.L (25 mM HEPES, 2 mM DTT, 10 μg/mL BSA, 50 mM KCl, 10 mM $MgCl_2$). Autophosphorylation reactions were initiated with 1 mM ATP and were quenched at the indicated timepoints with 0.1 M EDTA and 5% SDS loading buffer. Samples were analyzed with SDS-PAGE (50 ng enzyme per well) and western blotting with a phospho-specific Thr-348 antibody to monitor autophosphorylation and total eEF-2K as a control. Here we can see the incorporation of phospho-T348 from 0 – 5 min. We carried out additional lower time points to compare to pH 6.2 and were able to see a more dramatic progression of phosphate incorporation from 30 s – 4 min (right) (0 s control not shown). From this we see that in the absence of Ca^{2+}, if we take 2-5 min as fully saturated at pH 7.5, at pH 6.2 with 5 s being fully saturating autophosphorylation is at least 60 times faster.

Chapter 3: Effect of pH on eEF-2K Activity

3.1. ABSTRACT

Eukaryotic elongation factor 2 kinase (eEF-2K) is one of several proteins responsible for regulating protein translation. Eukaryotic elongation factor 2 (eEF-2) is the only known substrate of eEF-2K, which inhibits eEF-2 by phosphorylating it on Thr-56. Recent studies have elucidated the kinetic mechanism for eEF-2K; in summary, there is an initial binary on/on switch followed by a multitude of regulators that culminate into a volume control. Primarily, it has been various phosphorylation sites (and the cofactors and upstream regulators that responsible for the phosphorylations) whose effects on eEF-2K have been studied. Far fewer studies have been conducted on the nature of the effect of acidity on eEF-2K behavior. We have recently looked into the effect of low pH on eEF-2K activation and found that autophosphorylation is most profoundly affected/maintained in the absence of calcium. The data pointed to the notion that eEF-2K has an alternate interaction with CaM, which manifests even with a moderate 20-fold increase in H^+ ions from pH 7.5 to pH 6.2. The next logical step was to look into how the kinetics of substrate phosphorylation are affected. We found that the V_{max} values for peptide phosphorylation were relatively similar across pH and calcium concentration, suggesting that regardless of what ions are present CaM adopts a functionally similar conformation when bound to eEF-2K. Furthermore, we found that the difference in behavior observed at pH 6.2 and pH 7.5 was explained by the CaM dependency. We also found that H^+ ions augment the ability of Ca^{2+} ions to promote CaM binding, suggesting

that despite both ions promoting CaM binding, their underlying mechanisms exhibit distinct elements.

3.2. INTRODUCTION

Balancing protein synthesis and protein degradation is an integral part of cellular homeostasis. Various proteins are constantly being translated to adapt to the needs and environment of their cells. Protein synthesis is a major factor in cellular function and must be tightly controlled as this process alone can consume up to 40% of the cell's energy. Three ATP/GTP molecules per amino acid are required to translate mRNA into proteins, which is where the high-energy expenditure comes from. Eukaryotes have evolved several pathways to keep this process in check, including multiple factors required for the initiation, elongation and termination stages of translation[63,161–163]. One such factor is eukaryotic elongation factor 2 (eEF-2) which is responsible for moving the growing polypeptide chain from the A site to the P site in the ribosome[164–166]. Phosphorylation of eEF-2K on Thr-56 impedes its ability to bind the ribosome; eukaryotic elongation factor 2 kinase (eEF-2K) is responsible for this modification. eEF-2 is the only known substrate of eEF-2K, which therefore functions to halt global protein synthesis[10,64,65,167]. Surprisingly, eEF-2K has also been known to induce the translation of select transcripts which seems contradictory to its function[174]. This effect was observed in Aplysia sensory neurons; neurons are known for their tube-like cell body extensions and ability to utilize compartmentalization as a regulatory mechanism. In this context, it makes sense that eEF-2K may function in a location-specific manner to initiate specific

transcript translation. Still, understanding the ways that eEF-2K is regulated may help explain how such an effect is possible. More compellingly still, abnormal eEF-2K behavior is implicated in a variety of disease states, including several types of cancer, Alzheimer's and depression, which sets an even higher precedent for understanding this complex enzyme[87,101,179–181,107,111,122,125,175–178].

Upon its discovery eEF-2K was aptly named Ca^{2+}/CaM-dependent protein kinase 3 (CaMK-III) because it was identified as needing Ca^{2+}/CaM to exhibit activity[154,182,183]. Over the years it has been determined that Ca^{2+}/CaM is necessary for autophosphorylation of Thr-348 and that subsequent autophosphorylation of Ser-500 confers calcium-independent activity to eEF-2K[36,135]. Details behind these autophosphorylation sites remained elusive for nearly two decades, however we now know that the phosphorylation of Thr-348, located on a regulator loop (R-loop), stabilizes its binding to a conserved hydrophobic pocket near the catalytic domain that in turn allows eEF-2K to bind its substrate[20,21,54]. Studies have also shown that CaM, though not always calcium, is essential for both activation (Thr-348 autophosphorylation) and activity (substrate phosphorylation)[36,54,64,182]. Furthermore, although the precise mechanism is unclear, it has been demonstrated that Ser-500 autophosphorylation (or phosphorylation via cAMP activated protein kinase (PKA)) serves to enhance eEF-2K substrate phosphorylation and enhances the enzyme's response to CaM both calcium bound and in its apo form[21,36,138].

The multisite-phosphorylation regulation of eEF-2K continues with additional sites via upstream pathways; various growth factors, via the mitogen-activated protein

kinases (MAPKs) and mammalian target of rapamycin mTORC1 pathways, have an inhibiting effect on eEF-2K by phosphorylating Ser-78 and Ser-359/Ser-366[52,91,169,184–186]. AMPK on the other hand has been shown to have an activating effect on eEF-2K by relieving inhibition of eEF-2K by mTOR as well as phosphorylating eEF-2K on Ser-491/Ser-492[185]. An additional layer of regulation, seemingly independent of upstream enzymes and phosphorylation sites is pH, which has been shown to activate the enzyme and may have physiological significance for slowing down protein synthesis during states of stress such as anoxia and hypoxia[8,159]. However, to date our studies indicate that most, if not all, post-translational modifications impinge upon the dynamics and affinity of Ca^{2+}/CaM binding and the rate of Thr-348 autophosphorylation.

pH is a condition that has the potential to affect Ca^{2+}/CaM binding, as acidity has been shown to cause CaM to mimic its calcium bound conformation[143]. Because CaM is a necessary ligand for both activation and activity of eEF-2K, pH therefore has the potential to affect either or both. Chapter 2 looked at the effect of pH on the activation step of eEF-2K and found that acidity was particularly activating in the absence of calcium. To look further into understanding how pH regulates eEF-2K, it would be most useful to look into how acidity affects the activity, in this case peptide substrate phosphorylation, of this enzyme. There has been a lack of mechanistic explanations in regards to this effect. Here we report that, contrary to previous reports, the V_{max} of eEF-2K does not change between high and low pH. Under more acidic conditions, in both the absence and presence of calcium, we show that the K_m for calmodulin decreases. This

suggests that acidity promotes the binding of CaM to eEF-2K to generate an active complex and that Ca^{2+} ions further augments the binding.

3.3. MATERIALS AND METHODS

3.3.1. Reagents, Strains, Plasmids and Equipment

Yeast extract, tryptone and agar were purchased from USB Corporation (Cleveland, OH). Isopropyl β-D-1-thiogalactopyranoside (IPTG) and dithiothreitol (DTT) were purchased from US Biological (Swampscott, MA). From Qiagen (Valencia, CA) Ni-NTA Agarose, QIAprep Spin Miniprep Kit, QIAquick PCR Purification Kit and QIAquick Gel Extraction Kit were purchased. Lambda Protein Phosphatase was from New England BioLabs (Ipswich, MA). BenchMark™ Protein Ladder was from Invitrogen Corporation. SIGMA*FAST*™ Protease inhibitor cocktail tablets for purification of His-tagged proteins, ultra-pure grade Tris-HCl, HEPES and calmodulin were from Sigma-Aldrich (St. Louis, MO). All other buffer components or chemicals were purchased from either Sigma-Aldrich or Fischer Scientific (Pittsburgh, PA). Amicon Ultrafiltration Stirred Cells, Ultracel Amicon Ultrafiltration Discs and Amicon Ultra Centrifugal Filter Units were from Millipore (Billerica, MA). MP Biomedicals (Solon, OH) supplied [γ-^{32}P]ATP.

Escherichia coli strain DH5α – for cloning – was obtained from Invitrogen Corporation, and BL21(DE3) and Rosetta-gami™ 2(DE3) – for recombinant protein expression – were from Novagen, EMD4Biosciences (Gibbstown, NJ). The pET-32α vector was obtained from Novagen.

The ÄKTA FPLC™ System, the HiPrep™ 26/60 Sephacryl™ S-200 HR gel filtration column and the HiLoad™ 16/60 Superdex™ 200 prep grade gel filtration column were from Amersham Biosciences / GE Healthcare Life Sciences (Piscataway, NJ). Absorbance readings were performed on a Cary 50 UV-Vis spectrophotometer. Radioactivity measurements were performed on either a Packard 1500 Lab TriCarb Liquid Scintillation Analyzer or a Wallac MicroBeta® TriLux Scintillation Counter from PerkinElmer (Waltham, MA). Proteins were resolved by Tris-glycine sodium dodecyl sulfate polyacrylamide gel electrophoresis (SDS-PAGE), under denaturing conditions on 10% gels, using the Mini-PROTEAN 3 vertical gel electrophoresis apparatus from Bio-Rad Laboratories (Hercules, CA). A Techne Genius Thermal Cycler purchased from Techne, Inc. (Burlington, NJ) was used for PCR. eEF-2K peptide substrate (pep-S; Acetyl-RKKYKFNEDTERRRFL-Amide (2,227.8 Da)) was custom ordered and purchased from AnaSpec Technologies (Fremont, CA). P81 cellulose filters were from Whatman / GE Healthcare Life Sciences (Florham Park, NJ).

3.3.2. Molecular Biology

p32TeEF-2K. The modified pET-32α vector (p32TeEF-2K) containing cDNA encoding human eEF-2K (GenBank entry NM_013302) was used for the expression of Trx-His6-tagged eEF-2K. This expression vector was originally chosen because of the thioredoxin tag (Trx-tag) for increased protein solubility and the hexa-histidine tag (His_6-tag) for nickel affinity chromatography purification. There was also an enterokinase protease recognition sequence site (DDDDK) that allows for cleavage of the tags,

however this site had been modified to a Tobacco Etch Virus (TEV) protease recognition sequence site (ENLYFQGDI). The vector was modified by the previous graduate student Clint Tavares[31] using site directed mutagenesis between the *Kpn*I (underlined) and *Eco*RV (italicized) recognition sites (Figure 2.1.A). Additional plasmid DNA was obtained by transforming the modified construct into DH5α cells and purifying the DNA using the Qiagen QIAprep Miniprep Kit. The sequence then verified by sequencing at the ICMB Core Facilities, UT Austin, using an Applied Biosystems automated DNA sequencer.

3.3.3. Expression and Purification of Proteins

Expression and Purification of eEF-2K. Recombinant human eEF-2K was expressed in the *E. coli* strain Rosetta-gami™ 2 (DE3) (Novagen) using the p32TeEF-2K expression vector. The Rosetta-gami™ 2 (DE3) cells were chosen because they carry the pRARE2 plasmid which supplies tRNAs for seven rare codons. eEF-2K contains 63 rare codons, an 8.7% of its 725 residues, so the aim with selecting these expression cells was to promote healthy and successful expression. Expression and purification were performed as described in Chapter 2.3 Materials and Methods of this dissertation.

Expression and purification of TEV protease. Tobacco Etch Virus protease was expressed from the pRK793 expression vector (gifted by Dr. John Tesmer, Life Sciences Institute, University of Michigan, Ann Arbor, MI). The construct was transformed into Rosetta-gami™ 2(DE3) cells, protein expression was induced with 0.5 mM IPTG at 28 °C

and the culture was incubated for 4h. The bacterial culture was centrifuged and the cells were harvested and purified according to protocols published earlier[170,171].

Expression and purification of calmodulin. The calmodulin (CaM) clone in the pET-23 expression vector was gift by Dr. Neal Waxham (Department of Neurobiology and Anatomy, University of Texas Medical School at Houston, Houston, TX). The construct was transformed into BL21(DE3) cells (Novagen). Expression and purification were carried out as described in Chapter 2.3 Materials and Methods of this dissertation. These methods were adapted from previous protocols[172,173].

3.3.4. Analytical Methods

General kinetic assays. eEF-2K was assayed at 30°C in Buffer 3A (25 mM buffer, 2 mM DTT, 10 μg/mL BSA, 50 mM KAcO, 10 mM $MgCl_2$, 100 μM EGTA, 150 μM pep-S) ±50μM free calcium (added as $CaCl_2$) in a final reaction volume of 100μL unless otherwise specified. 1 mM EGTA was added for assays performed in the absence of calcium. Changes in free calcium concentration over varied pH were accounted for using Stanford University's maxchelator calculator. 2 μM CaM was used in assays considered to be CaM saturated, varying concentrations (0-100 μM) of CaM were used for dose response curves. Assays were performed using 2 nM eEF-2K (untreated/not expressed with λ-phosphatase) and 1 mM [γ-^{32}P]ATP (100-1000 cpm/pmol). Either HEPES or Bis-Tris buffers were used for assays assessing pH dependence in their appropriate buffer range as calculated by The University of Liverpool's PFG buffer calculator. Samples were prepared on ice and all reactions and buffers were individually

adjusted to the proper pH (range of pH5.8-7.5). 90 µL of Buffer A was incubated at 30°C for 2 min, 5 µL of enzyme was mixed in and heated for an additional 3min, and the reaction was initiated by the addition of 5 µL ATP. Samples were quenched at various time points (1-8min) by spotting 10 µL reaction on P81 paper and immediately immersing in 0.1 M phosphoric acid. Samples were thrice washed for 15 minutes in phosphoric acid and once in acetone. Each data point was performed in duplicate. The pH of the remaining reaction was confirmed to be consistent with the assay start. The amount of labeled peptide associated with each paper was determined by measuring the counts per minute on a liquid scintillation counter. Kinase activity was determined by calculating the rate of phosphorylation of eEF-2 peptide ($\mu M.s^{-1}$). Data where K_C^{app}>20nM were fit to eqn. 3.1, and the data where K_c^{app}<20nM were fitted to equation 3.1.

$$k_{obs}^{app} = \frac{k_{cat}^{app}[C]}{K_c^{app} + [C]} \qquad \text{(Equation 3.1)}$$

$$k_{obs}^{app} = k_{cat}^{app} \frac{([E] + [C] + K_M^{app}) - \sqrt{([E] + [C] + K_M^{app}) - 4[E][C]}}{2[E]} \qquad \text{(Equation 3.2)}$$

The parameters are defined as follows: k_{obs}^{app}, apparent rate constant; k_{cat}^{app}, apparent catalytic constant; [C] is the concentration of varied co-activator CaM; [E] is the concentration of eEF-2K; K_c^{app} is the apparent CaM concentration required to achieve half maximal activity.

Data Fitting: Unless otherwise specified all data and equation fitting was performed using GraphPad Prism version 6.00 for Windows, GraphPad Software, La Jolla California USA, www.graphpad.com

3.4. Results and Discussion

The potential for pH to modify the conformation of CaM similarly to Ca^{2+} means that its interaction with eEF-2K may be affected. CaM is essential for both the activation and activity phases of the eEF-2K mechanism, and to isolate which step we are looking at dephosphorylated (lambda phosphatase co-expressed) enzyme was used to study activation in Chapter 2 and pre-activated enzyme will be used for the activity studies to follow. To obtain pre-activated (Thr-348 phosphorylated) enzyme, eEF-2K was purified and not co-expressed with lambda phosphatase. Although bacteria do not express CaM, we have seen that over extended (hours) periods of time, eEF-2K will autophosphorylate on Thr-148 without CaM. Presumably, this is not a viable *in vivo* method of autophosphorylation due to the presence of efficient phosphatases. However, since we use several cocktails of phosphatase inhibitors throughout the purification process, when not co-expressed with lambda phosphatase eEF-2K can be purified in a stoichiometrically phosphorylated state. This was confirmed using phospho-specific antibodies and western blotting (data not shown).

3.4.1. Characterizing the kinetic parameters of eEF-2K at low pH

pH Does Not Affect the Rate of eEF-2K Activity in the Presence of Calcium. The publication by Dorovkov et al.[11] was the only previous study to report quantified kinetics for eEF-2K at low pH. This study concluded that increased acidity increased the maximal velocity (V_{max}) of eEF-2K tenfold and had no effect on the K_m of substrates. Others[76,159] reported similar findings but without quantified data. Our previous data (Chapter 2) on the other hand pointed to the exact opposite, where increased acidity appeared to increase the affinity for CaM, but had a minimal effect on V_{max}. To more fully explore this effect, we performed a full CaM-dependence curve at pH 6.2 and pH 7.5 using saturating (50μM) free calcium. We used a maximal concentration of 1μM CaM with 10 serially diluted concentrations. Data were fit to equation 3.1. (Table 3.1). The k_{obs}^{app} under the two conditions were within two-fold : pH 6.2 was 20.9 ± 0.9 s^{-1} and pH 7.5 was 34.6 ± 0.9 s^{-1}. On the other hand, the K_c^{app} for pH 7.5 was 3.6 ± 0.6 nM and for pH 6.2 the K_c^{app} could not be resolved past >0.5nM. This is because at the lowest feasible concentration of CaM used the rate did not reach below half the maximal rate. Still, from these parameters we can see that there is at least a 7-fold difference in K_c^{app} between pH 6.2 and 7.5 where the increased acidity reflects tighter CaM binding. This effect can be visualized in Figure 3.1.

eEF-2K Activity Increases with Decreasing pH in the Absence of Calcium. From our previous autophosphorylation data (Chapter 2) we saw that acidity more prominently effected eEF-2K activity in the absence of calcium. This was of note because

there have been no reports for eEF-2K calcium independent activity unless Ser-500 had been phosphorylated. A report[143] that H^+ may have the same effect as Ca^{2+} on the conformation of CaM led to our hypothesis that the effects of low pH on eEF-2K activation are especially significant in the absence of calcium, because of the ability of H^+ ions to promote an 'active' CaM conformation and subsequent interaction with eEF-2K.

To determine the apparent catalytic constant and K_m for CaM, we performed a full CaM dose response curves with a minimum of ten serially diluted CaM concentrations. At pH 6.2 we used a max CaM concentration of 1μM which was sufficient to saturate and level out the maximum observed rate constant. As expected at pH 7.5 there was no observable activity at 1μM CaM or even 5μM. In attempt to level out the observed rate constant, or to see if we could saturate enough calmodulin to see any activity, we used additional concentrations of 10, 25, 50 and 100 μM. The kinetic parameters derived from these experiments are summarized in Table 3.1. The k_{cat}^{app} at pH 6.2 was 25.6±3.0 s^{-1} which is consistent with the k_{cat}^{app} of both pH 6.2 and 7.5 in the presence of calcium. On the other hand the k_{cat}^{app} for pH 7.5 without Ca^{2+} could not be determined, as even with 100 μM the observed rate constant did not level out; the information we could determine was k_{cat}^{app} >6 s^{-1}. Once again, the most notable difference was seen in the K_c^{app} where at pH 6.2 it is 36.0 ± 13.2 nM and at pH 7.5 could not be determined at all. The pH 6.2 without Ca^{2+} value is tenfold of the standard pH 7.5 with Ca^{2+}. Taking K_c^{app}, the concentration of CaM at half-maximal activity, as a reflection of

CaM binding to eEF-2K the data suggests that acidity promotes interaction where there would otherwise be none.

3.4.2. Mapping the pH dependence of eEF-2K activity

Data up to this point has supported the hypothesis that acidity promotes eEF-2K and CaM binding. To examine this in more detail we performed eEF-2K kinetic assays at 150 μM peptide, 1 μM CaM and excess EGTA (1 mM) to quench any free Ca^{2+} (Figure 3.3). For comparison we also evaluated the rate at pH 6.2 and pH 7.5 in the presence of saturating (50 μM) free Ca^{2+}. To stay within the buffer range limits, pH 5.8-6.6 were assayed in Bis-Tris and pH 6.8-7.5 were assayed in HEPES.

Here we report that in the absence of calcium the observed rate constant (k_{obs}^{app}) increases with an increasing H^+ concentration. This is evidenced by the slope of the plot of pH vs. k_{obs} where from pH 7.2 to pH 6.4 (the range where the effect by pH most changes) the slope is approximately 2 (Figure 3.3). In fact, a good fit through the data (green line) corresponds to a model whereby two protonations, corresponding to sites with pKa's of approximately 6.85 drive the proton-catalyzed reaction.

3.4.3 Bis-Tris does not significantly influence results in the absence of calcium

Because we use Bis-Tris for our buffer at low pH when normally eEF-2K assays are carried out in HEPES, we wanted to ensure that a change in buffer was not affecting our observations (Table 3.2). To test this we used 25 mM (assay concentration), 17 mM and 10 mM Bis-Tris with saturating peptide (150 μM pep-S), no Ca^{2+} and varying CaM

at pH 6.2 to observe any trend effects and, if possible, extrapolate the trend to zero buffer. The k_{max}^{obs} for 10, 17 and 25 mM respectively were: 25.8 ± 1.4, 26.7 ± 2.0 and 25.6 ± 3.0 s^{-1}. Which are consistent with no change. The K_{CaM}^{obs} values for 10, 17 and 25 mM Bis-Tris respectively were: 26.0 ± 4.8, 10.4 ± 3.8 and 36.0 ± 13.0 nM. Although the K_{CaM}^{obs} decreases for 17 mM, it does not appear to be due to concentration as it rises again from 10 to 25 mM. Since we did not see buffer effect here we also looked briefly at pH 6.8 at 10 mM and 25 mM Bis-Tris as a low and high buffer concentration to see if there was any difference. Overall, we did not observe any consistent trend by varying the concentration of Bis-Tris; 10 and 25 mM Bis-Tris values, respectively were: K_{CaM}^{obs} of 1.3 ± 0.4 µM and 1.4 ± 0.6 µM; k_{max}^{obs} of 27.3 ± 2.5 s^{-1} and 31.2 ± 3.1 s^{-1}.

3.6. CONCLUSION

Previous data (Chapter 2) revealed a novel mechanism where in the absence of Ca^{2+} ions, H^{+} ions were able to facilitate Thr-348 autophosphorylation of eEF-2K. Previous studies performed under standard conditions (pH 7.5) had reported Ca^{2+} to be necessary for eEF-2K activation, and calcium-independent activity was only observed after Ser-500 autophosphorylation, for which Thr-348 autophosphorylation was a prerequisite[36,53]. Our working hypothesis was that H^{+} ions have the potential to replace Ca^{2+} ions in altering the CaM conformation (as seen in the study by Villarroel et al.[143]) in order to promote binding to eEF-2K.

Here we report kinetics data that supports this hypothesis, but also provide data suggesting that H^{+} and Ca^{2+} ions augment each other's effect. These data are summarized

as the following points: 1) CaM-eEF-2K interaction is stronger at a lower pH in the presence of calcium as evidenced by K_{CaM}^{obs} whereas k_{cat}^{obs} (intrinsic activity/rate of substrate turnover) is not affected by pH. 2) We present a novel mechanism where H^+ ions can facilitate substrate phosphorylation of eEF-2K in compliment to calcium; H^+ ions promote CaM association in the presence of Ca^{2+} and maintain [a lower level of] activity and CaM association in its absence. That is, both Ca^{2+} and H^+ seem to increase the affinity of CaM to eEF-2K. 3) A qualitative assessment of how proton concentration affects k_{max}^{obs}, the increased activity caused by pH seems to be dependent on two protons.

With the activation and activity data gathered and described thus far, we have uncovered a compelling mechanism for calcium independent behavior of eEF-2K. This adds an additional layer to the many regulations of eEF-2K and may help us to understand how this versatile enzyme is able to respond to such a diverse array of cellular environments. Though we have demonstrated the positive effect of acidity on eEF-2K-CaM interaction, the underlying cause remains unclear. Further binding and mutagenesis studies will be critical for shedding light on this phenomenon.

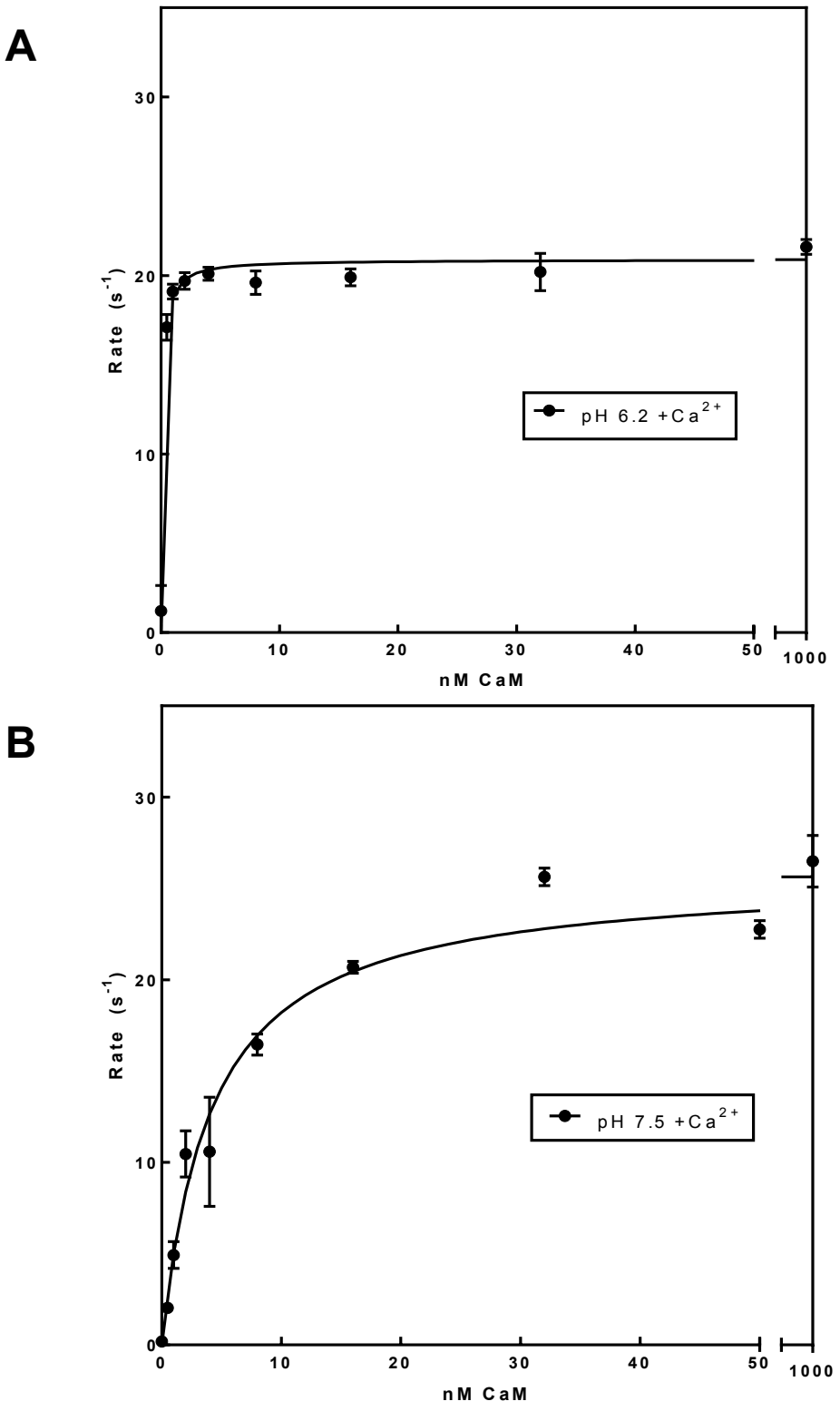

Figure 3.1. (See following page)

Figure 3.1 Examining the effect of low pH on eEF-2K activity in the presence of calcium.

2mM eEF-2K (untreated/not expressed with λ-phosphatase) was assayed at 30°C in Buffer 3A (25mM buffer, 2mM DTT, 10µg/mL BSA, 50mM KAcO, 10mM $MgCl_2$, 100µM EGTA, 150µM pep-S) +50µM free calcium (added as $CaCl_2$) in a final reaction volume of 100µL; varying concentrations (0-100µM) of CaM were used for dose response curves. Assays were initiated with 1mM [γ-^{32}P]ATP (100-1000cpm/pmol). HEPES was used for pH 7.5 (A) and Bis-Tris was used for pH 6.2 (B). Samples were quenched at various time points (1, 2, 3, 4, 6 and 8 min) by spotting 10µL reaction on P81 paper and immediately immersing in 0.1M phosphoric acid. Each data point was performed in duplicate. The pH of the remaining reaction was confirmed to be consistent with the assay start. The amount of labeled peptide associated with each paper was determined by measuring the counts per minute on a liquid scintillation counter. The rate for each CaM concentration was determined by finding the slope of phosphate incorporated over time; kinetic parameters were determined by plotting the rates of phosphorylation of eEF-2 peptide ($\mu M.s^{-1}$) against CaM concentration and fitting the curves to equation 3.1 (modified Michaelis-Menten). Calculated parameters are as follows: at pH 6.2 K_c^{app} = 0.004±0.01 (undeterminable due to assay limits, <0.5 nM) nM and k_{cat}^{app} = 20.9±0.7 s^{-1} and at pH 7.5 K_c^{app} = 3.6±0.6 nM and k_{cat}^{app} = 25.6 ± 0.6 s^{-1}. Between the two pH, the max rate (k_{cat}^{app}) did not significantly differ and the CaM K_m (K_c^{app}) were too low to accurately identify however it can be seen by the sharper curve that binding is tighter at pH 6.2.

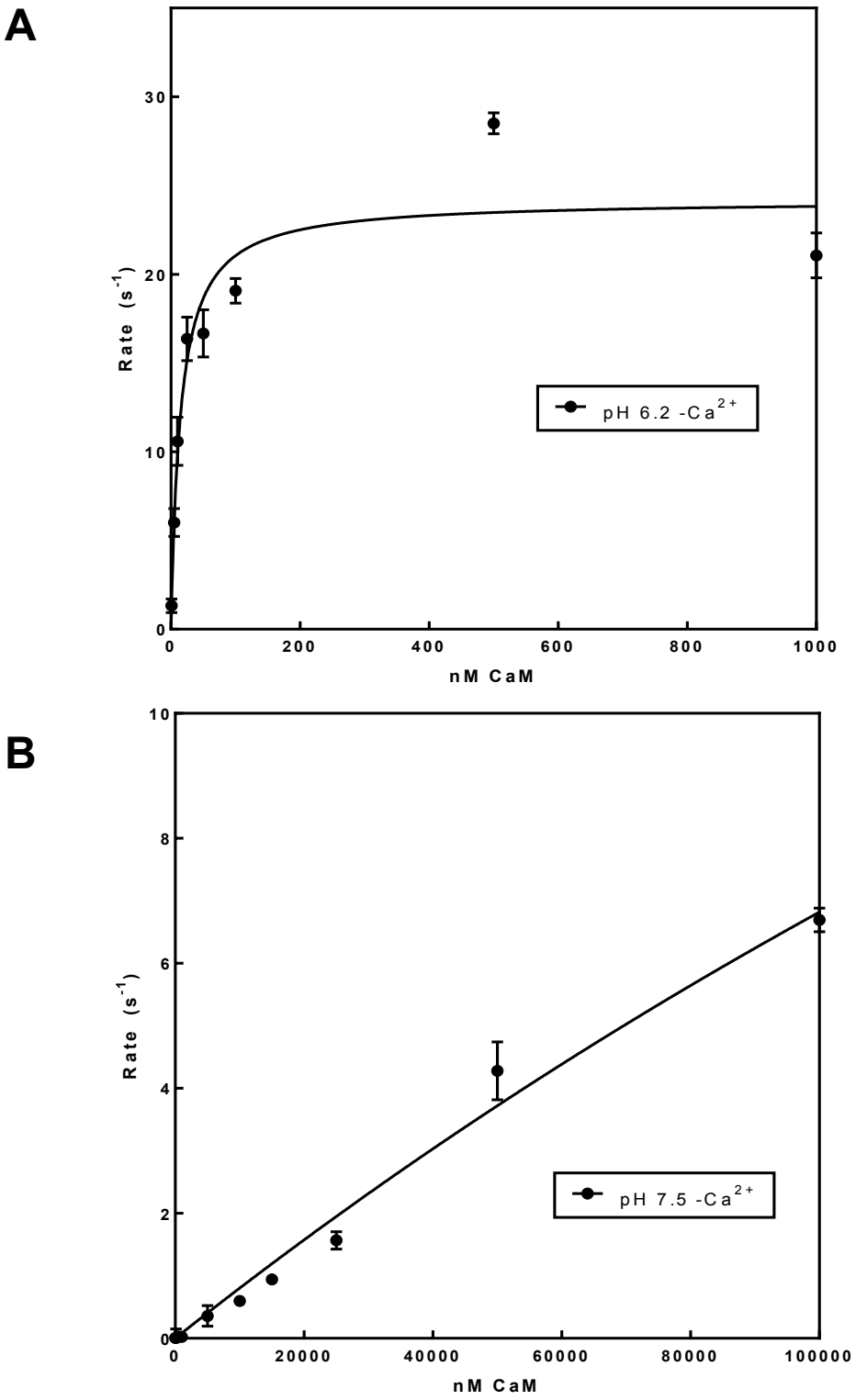

Figure 3.2. (See following page)

Figure 3.2. Examining the effect of low pH on eEF-2K activity in the absence of calcium.

2 nM eEF-2K (untreated/not expressed with λ-phosphatase) was assayed at 30°C in Buffer 3A (25 mM buffer, 2 mM DTT, 10 μg/mL BSA, 50 mM KAcO, 10 mM $MgCl_2$, 1 mM EGTA, 150 μM pep-S) in a final reaction volume of 100μL and initiated with 1mM [γ-^{32}P]ATP (100-1000cpm/pmol). HEPES was used for pH 7.5 and Bis-Tris was used for pH 6.2. Samples were quenched at various time points (1, 2, 3, 4, 6 and 8 min) by spotting 10μL reaction on P81 paper and immediately immersing in 0.1M phosphoric acid. The pH of the remaining reaction was confirmed to be consistent with the assay start. The amount of labeled peptide associated with each paper was determined by measuring the counts per minute on a liquid scintillation counter. The rate for each CaM concentration was determined by finding the slope of phosphate incorporated over time; kinetic parameters were determined by plotting the rates of phosphorylation of eEF-2 peptide ($\mu M.s^{-1}$) against CaM concentration and fitting the curves to equation 3.2 (modified quadratic equation). Kinetic parameters were calculated to be: at pH 6.2 K_c^{app} = 36.0 ± 13.2 nM and k_{cat}^{app} = 25.6 ± 3.0 s^{-1} and at pH 7.5 K_c^{app} was undeterminable because the rate never reached a saturating or maximal limit, even at 100μM CaM (standard assays use 2μM for saturating CaM. This data supports the hypothesis that eEF-2K and CaM interact differently at low pH, and that H^+ may take the place of Ca^{2+} in terms of stabilizing this interaction.

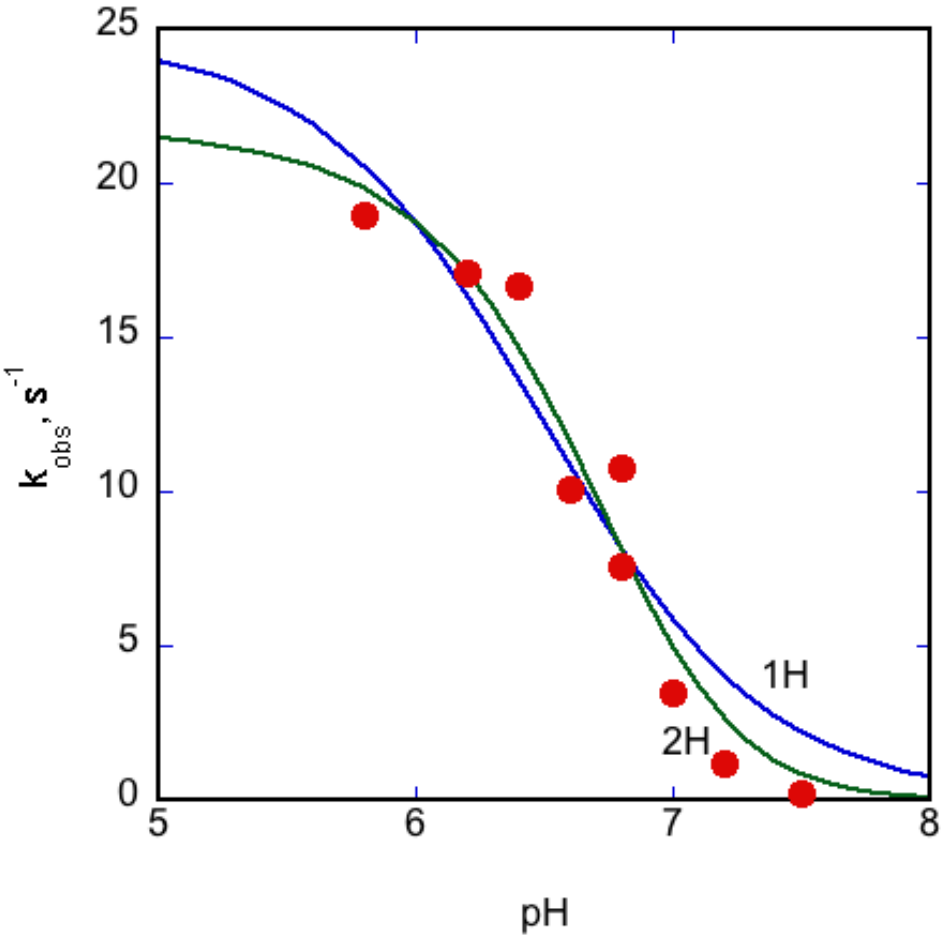

Figure 3.3. Mapping the pH dependence of eEF-2K activity.

To determine the continuance of observed effects across the pH range, general kinetic assays were performed: 2 nM eEF-2K (untreated/not expressed with λ-phosphatase) was assayed at 30°C in Buffer 3A (25 mM buffer, 2 mM DTT, 10 µg/mL BSA, 50 mM KAcO, 10 mM MgCl2, 100 µM EGTA, 150 µM pep-S), 1 µM CaM and either 50 µM free calcium (added as $CaCl_2$) or a total of 1 mM EGTA in a final reaction volume of 100µL and were initiated with 1mM [γ-^{32}P]ATP (100-1000cpm/pmol). Changes in free calcium concentration over varied pH were accounted for using Stanford University's maxchelator calculator. HEPES was used for pH conditions above pH 6.8 and Bis-Tris

was used for assays pH 6.8 and below. Samples were quenched at various time points (1-8min) by spotting 10μL reaction on P81 paper and immediately immersing in 0.1M phosphoric acid. The pH of the remaining reaction was confirmed to be consistent with the assay start. The amount of labeled peptide associated with each paper was determined by measuring the counts per minute on a liquid scintillation counter. The rate for each pH was determined by finding the slope of phosphate incorporated over time. The best fit through the data (green line, k_1 = 21.8 s^{-1}, K_a = 1.4 x 10^{-7} M) was obtained by fitting the data to $k_{obs} = (k_1H^2)/(H^2+K_aH+K_a^2)$, where k_1 is the observed rate constant for the CaM•eEF2K complex at low pH, H is the concentration of protons, and K_a is the pK_a of each of two protonated residues within the CaM•eEF2K complex. The alternative fit through the data (blue line, k_1 = 24.7 s^{-1}, K_a = 3.2 x 10^{-7} M) corresponded to $k_{obs} = (k_1H)/(H+K_a)$, where it is assumed that only one protonated species contributes to the observed reaction at low pH.

Table 3.1 A summary of various kinetic parameters for eEF-2K under a CaM dose dependence curve.

	pH 6.2		pH 7.5	
	-Ca^{2+}	**+ Ca^{2+}**	**-Ca^{2+}**	**+ Ca^{2+}**
k_{cat}^{app} **(s^{-1})**	25.6±3.0	20.9±0.7	>6	25.6±0.6
K_c^{app} **(nM)**	36.0±13.2	<0.5	n/a	3.6±0.6

This table depicts the kinetic parameters as defined in Figures 3.1 and 3.2. General kinetic assays used 2 nM eEF-2K, 1 mM ATP, 150 μM peptide substrate ± 50 μM free $Ca2^{+}$ with 10 concentrations of varying CaM in reaction buffer (HEPES for pH 7.5 and Bis-Tris for pH 6.2). Parameters in the presence of calcium were fit with equation 3.1 and parameters in the absence of calcium were fit to equation 3.2. pH 6.2 K_c^{app} in the presence of calcium could not be determined beyond lower than the lowest feasible concentration of CaM used. pH 7.5 K_c^{app} in the absence of calcium could not be determined because the rate did not reach a saturating/maximal limit.

Table 3.2. Bis-Tris concentration does not affect kinetic parameters for eEF-2K under a CaM dose dependence curve in the absence of Ca^{2+}.

	[Bis-Tris]:	10 mM	17 mM	25 mM
pH 6.2	k_{max}^{app}(s^{-1})	25.8 ± 1.4	26.7 ± 2.0	25.6±3.0
	K_{CaM}^{app}(nM)	26.0 ± 4.8	10.4 ± 3.4	36.0±13.2
pH 6.8	k_{max}^{app}(s^{-1})	27.3 ± 2.5		27.4 ± 5.8
	K_{CaM}^{app}(μM)	1.3 ± 0.4		1.4 ± 0.6

To determine whether Bis-Tris concentration affects experimental results, general kinetic assays were performed using 2 nM eEF-2K, 1 mM ATP, 150 μM peptide substrate, 1 mM EGTA and no $Ca2^{+}$ with varying CaM in reaction buffer (concentration of Bis-Tris as shown). Assays were initiated with 1mM [γ-^{32}P]ATP (100-1000cpm/pmol). Samples were quenched at various time points (1-8min) by spotting 10μL reaction on P81 paper and immediately immersing in 0.1M phosphoric acid. The pH of the remaining reaction was confirmed to be consistent with the assay start. The amount of labeled peptide associated with each paper was determined by measuring the counts per minute on a liquid scintillation counter. The rate for each pH was determined by finding the slope of phosphate incorporated over time. Each rate value was plotted against its CaM concentration and data were fit to Eqn 3.1. to calculate values shown in the table. Data suggests that Bis-Tris does not affect experimental results.

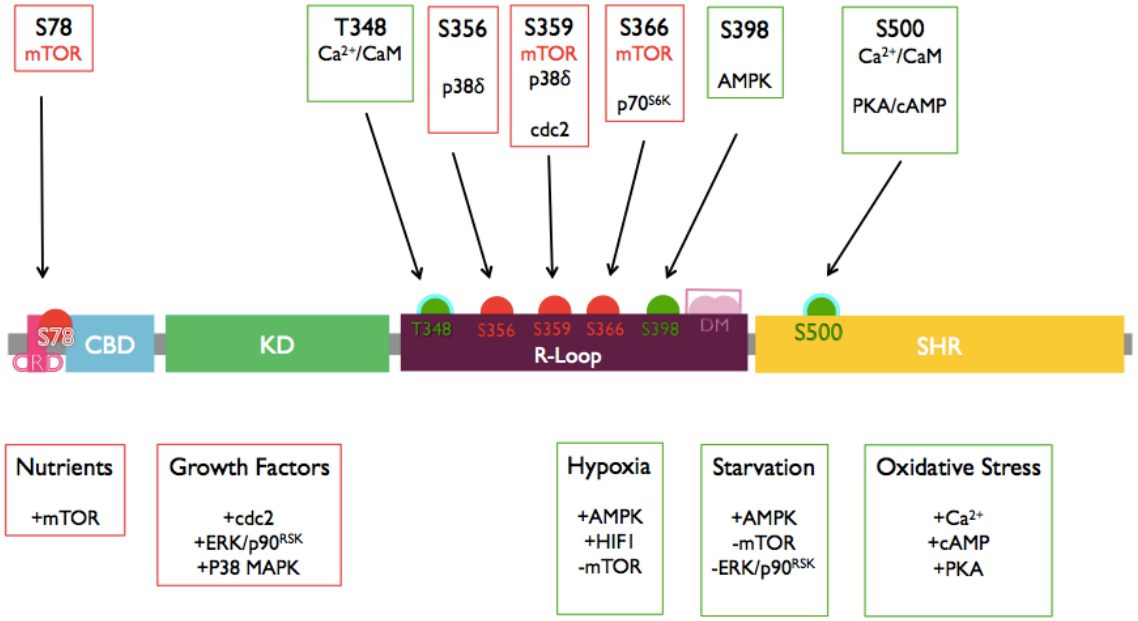

Scheme 3.1. Regulation of eEF-2K activity by multisite phosphorylation.

Between CaM/Ca^{2+} control and the various possible phosphorylation states (colored circles; green for activating and red for inhibiting) it is clear that there are many layers to eEF-2K regulation that allow the complex integration of cellular signals. Current studies suggest that CaM binding acts as an on/off binary switch while the phosphorylation sites act in combination as a volume dial, determining the level of activity[54]. Of the phosphorylation sites discussed here, T348 and S500 are autophosphorylated upon Ca^{2+}/CaM stimulation (light blue outline)[135], S398 is phosphorylated by AMPK under energy stress[90], and S500 can be additionally phosphorylated by cAMP-dependent protein kinase (PKA)[138]; these three sites are activating. On the other hand, mTOR via downstream kinases phosphorylates the three inhibitory sites: S78 which is thought to affect CaM binding[95], S359 which is specifically influenced by cdc2-cyclin B[59] and p38δ[160], and S366 which is influenced by p70 S6 kinase as well as Erk-activated $p90^{RSK1}$

[95]. It is not clear what prompts the diphosphorylation site in the degron motif (DM), but it is hypothesized to be the T348 and S500 autophosphorylations[151]. Studies have also made progress into detailing the mechanisms by which these sites exert control over eEF-2K activity, especially in regards to T348 and S500. CaM/Ca^{2+} has been shown to increase the ability of eEF-2K to autophosphorylate T348, which can then bind to a basic allosteric binding pocket that is likely to cause a conformational change in the R-loop that allows for enhanced efficiency to phosphorylate substrate[54,135]. Additionally, phosphorylation of S500 has been implicated in imparting Ca^{2+} independent activity of eEF-2K[53] and because S500 can also be phosphorylated by PKA, under cellular conditions of elevated cAMP it could help maintain significant translational pause without calcium signaling[138]. In summary, there are many complex layers of eEF-2K regulation, some yet to be unraveled, to be considered when studying mechanism.

Chapter 4: Role of Acidity in the Interaction between Calmodulin and Eukaryotic Elongation Factor 2 Kinase

4.1. ABSTRACT

Eukaryotic elongation factor 2 kinase (eEF-2K) is an enzyme whose activity results in global downregulation of protein synthesis, making it a key enzyme in cell cycle and energy regulation. The initial activation of eEF-2K requires calmodulin (CaM), which typically has two calcium (Ca^{2+}) ions when it binds eEF-2K. The binding of CaM to eEF-2K allows for the activating autophosphorylation of Thr-348. eEF-2K has one known substrate: eukaryotic elongation factor 2, which is inactivated by eEF-2K and is responsible for moving tRNA molecules and growing polypeptide chains through the ribosome. The inactivating phosphorylation of eEF-2 on Thr-56 by eEF-2K also requires CaM. While CaM is necessary for both activation and substrate phosphorylation, studies have shown that Ca^{2+} is not; either will occur without calcium albeit very slowly. Furthermore, phosphorylation of Ser-500 on eEF-2K has been shown to cause calcium independent activation and activity comparable to standard/saturating conditions. Our data (chapters 2 & 3) were the first to demonstrate calcium-independent activation and substrate phosphorylation outside of a post-translational modification; an effect observed under acidic conditions. We also observed a tighter interaction between eEF-2K and CaM at low pH in the presence of calcium; all of our data up to this point cumulates to the hypothesis that H^+ ions can replace Ca^{2+} ions in altering CaM conformation, resulting in tighter binding to eEF-2K. In this chapter we continue to explore the nature of the effect

of pH on eEF-2K and provide lifetime fluorescence binding data that supports this hypothesis.

4.2. INTRODUCTION

Eukaryotic elongation factor 2 (eEF-2) is responsible for moving the tRNA and growing polypeptide chain from the A site to the P site in the ribosome. eEF-2 is the only known substrate of eukaryotic elongation factor 2 kinase (eEF-2K) which phosphorylates eEF-2K on Thr-56, impeding its ability to bind the ribosome[34,64,167,187]. eEF-2K activity therefore has a direct correlation to global downregulation of protein synthesis. Upon its initial discovery, eEF-2K was known as Ca^{2+}/CaM-dependent protein kinase III (CaMK-III), as the study reported it requiring both Ca^{2+} and CaM to be active, though studies have since then demonstrated calcium independent activity[20,34–36]. While there is a Ca^{2+}/CaM-dependent kinase (CAMK) family of protein kinases, eEF-2K is actually classified as an alpha protein kinase, the only CaM/Ca^{2+} dependent kinase in this family. The alpha protein kinase family is a subset of atypical protein kinases (APK) which represent the 10% of protein kinases that lack of sequence homology to the 90% of conventional protein kinases[16,17,39]. Alpha kinases are unique to eukaryotes as they appeared relatively recently in evolution. Subfamilies of alpha kinases have very different domain structures, but share a catalytic domain homology to the myosin heavy chain kinases (MHCK)[16,17,42]. Many, but not all, of the alpha kinases target substrate residues within an alpha-helix conformation which is how the family got its name[43,44].

A crystal structure for eEF-2K has not successfully been defined, likely due to the flexible regulatory loop located in the middle of the protein. A cumulation of many studies over the decades has allowed us to compile a working model for the domain structure and organization of eEF-2K (Scheme 4.1)[30,33,48,54,57,58,188]. Starting at the N-terminus, there is a DXDXDG motif that is a potential Ca^{2+} binding domain (CRD) whose role is currently unknown[49], followed by the Ser-78 phosphorylation site and a calmodulin (CaM) binding domain (CBD) that is critical for activation and the atypical α-kinase catalytic kinase domain (KD). C-terminal to the KD is a regulatory loop (R-loop) that carries four of the main regulatory phosphorylation sites (Thr-348, Ser-359, Ser-366, and Ser-398) and a ^{440}DSGXXS^{445} degron motif (DM). Autophosphorylation of Thr-348 and its subsequent binding to a conserved binding pocket in the kinase domain is a prerequisite for kinase activity[54,57]. The degron motif involved in recognition by the $SCF^{\beta TrCP}$ ubiquitin ligase and ensuing degradation of eEF-2K. Activation of eEF-2K and subsequent diphosphorylation of the serine residues in the DM provide an efficient and precise control for translational depression and rapid resumption[54–56]. Proceeding the DM is the Ser-500 phosphorylation site and finally at the C-terminus there are three helical SEL1-type domains (SHR) and a C-terminal tail that interact with the KD and are necessary for substrate phosphorylation, but not intrinsic activity. This implicates a role in protein-protein interactions, although it has been suggested that the extreme C-terminal domain of eEF-2K is not a primary eEF-2 docking site on its own[33,58].

The many phosphorylation sites mentioned above provide a flexible and multi-input method for the cell to fine-tune eEF-2K activity. The first step for regulating eEF-

2K, as mentioned above, is the binding of CaM/Ca^{2+} that allows for autophosphorylation of Thr-348 and activation of the enzyme[54,135]. CaM is also required for substrate phosphorylation[54], and so studying the nature of the interaction between CaM and eEF-2K can give us insight into understanding the nature of regulation on eEF-2K by CaM. A recent study on the mechanism by which CaM affects eEF-2K employed a number of methods, including mass spectrometry, small angle x-ray scattering, NMR and computational modeling, to gain insight to eEF-2K conformation and binding to CaM. Other CaM regulated kinases operate on a release-of-inhibition mode of activation upon CaM binding where this event causes a the rearrangement of a substrate-like-moiety away from the substrate recognition site[53,139,140]. This is not the case for eEF-2K; the study demonstrated that in each step of CaM binding, i.e. during activation and substrate phosphorylation, there is a favorable change in conformation, allowing for either autophosphorylation or substrate interaction[139]. That is, eEF-2K is rearranged to result in a form with an increased intrinsic activity/ability to phosphorylate, rather than an increase in ability to bind a substrate[53].

Structural details of the CaM-eEF-2K binding interaction have been reported, but it is first important to understand some details of the CaM structure. CaM is a well-studied calcium modulated protein and at 148 amino acids, it is one of the smaller proteins. CaM is composed of two globular domains connected by a flexible linker, where each globular domain has two "hands" which can bind Ca^{2+} ions; CaM can bind a total of four Ca^{2+} ions[189,190]. This allows CaM to be versatile in its calcium sensitivity as its conformation, along with its affinity for other proteins, changes and adapts with each

ion it binds[142]. Interestingly, even in high calcium concentrations CaM binds eEF-2K with only two Ca^{2+} ions bound in the N-terminus. It is the C-terminus of CaM that binds the calmodulin-binding domain (CBD) of eEF-2K - the conserved W85 residue on eEF-2K inserts deep into a hydrophobic cavity on CaM. Meanwhile the Ca^{2+}-loaded N-terminus of CaM forms sparse and weak interactions elsewhere on the enzyme[126,141,142]. Furthermore, a study of the effect of acidity on the conformation of CaM demonstrated that H^+ ions have the capability of promoting a similar conformational change in CaM similar to Ca^{2+} binding[142,143].

While CaM is always required for eEF-2K activation and substrate phosphorylation, these events will still occur under standard saturating conditions, though it is on the timescale of minutes to hours instead of seconds[54]. Phosphorylation of Ser-500 imparts further Ca^{2+}-independent activity of eEF-2K[53] where autophosphorylation and substrate phosphorylation rates are comparable to standard saturating conditions. Ser-500 can also be phosphorylated by PKA, under cellular conditions of elevated cAMP it could help maintain significant translational pause without calcium signaling[138]. Our data (chapters 2-3) have shown a novel mechanism for a calcium-independent mechanism of eEF-2K via acidic conditions, which would provide an additional layer of physiological regulation to help explain the *in vivo* functions of eEF-2K. Our hypothesis and working model suggests that protons supplement Ca^{2+} in favorably altering CaM concentration to bind eEF-2K. Our data examining autophosphorylation and substrate phosphorylation at low pH support this model however we have not directly tested CaM binding. Our previous experiments that look at phosphorylation did not have the resolution to separate

the CaM binding and phosphorylation steps (Figure 4.2). By looking at binding directly we will gain direct insight into the interaction of CaM and eEF-2K at low pH. In the current study we report that in the absence of calcium, eEF-2K is only able to bind CaM at low pH. This supports a model where H^+ ions supplement Ca^{2+} ions in causing a conformational change in CaM that is favorable to binding eEF-2K.

4.3. MATERIALS AND METHODS

4.3.1. Reagents, Strains, Plasmids and Equipment

Yeast extract, tryptone and agar were purchased from USB Corporation (Cleveland, OH). Isopropyl β-D-1-thiogalactopyranoside (IPTG) and dithiothreitol (DTT) were purchased from US Biological (Swampscott, MA). From Qiagen (Valencia, CA) Ni-NTA Agarose, QIAprep Spin Miniprep Kit, QIAquick PCR Purification Kit and QIAquick Gel Extraction Kit were purchased. Lambda Protein Phosphatase was from New England BioLabs (Ipswich, MA). BenchMark™ Protein Ladder was from Invitrogen Corporation. SIGMA*FAST*™ Protease inhibitor cocktail tablets for purification of His-tagged proteins, ultra-pure grade Tris-HCl, HEPES and calmodulin were from Sigma-Aldrich (St. Louis, MO). All other buffer components or chemicals were purchased from either Sigma-Aldrich or Fischer Scientific (Pittsburgh, PA). Amicon Ultrafiltration Stirred Cells, Ultracel Amicon Ultrafiltration Discs and Amicon Ultra Centrifugal Filter Units were from Millipore (Billerica, MA). MP Biomedicals (Solon, OH) supplied [γ-^{32}P]ATP.

Escherichia coli strain DH5α – for cloning – was obtained from Invitrogen Corporation, and BL21(DE3) and Rosetta-gami™ 2(DE3) – for recombinant protein expression – were from Novagen, EMD4Biosciences (Gibbstown, NJ). The pET-32α vector was obtained from Novagen.

The ÄKTA FPLC™ System, the HiPrep™ 26/60 Sephacryl™ S-200 HR gel filtration column and the HiLoad™ 16/60 Superdex™ 200 prep grade gel filtration column were from Amersham Biosciences / GE Healthcare Life Sciences (Piscataway, NJ). Absorbance readings were performed on a Cary 50 UV-Vis spectrophotometer. Proteins were resolved by Tris-glycine sodium dodecyl sulfate polyacrylamide gel electrophoresis (SDS-PAGE), under denaturing conditions on 10% gels, using the Mini-PROTEAN 3 vertical gel electrophoresis apparatus from Bio-Rad Laboratories (Hercules, CA). A Techne Genius Thermal Cycler purchased from Techne, Inc. (Burlington, NJ) was used for PCR.

4.3.2. Molecular Biology

p32TeEF-2K. The modified pET-32α vector (p32TeEF-2K) containing cDNA encoding human eEF-2K (GenBank entry NM_013302) was used for the expression of Trx-His6-tagged eEF-2K. This expression vector was originally chosen because of the thioredoxin tag (Trx-tag) for increased protein solubility and the hexa-histidine tag (His_6-tag) for nickel affinity chromatography purification. There was also an enterokinase protease recognition sequence site (DDDDK) that allows for cleavage of the tags, however this site had been modified to a Tobacco Etch Virus (TEV) protease recognition

sequence site (ENLYFQGDI). The vector was modified by the previous graduate student Clint Tavares[31] using site directed mutagenesis between the *Kpn*I (underlined) and *Eco*RV (italicized) recognition sites (Figure 2.1.A). Additional plasmid DNA was obtained by transforming the modified construct into DH5α cells and purifying the DNA using the Qiagen QIAprep Miniprep Kit. The sequence then verified by sequencing at the ICMB Core Facilities, UT Austin, using an Applied Biosystems automated DNA sequencer.

4.3.3. Expression and Purification of Proteins

Expression and Purification of wild type eEF-2K. Recombinant human eEF-2K was expressed in the *E. coli* strain Rosetta-gami™ 2(DE3) (Novagen) using the p32TeEF-2K expression vector. The Rosetta-gami™ 2(DE3) cells were chosen because they carry the pRARE2 plasmid which supplies tRNAs for seven rare codons. eEF-2K contains 63 rare codons, an 8.7% of its 725 residues, so the aim with selecting these expression cells was to promote healthy and successful expression. Expression and purification were performed as described in Chapter 2.3 Materials and Methods of this dissertation.

Expression and purification of TEV protease. Tobacco Etch Virus protease was expressed from the pRK793 expression vector (gifted by Dr. John Tesmer, Life Sciences Institute, University of Michigan, Ann Arbor, MI). The construct was transformed into Rosetta-gami™ 2(DE3) cells, protein expression was induced with 0.5 mM IPTG at 28 °C and the culture was incubated for 4h. The bacterial culture was centrifuged and the cells were harvested and purified according to protocols published earlier[170,171].

Expression and purification of calmodulin. The calmodulin (CaM) clone in the pET-23 expression vector was gift by Dr. Neal Waxham (Department of Neurobiology and Anatomy, University of Texas Medical School at Houston, Houston, TX). The construct was transformed into BL21(DE3) cells (Novagen). Expression and purification were carried out as described in Chapter 2.3 Materials and Methods of this dissertation. These methods were adapted from previous protocols[172,173].

4.3.4. Analytical Methods

Analysis of calmodulin binding by fluorescence. eEF-2K was assayed at 27°C in Buffer 4.A (25mM buffer, 2mM DTT, 10µg/mL BSA, 50mM KCl, 100µM EGTA, 0.1µM $CaM(C75)_{IAE}$ (labeled using a protocol as previously described[144]) ±50µM free calcium (added as $CaCl_2$, calculated as previously described) in a final reaction volume of 500µL. Buffer 4.A was incubated at 27°C for 5min and $CaM(C75)_{IAE}$ was excited at 345 nm before an emission spectrum was taken. The emission spectrum was used to optimize the wavelength for measuring the fluorescence lifetime.

For a dose response binding curve: eEF-2K (unphosphorylated; co-expressed with λ-phosphatase) was titrated in incrementally (ranged from 0.5nM-4µM). Either HEPES or Bis-Tris buffers were used as previously described and the pH was confirmed and adjusted periodically through the titrations.

For pH dependence: 1µM eEF-2K was added to Buffer 4.A (with Bis-Tris) at pH6.8 and HCl was titrated in to reduce the pH 0.2 units per measurement.

In both experiments the lifetime fluorescence spectrum was taken after each titration. The emission spectrum was taken periodically to account for fluctuations and the lifetime measurements were adjusted accordingly (average range 470-480nm). All fluorescent measurements were taken with a lifetime fluorometer (Horiba Scientific, Kyoto, Japan).

Data Fitting. We used the time-correlated single photon counting (TCSPC) lifetime fluorescence technique which is particularly useful for short-term decays, as we would expect for binding. This by nature requires the data to be digitally processed as it is received by the fluorescence machine, and to complete the analysis we used the PTI FelixGX program, developed by Horiba Scientific and integrated into the data collection process. To determine the number of lifetimes (distinct steps/enzyme species) in CaM/eEF-2K binding, we looked at the population of species (defined by different intensities) separated into their corresponding time bins (how long each species spends in an excited state before emitting a photon) with saturating CaM and eEF-2K (100nM CaM with 1μM eEF-2K at pH 7.5). We observed two distinct species and so to fit our lifetime binding data we used two lifetime parameters, a double exponential equation (Eqn 4.1)

$$I(t) = \alpha_1 \times e^{-t/\tau_1} + \alpha_2 \times e^{-t/\tau_2} \qquad \text{(Equation 4.1)}$$

Where I(t) describes the decay of the fluorophore from the excited state to ground state; α describes the fraction of bound species; t describes elapsed time; and τ describes the lifetime, typically in seconds.

The fraction of bound species (α) was plotted against concentration of enzyme and data were fit to equation 4.2:

$$\alpha(t) = F + dF\frac{([C] + [X] + K_D^{app}) - \sqrt{\left([C] + [X] + K_D^{app}\right) - 4[X][C]}}{2[X]} \quad \text{(Equation 4.2)}$$

where α(t) describes the fraction of bound species over time; F is a correction factor defined by the lowest α value; dF is a correction factor defined by the ratio of $\alpha_{max} - \alpha_{min}$ / $[X]_{max}$-$[X]_{min}$; [C] is concentration of CaM; [X] is concentration of variable addition (usually eEF-2K or $[H^+]$ in the case of varied pH); and K_D^{app} is the apparent concentration of the variable at half max bound species.

4.4. Results & Discussion

4.4.1. Acidity Rescues Binding in the Absence of Calcium

We have previously shown (Chapters 2-3) with unphosphorylated enzyme that H^+ promotes autophosphorylation in the absence of calcium and with Thr-348-phosphorphorylated (pre-activated) eEF-2K that H^+ promotes substrate phosphorylation in the absence of calcium. CaM binding is a pre-requisite for both of these steps. In the assays used to study these steps CaM and eEF-2K were incubated before the addition of ATP to initiate the phosphorylation reaction. The autophosphorylation assays we performed did not have the resolution to differentiate between the effect of pH on CaM binding vs. intrinsic enzyme activity (Scheme 4.2). However, the substrate phosphorylation assay does suggest that the increased activity at low pH is derived from

increased binding of CaM. These experiments were useful to establish an effect by pH and led to our hypothesis that H^+ ions supplements Ca^{2+} ions in favorably altering the conformation of CaM for eEF-2K binding. Here we use a fluorescent assay to study directly the effect of pH on CaM binding to eEF-2K in the absence of calcium.

First we wanted to address whether H^+ ions were capable of promoting CaM binding in the absence of calcium, so we used a fluorescence lifetime assay to compare binding at high and low pH. Fluorescence lifetime measures the amount of time a fluorophore spends in an excited state before emitting a photon and returning to the ground state; this technique has an advantage over other fluorescence techniques as it an absolute measurement and does not rely on fluorescence intensity[191]. In the assays we used 100 nM i-CaM in reaction buffer (Buffer 4.A), incubated this at 27°C in a 500µL quartz cuvette and unphosphorylated eEF-2K was titrated in from 0-1000nM. We used unphosphorylated eEF-2K (co-expressed with lambda phosphatase) so that we could ensure we were looking at the first CaM binding step in isolation. All assays were performed in the absence of calcium and 10mM EGTA. Emission spectra were taken periodically to optimize the wavelength for the lifetime spectra, as addition of eEF-2K alters emission wavelengths by nm amounts (range of 475-485nM from 0-1000nM eEF-2K). The lifetime curves of the varying eEF-2K concentrations were fit to a double exponential equation (Eqn. 4.1, see Materials and Methods) for the two observed lifetimes, whose relative amplitude change upon eEF-2K binding. This equation starts off with four variables (two per lifetime); to increase accuracy of fitting, both *T* values (representing the time spent in a lifetime) were locked because theoretically *T* values

should not change and the lifetime spectra is a blend of the two α values. The values of α_1 and α_2 (for unbound CaM) were calculated by averaging the fitting of the lifetime fluorescence with just CaM and buffer (no enzyme) to a double exponential where T_1 = 1.5s and T_2 = 15.6s. The values of α_1 and α_2 for bound CaM was calculated by fitting a double exponential equation to the observed lifetime spectra in the presence of 5μM enzyme using T_1 = 1.5s and T_2 = 15.6s. To calculate the fraction of binding the value of α_1 and α_2 are compared to those at zero and complete binding.

In Figure 4.1 we can see at pH 6.2 binding is saturated with the addition of 900nM eEF-2K whereas at pH 7.5 there is no change in lifetime fluorescence from 0-1.5μM. For pH 6.2, % bound CaM was plotted against eEF-2K concentration and data were fit to a quadratic equation (Eqn. 4.2, see Materials and Methods) to examine the eEF-2K dependence of i-CaM binding. Here we can see that for pH 6.2, eEF-2K is half bound at 130 ± 22nM.

4.4.3. Ability of Mg^{2+} to replace Ca^{2+} in CaM binding

Calmodulin has four so-called EF-hand structural motifs, which are common helix-loop-helix structures found in proteins that need to bind Ca^{2+}. Under resting cellular conditions magnesium (Mg^{2+}), a chemically similar divalent ion to Ca^{2+}, can exist in 1000x excess to Ca^{2+}. In order to be a competent calcium signaling protein, CaM must be able to distinguish between Mg^{2+} and Ca^{2+}[192,193]. While it has been shown that Mg^{2+} is likely too small to engage and bind EF-hands similarly to calcium, there have also been reports of Mg^{2+} associating with both the two N-terminal (I & II) and the two C-terminal

(III & IV) EF-hands of CaM. Some reports show Mg^{2+} being unable to bind EF-hands (EF-hand III), some show that Mg^{2+} binds and induces a local conformational change (EF-hand IV), and others show that Mg^{2+} binds (EF-hands I & II) in a way that stabilizes the apo-form of CaM[192,194,195]. The exact mechanism of when and how Mg^{2+} affects CaM is not fully understood, our concern remained that Mg^{2+} is used as a stabilizing component for ATP in our assays. Reports show that Ca^{2+} has a much higher affinity for CaM than Mg^{2+} but as we are primarily looking at the effect of H^{+} on eEF-2K in the absence of Ca^{2+}, we wanted to verify that our observed effects are independent of Mg^{2+}. To do this all assays were performed in the absence of Ca^{2+} using 100 nM $CaM(C75)_{IAE}$ (i-CaM) in reaction buffer (Buffer 4.A) with 1mM Mg^{2+}; the reaction was incubated at 27°C in a 500µL quartz cuvette.

For determination of % CaM bound (Figure 4.2.A)*:* unphosphorylated/inactive eEF-2K was titrated in from 0-1000nM. Emission spectra were taken periodically to optimize the wavelength for the lifetime spectra as addition of eEF-2K alters emission wavelengths by nm amounts (range of 475-485nM from 0-1000nM eEF-2K). The lifetime curves were fit to a double exponential equation (Eqn. 4.1, see Materials and Methods) for the two lifetimes to calculate % bound CaM. Additional controls were performed (not shown) where a total of 10mM magnesium was added (no additional effect) and where magnesium was added after binding was saturated with eEF-2K (no additional effect). Our data shows that magnesium did not enhance eEF-2K and i-CaM binding.

For determination of eEF-2K dependence of CaM binding (Figure 4.2.B): % bound CaM were plotted against eEF-2K concentration and data were fit to a quadratic equation (Eqn. 4.2, see Materials and Methods) to examine the eEF-2K dependence of CaM binding. The concentration of half bound eEF-2K (K_d^{eEF-2K}) was similar for high pH (142.5 ± 53.7nM without Mg^{2+} and 111.3 ± 54.2nM with Mg^{2+}) but had a nearly two-fold difference under low pH (130.3 ± 21.8nM without Mg^{2+} and 236.4 ± 16.9 nM with Mg^{2+}). This suggests that Mg^{2+} may compete slightly with H^+ to disturb the binding equilibrium.

4.4.4. H^+ Dependence of CaM Binding in the Absence of Calcium

Our binding data up to this point has supported the model for H^+ to promote Ca^{2+}-independent CaM binding to eEF-2K. In order to study the nature of the effect of acidity on binding, we performed a pH dependence curve. This can provide information on the dependence of binding on the concentrations of H^+ ions. To do this we used 100 nM $CaM(C75)_{IAE}$ (i-CaM) and 1μM eEF-2K in reaction buffer (Buffer 4.A) incubated at 27°C in a 500μL quartz cuvette. All assays were performed in the absence of calcium and pH was titrated downwards using HCl; the pH was verified after each titration. This occurred in two steps to accommodate buffer limits; HEPES was used from pH 7.5-7.0 and Bis-Tris was used from 6.8-5.8. Emission spectra were taken periodically to optimize the wavelength for the lifetime spectra to check whether addition of acid alters emission wavelengths by nm amounts (range of 83-485nM from pH 5.8-7.5 was used). We performed several controls (not shown) where we started with titrating in eEF-2K before

titrating down in pH (no additional effect), where we added in excess eEF-2K after titrating down in pH and reaching saturation of H^+ (no additional effect). The lifetime curves were fit to a double exponential equation (Eqn. 4.1, see Materials and Methods) for the two lifetimes to get the % bound CaM. % bound CaM values were then plotted against pH. Here we see that binding increases as pH decreases and saturation occurs at pH 6.2 and from pH 6.5 to pH 7.5 is roughly a slope of 2 over a ten-fold change in H^+ concentration, indicating the involvement of 2 protons in this process.

4.5. CONCLUSION

Due to the high-energy demand of translation, regulation of protein synthesis is a central part of maintaining cellular homeostasis. One such method for inhibiting translation is the phosphorylation of eEF-2 by eEF-2K, which prevents the movement of tRNA molecules through the ribosome[76,167]. eEF-2K in turn has many regulatory inputs that it must integrate into its overall activity; Ca^{2+}, CaM, upstream kinases and pH have a combination of activating and inhibiting effects on the enzyme. eEF-2K has been shown to be important under various physiological circumstances such as during the cell cycle, during cell stress, and during various neuronal processes[59,93,115,196,197]. It has also been implicated in various diseases including several types of cancer, Alzheimer's and depression[71,111,123,198,199]. eEF-2K has also seemingly paradoxically been reported to promote the translation of select transcripts, and the mechanism behind this remains undefined[174,200]. Understanding the nature of the effect these inputs have on eEF-2K is crucial for understanding how this enzyme functions.

Previous data (chapters 2-3) demonstrated that H^+ are capable of replacing Ca^{2+} in promoting the autophosphorylation and substrate phosphorylation; each are steps that require CaM binding[54]. This was reflected in: 1) The faster rate of autophosphorylation at low pH in the absence of calcium. 2) The rescued activity (k_{max}^{app} = 25.6 ± 3.0 s^{-1}) and affinity (K_{CaM}^{app} = 36.6±13.2nM) at pH 6.2 in the absence of calcium (pH 7.5 kinetic parameters could not be determined as rate of substrate phosphorylation failed to reach saturation even at 100μM CaM).

Our above data, combined with the study that reported a similar effect of H^+ as Ca^{2+} on CaM conformation[142] led us to the hypothesis that H^+ supplements Ca^{2+} in promoting CaM binding to eEF-2K. We initially suspected H^+ may replace, rather than supplement, Ca^{2+} in this effect however in the presence of Ca^{2+} low pH caused at least a 7-fold decrease in K_{CaM}^{app}. Our data up to this point established an effect by low pH and a novel mechanism for Ca^{2+}-independent intrinsic activity, however we have not directly assessed CaM binding. To look at eEF-2K and CaM binding directly we used lifetime fluorescence. We studied unphosphorylated/inactivate enzyme (co-expressed with lambda phosphatase) in the absence of calcium. Here we reveal that low pH promotes the binding of CaM and eEF-2K in a calcium independent manner, which supports our hypothesis that H^+ directly impacts the affinity of CaM for eEF-2K. Highlights from our data include: 1) We present a novel mechanism where H^+ promotes calcium-independent binding to eEF-2K. 2) H^+ overrides any effect Mg^{2+} may have on CaM-eEF-2K binding. 3) The increase in CaM binding appears to mirror the sensitivity of k_{obs} to pH, supporting the notion that the binding of two protons drive the binding of CaM to eEF-2K.

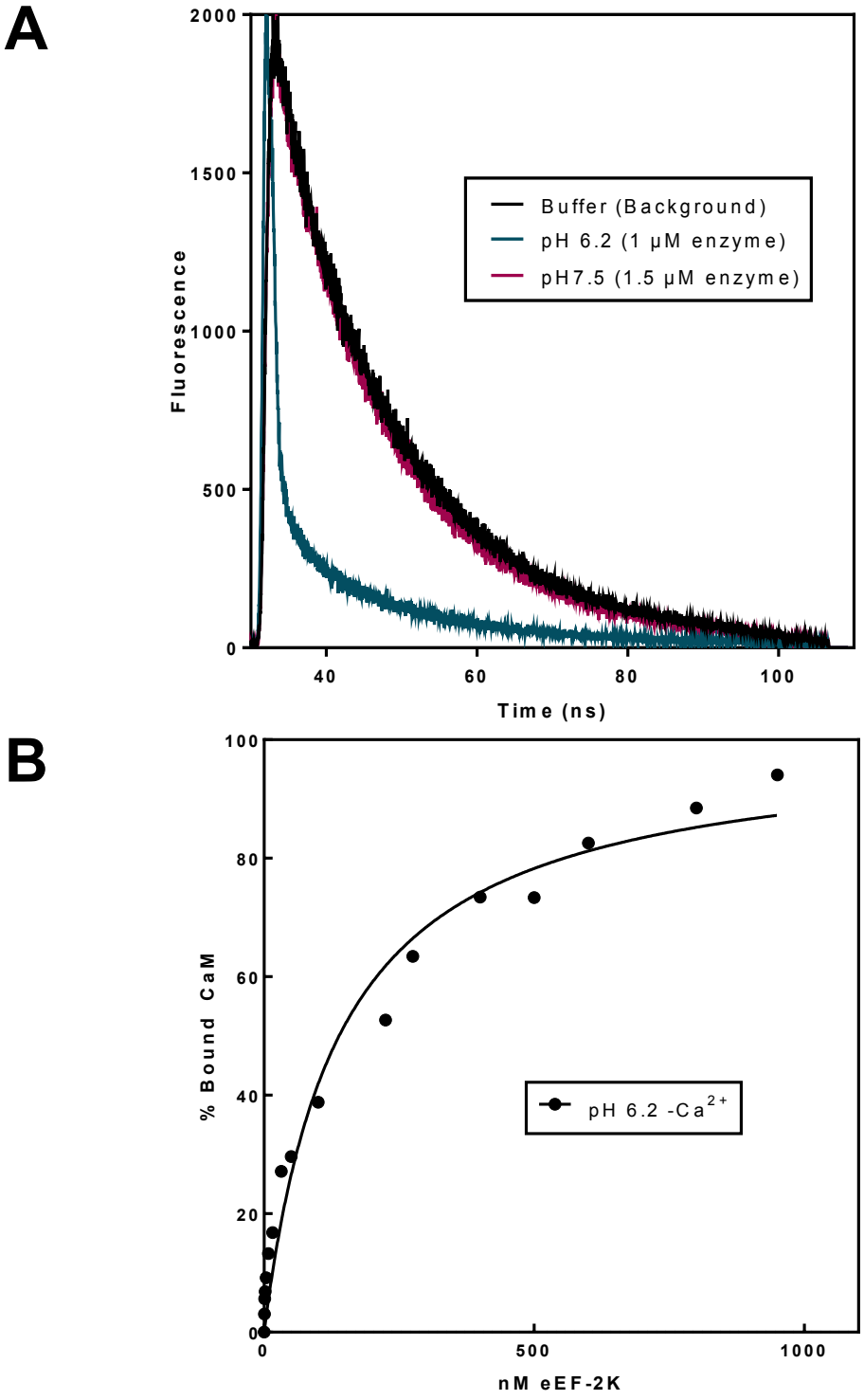

Figure 4.1. (See following page)

Figure 4.1. Acidity rescues CaM binding in the absence of calcium.

All studies were performed in the absence of calcium. **(A)** To study the binding of CaM and eEF-2K, we looked at the lifetime fluorescence spectra of $CaM(C75)_{IAE}$ (i-CaM). 100 nM i-CaM in reaction buffer (25 mM buffer, 2 mM DTT, 10 µg/mL BSA, 50 mM KCl, 1 mM EGTA,) was incubated at 27°C in a 500µL quartz cuvette and unphosphorylated eEF-2K was titrated in from 0-1000nM. HEPES was used for pH 7.5 and Bis-Tris was used for pH 6.2. Emission spectra were taken periodically to optimize the wavelength for the lifetime spectra as addition of eEF-2K alters emission wavelengths by nm amounts (range of 475-485nM from 0-1000nM eEF-2K). The lifetime curves of the varying eEF-2K concentrations were fit to a double exponential equation (Eqn. 4.1, see Materials and Methods) for the two lifetimes; the first lifetime represents i-CaM without eEF-2K bound and the second i-CaM with eEF-2K bound. Here we can see at pH 6.2 binding is saturated with the addition of 850nM eEF-2K whereas at pH 7.5 there is not an change in lifetime fluorescence (no change in binding) from 0-1.5µM enzyme. This was the first step in establishing an effect on CaM binding that was dependent on pH. **(B)** % CaM bound was plotted against respective eEF-2K concentrations and data were fit to a quadratic equation (Eqn. 4.2, see Materials and Methods) to examine the eEF-2K dependence of i-CaM binding. Due to artifacts of the experiment even saturating quantities of eEF-2K did not appear to reach 100% bound CaM, so we defined the calculated V_{max}^{app} for each condition (75.1% for pH 6.2 $-Ca^{2+}$) as 100% and replotted these calculations against corresponding CaM concentrations. There was no binding at pH 7.5 here in the absence of calcium.

A

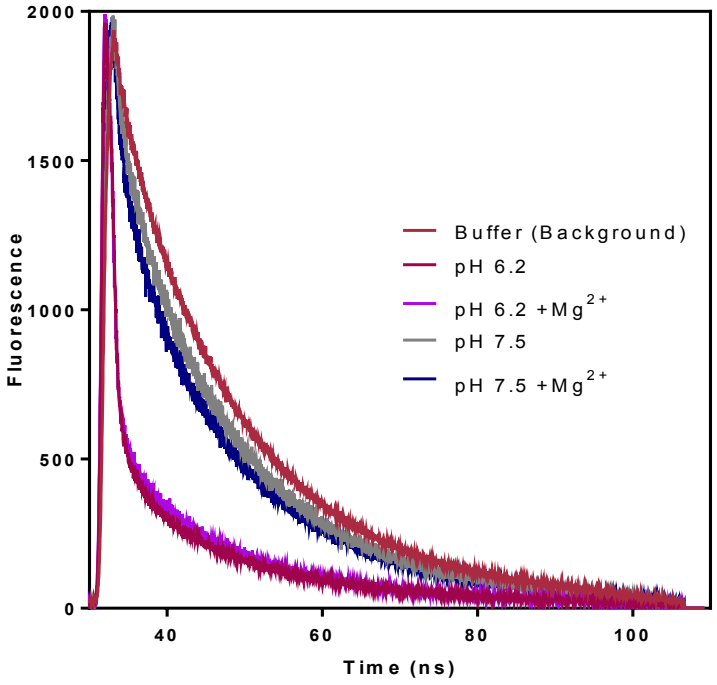

B

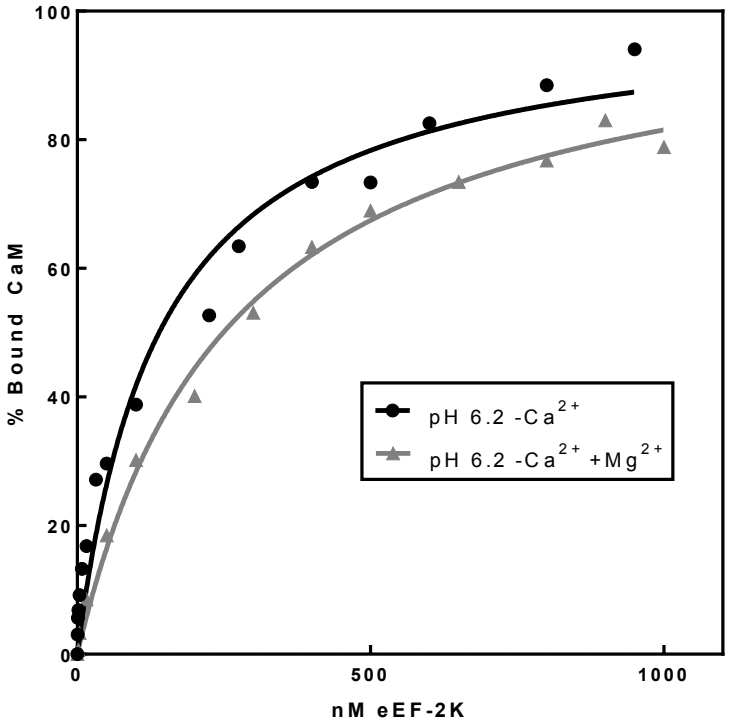

Figure 4.2. (See following page)

Figure 4.2. Binding is not promoted by magnesium.

All studies were performed in the absence of calcium. It has been reported that magnesium may have a similar effect on CaM conformation as calcium. Since phosphorylation assays and physiological events use magnesium, oftentimes to stabilize ATP, we wanted to check whether magnesium could be contributing to any observed effects. **(A)** 100 nM $CaM(C75)_{IAE}$ (i-CaM) in reaction buffer (25 mM buffer, 2 mM DTT, 10 μg/mL BSA, 50 mM KCl, 1 mM EGTA,) with 1 mM Mg^{2+} was incubated at 27°C in a 500μL quartz cuvette and unphosphorylated eEF-2K was titrated in from 0-1000nM. HEPES was used for pH 7.5 and Bis-Tris for pH 6.2. Emission spectra were taken periodically to optimize the wavelength for the lifetime spectra as addition of eEF-2K alters emission wavelengths by nm amounts (range of 475-485nM from 0-1000nM eEF-2K). The lifetime curves were fit to a double exponential equation (Eqn. 4.1, see Materials and Methods) for the two lifetimes. Here we see that magnesium did not significantly alter eEF-2K and i-CaM binding at pH 6.2 or pH 7.5. **(B)** To quantify these results, we looked at eEF-2K dependence of CaM binding by plotting % bound CaM against eEF-2K concentration and data were fit to a quadratic equation (Eqn. 4.2, see Materials and Methods).

A

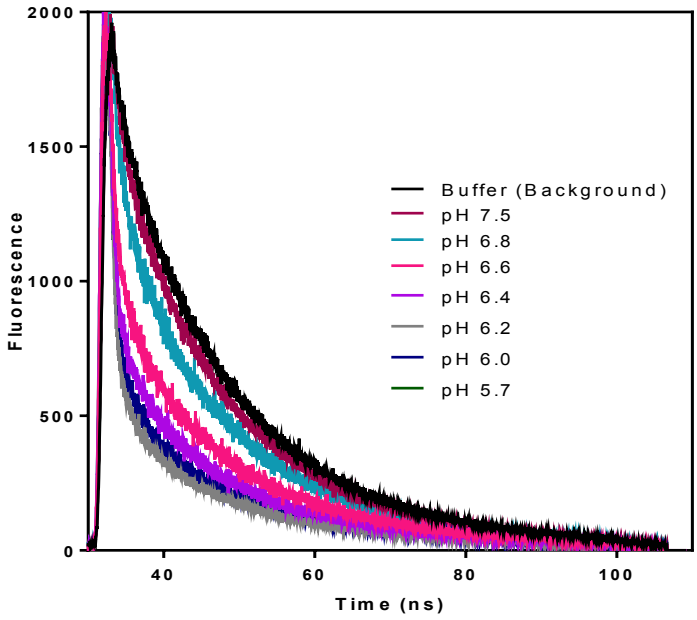

Figure 4.3. (Continued on following page)

B

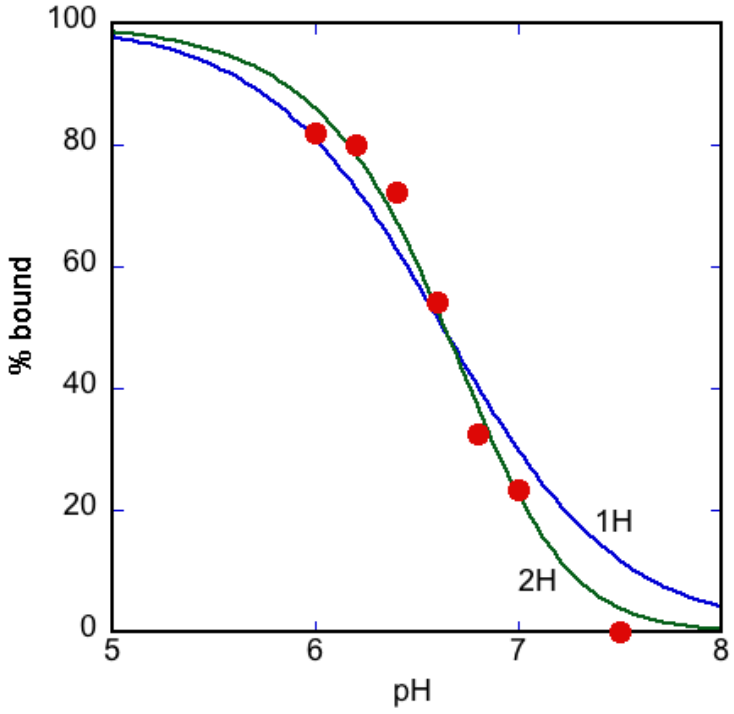

C

pH	% Bound CaM	Error
7.5	0.1	0.3
7.0	23.2	0.5
6.8	32.5	0.7
6.6	54.3	0.6
6.4	72.2	0.6
6.2	79.9	0.6
6.0	81.9	0.5

Figure 4.3. (See following page)

Figure 4.3. Correlation of pH to CaM binding in the absence of calcium.

All studies were performed in the absence of calcium. In order to study the nature of the effect of acidity on binding, we performed a pH dependence curve. **(A)** 100 nM $CaM(C75)_{IAE}$ (i-CaM) and 1μM eEF-2K in reaction buffer (25 mM buffer, 2 mM DTT, 10 μg/mL BSA, 50 mM KCl, 1 mM EGTA,) were incubated at 27°C in a 500μL quartz cuvette and pH was titrated downwards using HCl; the pH was verified after each titration. This occurred in two steps to accommodate buffer limits; HEPES was used from pH 7.5-7.0 and Bis-Tris was used from 6.8-5.8. Emission spectra were taken periodically to optimize the wavelength for the lifetime spectra to check whether addition of acid alters emission wavelengths by nm amounts (range of 83-485nM from pH 5.8-7.5 was used). The lifetime curves were fit to a double exponential equation (Eqn. 4.1, see Materials and Methods) for the two lifetimes to get the % bound CaM. **(B)** % bound CaM were plotted against pH. Here we see that binding increases as pH decreases and saturation occurs at pH 6.2. The best fit through the data (green line, $K_a = 1.4 \times 10^{-7}$ M) was obtained by fitting the data to $\%bound = 100\% \times (H^2)/(H^2+K_aH+K_a^2)$, where H is the concentration of protons, and K_a is the pK_a of each of two protonated residues within the CaM•eEF2K complex. The alternative fit through the data (blue line, $K_a = 2.35 \times 10^{-7}$ M) corresponded to $\%bound = 100\% \times (H)/(H+K_a)$, where it is assumed that only one protonated species contributes to the observed reaction at low pH. **(C)** Shows a table of the pH dependence values, an average of duplicate assays.

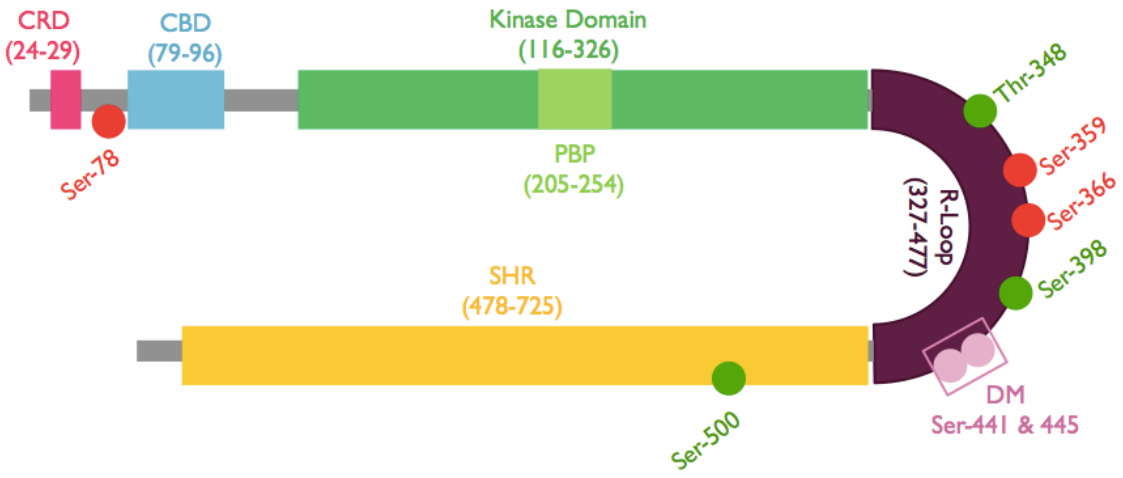

Scheme 4.1. Proposed domains and regulatory regions in eEF-2K.

Depiction of the structural layout and regulatory sites of eEF-2K based on various truncation studies and homology models[48,53,54,57,58,172,201,202]. The highlighted domains include the proposed DXDXDG Ca^{2+}-binding site (CRD, pink), the CaM-binding region (CBD, blue), the kinase catalytic domain and phosphate binding pocket (PBP) (green), the regulatory loop (R-loop) and associated phosphorylation sites, the degron motif (DM, lavender), and the C-terminal helical domain (SHR, yellow) containing three SEL1-like helical repeats required for eEF-2 binding. The residue numbers assigned are estimates based on previous experimental studies and the prediction software[30,42,48]. Activating phosphorylation sites are shown in green (Thr-348, Ser-398, Ser-500) and inhibitory phosphorylation sites are shown in red (Ser-78, Ser-359, Ser-366).

A

$$E + CaM \underset{k_{-1}}{\overset{k_{1\,[CaM]}}{\longleftrightarrow}} E{\bullet}CaM \xrightarrow{k_2^{auto}} E^p{\bullet}CaM$$

B

$$E^p + CaM + S \underset{k_{-3}}{\overset{k_3}{\longleftrightarrow}} E^p{\bullet}CaM{\bullet}S \xrightarrow{k_4^{phos}} E^p{\bullet}CaM{\bullet}P$$

Scheme 4.2. Model for CaM binding and eEF-2K intrinsic activity.

A) eEF-2K (E) activation consists of two steps: 1) CaM binding (defined by the equilibrium k_1/k_{-1}) which induces a conformational change of eEF-2K; and 2) eEF-2K autophosphorylation of Thr-348 (defined by the rate k_2, phosphorylated enzyme denoted as E^p). The autophosphorylation assay (Chapter 1) does not have the resolution to distinguish between these two steps. **B)** Autophosphorylation of Thr-348 induces a conformational change with the allosteric interaction between the phospho-Thr-348 residue and a phosphate-binding pocket on the kinase domain of eEF-2K. CaM is required for substrate phosphorylation however it is not a prerequisite for substrate (S) binding; the first step is denoted as a single binding equilibrium (ratio of k_3/k_{-3}) however it likely exists as several binding equilibria between E^P, CaM, S and ATP (not shown). Once everything is bound, substrate phosphorylation occurs (resulting in formation of P) which is here defined by the rate k_4. Activity assays measure the entirety of these binding and phosphorylation steps and does not have the resolution to distinguish between them.

Chapter 5: Characterization of eEF-2K Histidine Mutants at low pH

5.1. ABSTRACT

Acidification is a physiological phenomenon occurring under conditions such as high-intensity exercise, ischemia, septic shock, diabetic ketoacidosis and solid tumors. These are all processes that involve severe cell stress and many involve anaerobic glycolysis, which puts cells in a state of high-energy demand. This makes it favorable to conserve energy and shut down energy consuming processes such as protein synthesis, which use up to 40% of cellular energy. One such mechanism to accomplish this is activation of eukaryotic elongation factor 2 kinase (eEF-2K), which phosphorylates and inactivates its only known substrate, eukaryotic elongation factor 2 (eEF-2). This prevents movement of tRNA through the ribosome and effectively shuts down protein translation via the elongation step. eEF-2K has also been shown to promote translation of specific transcripts, which is seemingly contradictory and a poorly understood mechanism.

eEF-2K has many regulatory inputs including calmodulin (CaM) and calcium (Ca^{2+}) concentration and availability, upstream regulators (cAMP-dependent protein kinase A (PKA), mammalian target of rapamycin (mTOR), MAPK (MEK/ERK), AMP-activated protein kinase AMPK), transient receptor potential cation channel, subfamily M, member 7 (TRPM7)) and pH. Many of these are communicated through activating or inhibiting multi-site phosphorylations and autophosphorylations, with the exception of pH for which the mechanism of regulation is not understood. We have previously demonstrated (chapters 2-4) a novel mechanism of H^+ ion-promoted calcium-independent

intrinsic activity and CaM binding of eEF-2K. From this we have developed a hypothesis that H^+ overrides the need for calcium in promoting CaM conformations favorable for eEF-2K binding. Based on a study by Pandey et. al (2014), our model for the mechanism behind this is that H^+ and Ca^{2+} affect CaM conformation similarly, promoting CaM binding to eEF-2K in the absence of calcium. This was supported by our binding data from chapter 4, however an alternative hypothesis suggested by Xie et al. (2015) is that low pH directly affects eEF-2K (or CaM) by ionizing histidine residues. Here we use kinetic characterization to identify five histidine residues in eEF-2K that may be important for its sustained activity under calcium-independent acidic conditions.

5.2. INTRODUCTION

Since its discovery in the early 1980's eukaryotic elongation factor 2 kinase (eEF-2K) has been established as an important regulator of protein synthesis. Its dysregulation has been associated with numerous diseases and aberrant cellular conditions including breast cancer, pancreatic cancer, glioblastoma, hypoxia, nutrient deprivation, ischemia, depression and Alzheimer's[83,103,111,123,177,203–205]; this has identified eEF-2K as a potential target for therapeutic treatment and prompted the appearance of many studies in understanding this enzyme. Under baseline conditions, eEF-2K is physiologically important for the cell cycle, learning, memory and synaptic plasticity[6,148,197,206] . eEF-2K is likely critically beneficial to all of these conditions because of its ability to tightly regulate protein translation, which is a large consumer of cellular energy, to resources[34,166,207].

Eukaryotic elongation factor 2 (eEF-2) is the only validated physiological substrate of eEF-2K[34]. As its name suggests, eEF-2 aids in the elongation phase of translation, facilitating the movement of the t-RNA molecules and their associated peptide chains through the ribosome from the A-site to the P-site[164]. Phosphorylation on Thr-56 via eEF-2K prevents eEF-2 from binding to the ribosome, thereby effectively halting global protein synthesis[137,154,167]. eEF-2K activity has also been correlated to the increased translation of select transcripts in neurons[174,207]. While this is seemingly contradictory it is likely possible due to localized regulation or scaffolding across the extended neuron cell bodies, though the mechanism for this effect remains undefined. It is certainly possible with the multitude of signals imposed in eEF-2K to allow for its tight regulation.

Among these signals include regulation via $Ca^{2+/}$CaM binding and multi-site phosphorylations by upstream kinases and intramolecular autophosphorylation[36,54]. Pathways involved in responding to cell stress often activate eEF-2K (i.e. AMP-activated protein kinase (AMPK)[55,80,208–210]) whereas those involved in growth and proliferation often inhibit eEF-2K (mammalian target of rapamycin (mTOR), MAPK (MEK/ERK), cdc2-cyclin B complex, transient receptor potential cation channel, subfamily M, member 7 (TRPM7))[79,148,211–214]. Interestingly, though CaM is always a prerequisite for intrinsic activity, phosphorylation on Ser-500 (either via cAMP-dependent protein kinase (PKA) or autophosphorylation) has been shown to impart Ca^{2+}-independent activity[21,138,215]. We have suggested (Chapters 1-4) that low pH (elevated H^+ ion concentrations) is a novel

mechanism for imparting calcium-independent intrinsic activity and CaM binding to eEF-2K.

Acidification of tissues is often associated with conditions of extreme stress, including high-intensity exercise, ischemia, septic shock, diabetic ketoacidosis and solid tumors, so it is logical that eEF-2K would be beneficial in these circumstances to shut down protein synthesis so cells may better focus on regaining homeostasis[178,216–219]. Our data thus far (looking at activation, substrate phosphorylation and CaM binding) has supported the model that H^+ and Ca^{2+} impart similar conformational changes in CaM making it favorable to bind eEF-2K. An alternative mechanism explaining the effects of low pH on eEF-2K was proposed by a recent study by Xie et. al (2015) where ionizable histidine residues may boost CaM binding, intrinsic eEF-2K activity or both. Because these studies were performed with GST-tagged eEF-2K, which has notoriously minimal activity, we wanted to study the potential effects of histidines at low pH on our recombinant human eEF-2K using His to Gln mutants. Here we report five histidine mutants: H103Q, H201Q, H227Q, H230Q, and H288Q which have remarkably blunted activity at pH 6.2 in the absence of calcium as compared to wild type eEF-2K.

5.3. Materials and Methods

5.3.1. Reagents, Strains, Plasmids and Equipment

Yeast extract, tryptone and agar were purchased from USB Corporation (Cleveland, OH). Isopropyl β-D-1-thiogalactopyranoside (IPTG) and dithiothreitol (DTT) were purchased from US Biological (Swampscott, MA). From Qiagen (Valencia,

CA) Ni-NTA Agarose, QIAprep Spin Miniprep Kit, QIAquick PCR Purification Kit and QIAquick Gel Extraction Kit were purchased. Lambda Protein Phosphatase was from New England BioLabs (Ipswich, MA). BenchMark™ Protein Ladder was from Invitrogen Corporation. SIGMA*FAST*™ Protease inhibitor cocktail tablets for purification of His-tagged proteins, ultra-pure grade Tris-HCl, HEPES and calmodulin were from Sigma-Aldrich (St. Louis, MO). All other buffer components or chemicals were purchased from either Sigma-Aldrich or Fischer Scientific (Pittsburgh, PA). Amicon Ultrafiltration Stirred Cells, Ultracel Amicon Ultrafiltration Discs and Amicon Ultra Centrifugal Filter Units were from Millipore (Billerica, MA). MP Biomedicals (Solon, OH) supplied [γ-^{32}P]ATP.

Escherichia coli strain DH5α – for cloning – was obtained from Invitrogen Corporation, and BL21(DE3) and Rosetta-gami™ 2(DE3) – for recombinant protein expression – were from Novagen, EMD4Biosciences (Gibbstown, NJ). The pET-32α vector was obtained from Novagen.

The ÄKTA FPLC™ System, the HiPrep™ 26/60 Sephacryl™ S-200 HR gel filtration column and the HiLoad™ 16/60 Superdex™ 200 prep grade gel filtration column were from Amersham Biosciences / GE Healthcare Life Sciences (Piscataway, NJ). Absorbance readings were performed on a Cary 50 UV-Vis spectrophotometer. Proteins were resolved by Tris-glycine sodium dodecyl sulfate polyacrylamide gel electrophoresis (SDS-PAGE), under denaturing conditions on 10% gels, using the Mini-PROTEAN 3 vertical gel electrophoresis apparatus from Bio-Rad Laboratories (Hercules, CA). A Techne Genius Thermal Cycler purchased from Techne, Inc. (Burlington, NJ) was used

for PCR. P81 cellulose filters were from Whatman / GE Healthcare Life Sciences (Florham Park, NJ). eEF-2K peptide substrate (pep-S; Acetyl-RKKYKFNEDTERRRFL-Amide (2,227.8 Da)) was custom ordered and purchased from AnaSpec Technologies (Fremont, CA).

5.3.2. Molecular Biology

p32TeEF-2K. The modified pET-32α vector (p32TeEF-2K) containing cDNA encoding human eEF-2K (GenBank entry NM_013302) was used for the expression of Trx-His6-tagged eEF-2K. This expression vector was originally chosen because of the thioredoxin tag (Trx-tag) for increased protein solubility and the hexa-histidine tag (His_6-tag) for nickel affinity chromatography purification. There was also an enterokinase protease recognition sequence site (DDDDK) that allows for cleavage of the tags, however this site had been modified to a Tobacco Etch Virus (TEV) protease recognition sequence site (ENLYFQGDI). The vector was modified by the previous graduate student Clint Tavares[31] using site directed mutagenesis between the *Kpn*I (underlined) and *Eco*RV (italicized) recognition sites (Figure 2.1.A). Additional plasmid DNA was obtained by transforming the modified construct into DH5α cells and purifying the DNA using the Qiagen QIAprep Miniprep Kit. The sequence then verified by sequencing at the ICMB Core Facilities, UT Austin, using an Applied Biosystems automated DNA sequencer.

G6 eEF-2K. The modified eEF-2K construct with a truncated N-terminus and R-loop was a generous gift from the Ghose Lab. This construct was generated to be a

stripped-down simplified but functional model for full-length wild type eEF-2K and had been shown to exhibit tight 1:1 binding with Ca^{2+}/CaM and require Ca^{2+}/CaM for activation and activity under standard conditions in an identical manner to wild type eEF-2K. This was the construct used to generate the histidine mutants and so is the control comparison for experiments in this chapter. The G6-eEF-2K construct was modified as follows: residues 0-70 (N-terminus) and 359-489 (part of the R-loop) were truncated and the R-loop truncation was replaced with a 6-residue glycine linker.

eEF-2K mutants. Mutant eEF-2K DNA were a generous gift from the Ghose Lab (The City College of New York, NY). Mutants were histidine to glutamine mutations (HxQ) on the G6 eEF-2K construct and were cloned into pET15b-SUMO plasmids. They are ampicillin resistant and carry a histidine tag for Ni-NTA purification. A list of gifted mutants are as follows: H80Q, H87Q, H94Q, H103Q, H115Q, H157Q, H201Q, H227Q, H230Q, H268Q, H288Q, H495Q, H527Q, H534Q, H554Q, H557Q, H579Q, H580Q and H639Q. These histidine sites were all chosen for their proximity to key domains, such as the CaM binding domain, substrate binding domain and catalytic domain.

5.3.3. Expression and Purification of Proteins

Expression and Purification of wild type eEF-2K. Recombinant human eEF-2K was expressed in the *E. coli* strain Rosetta-gami™ 2(DE3) (Novagen) using the p32TeEF-2K expression vector. The Rosetta-gami™ 2(DE3) cells were chosen because they carry the pRARE2 plasmid which supplies tRNAs for seven rare codons. eEF-2K contains 63 rare codons, an 8.7% of its 725 residues, so the aim with selecting these expression cells

was to promote healthy and successful expression. Expression and purification were performed as described in Chapter 2.3 Materials and Methods of this dissertation.

Expression and Purification of eEF-2K histidine mutants. eEF-2K mutants were co-expressed with lambda phosphatase (encoded in a pCDF-Duet (Novagen) expression vector); 70ng each of pet15b-SUMO mutant and phosphatase DNA were transformed into the Rosetta-gami™ 2(DE3) cells. A single colony of freshly transformed cells was used to inoculate a starter culture of LB media containing 135 μM ampicillin, 300 μM chloramphenicol, 20μM spectinomycin and 20 μM tetracycline, and grown overnight at 37 ˚C on a shaker (225 rpm). The culture was diluted 20-fold into 500mL LB media containing the same concentration of antibiotics and incubated at 37 ˚C on a shaker (225 rpm) for 3-4 h until it reached an OD_{600} of 0.6-0.8. To induce protein expression the temperature was reduced to 22 ˚C, 0.4 mM isopropyl β-D-1-thiogalactopyranoside (IPTG) was added and the cultures were incubated for 18h. The cells were harvested by centrifugation (7000*g* for 10 min at 4 ˚C), flash frozen in liquid nitrogen and stored at -80 ˚C.

All mutants were purified with Ni-NTA chromatography, possible because of the His_6 tag in the pet15b-SUMO vector. To start purification the bacterial pellet (typically 1.5 wet cells per 500L of cultured LB) was thawed on ice and resuspended in 25 mL of Buffer 4.A (20 mM tris-HCl (pH 8.0), 0.5 M NaCl, 5 mM imidazole, 5 mM $MgCl_2$, 1% triton X-100 (*v/v*), 0.03% brij 30 (*v/v*), 0.1% 2-mercaptoethanol (*v/v*), 1 mM benzamidine hydrochloride hydrate, 0.1 mM tosyl phenylalanyl chloromethyl ketone (TPCK), 0.1 mM phenylmethanesulfonyl fluoride (PMSF) and 7 μM lysozyme). The suspension was

sonicated for 12min (10s pulses) and the temperature was monitored and maintained between 4-6 ˚C. The lysate suspension was centrifuged (Sorvall – SS34 rotor) at 27,000*g* for 30 min at 4 ˚C. The supernatant was gently agitated with 300 µL of Ni-NTA beads (Qiagen) for 1 h at 4 ˚C. Prior to agitation, the beads were equilibrated in a chromatography column with 50 mL of Buffer 4.A and after agitation the beads were washed with 50mL of Buffer 4.B (20 mM tris-HCl (pH 8.0), 0.25 M NaCl, 40 mM imidazole, 0.03% brij 30 (*v/v*), 0.1% 2-mercaptoethanol (*v/v*), 1 mM benzamidine hydrochloride hydrate, 0.1 mM TPCK and 0.1 mM PMSF). Each mutant was eluted in three fractions of 3mL of Buffer 4.C (20 mM tris-HCl (pH 8.0), 0.25 M NaCl, 250 mM imidazole, 0.03% brij 30 (*v/v*), 0.1% 2-mercaptoethanol (*v/v*), 1 mM benzamidine hydrochloride hydrate, 0.1 mM TPCK and 0.1 mM PMSF). The purification stages were monitored via SDS-PAGE: uninduced culture, induced culture, lysis suspension post sonication, centrifuged pellet, centrifuged supernatant, chromatography column wash flow-through and the various elution fractions.

The eluted fractions containing SUMO-His_6-tagged eEF-2K mutants from the Ni-NTA purification were pooled and dialyzed against Buffer 4.D (25 mM HEPES (pH 7.5), 2 mM DTT, 50 mM KCl, 0.1 mM EGTA, 0.1 mM EDTA and 10% glycerol). The dialyzed protein was concentrated using a centrifugal filter unit to 5-10 µM, aliquoted, flash frozen in liquid nitrogen and stored at -80°C. The concentration of eEF-2K was calculated using its absorbance at 280 nm and the extinction coefficient (A280) of 97150$cm^{-1}M^{-1}$.

Expression and purification of TEV protease. Tobacco Etch Virus protease was expressed from the pRK793 expression vector (gifted by Dr. John Tesmer, Life Sciences Institute, University of Michigan, Ann Arbor, MI). The construct was transformed into Rosetta-gami™ 2(DE3) cells, protein expression was induced with 0.5 mM IPTG at 28 °C and the culture was incubated for 4h. The bacterial culture was centrifuged and the cells were harvested and purified according to protocols published earlier[170,171].

Expression and purification of calmodulin. The calmodulin (CaM) clone in the pET-23 expression vector was gift by Dr. Neal Waxham (Department of Neurobiology and Anatomy, University of Texas Medical School at Houston, Houston, TX). The construct was transformed into BL21(DE3) cells (Novagen). Expression and purification were carried out as described in Chapter 2.3 Materials and Methods of this dissertation. These methods were adapted from previous protocols[172,173].

5.3.4. General Analytical Methods

General kinetic assays. eEF-2K mutants were assayed at 30°C in Buffer 5.A (25 mM buffer, 2 mM DTT, 10 μg/mL BSA, 50 mM KAcO, 10 mM $MgCl_2$, 100 μM EGTA, 150 μM pep-S) ±50 μM free calcium (added as $CaCl_2$) in a final reaction volume of 100 μL. 1 mM EGTA was added for assays performed in the absence of calcium. Changes in free calcium concentration over varied pH were accounted for using Stanford University's maxchelator calculator. 1 μM CaM was used in assays considered to be CaM saturated. Assays were performed using 2 nM eEF-2K and 1 mM [γ-^{32}P]ATP (100-1000cpm/pmol). Either HEPES or Bis-Tris buffers were used for assays assessing pH

dependence in their appropriate buffer range as calculated by The University of Liverpool's PFG buffer calculator. Samples were prepared on ice and all reactions and buffers were individually adjusted to the proper pH (range of pH5.8-7.5). 90 µL of Buffer 5.A was incubated at 30°C for 2 min, 5µL of enzyme was mixed in and heated for an additional 3min, and the reaction was initiated by the addition of 5 µL ATP. Samples were quenched at various time points (1-8min) by spotting 10 µL reaction on P81 paper and immediately immersing in 0.1 M phosphoric acid. Samples were thrice washed for 15minutes in phosphoric acid and once in acetone. Each data point was performed in duplicate. The pH of the remaining reaction was confirmed to be consistent with the assay start. The amount of labeled peptide associated with each paper was determined by measuring the counts per minute on a liquid scintillation counter. Kinase activity was determined by calculating the rate of phosphorylation of eEF-2 peptide ($\mu M.s^{-1}$). Data where K_C^{app}>20 nM were fit to eqn. 3.1, and the data where K_c^{app}<20 nM were fitted to equation 5.1.

$$k_{obs}^{app} = \frac{k_{cat}^{app}[C]}{K_c^{app} + [C]} \qquad \text{(Equation 5.1)}$$

$$k_{obs}^{app} = k_{cat}^{app} \frac{([E] + [C] + K_M^{app}) - \sqrt{([E] + [C] + K_M^{app}) - 4[E][C]}}{2[E]} \qquad \text{(Equation 5.2)}$$

The parameters are defined as follows: k_{obs}^{app}, apparent rate constant; k_{cat}^{app}, apparent catalytic constant; [C] is the concentration of varied co-activator CaM; [E] is the

concentration of eEF-2K; K_c^{app} is the apparent CaM concentration required to achieve half maximal activity.

CaM Dependence. Calmodulin dose response assays were performed on mutants that were selected for further analysis. The same protocol as general kinetic assays were performed, except each mutant was assayed under ten varying CaM concentrations: 0, 1, 5, 10, 25, 500, 100, 250, 500, 1000 nM.

Data Fitting: Unless otherwise specified all data and equation fitting was performed using GraphPad Prism version 6.00 for Windows, GraphPad Software, La Jolla California USA, www.graphpad.com

5.4. RESULTS & DISCUSSION

5.4.1. Initial screening of eEF-2K histidine mutants

eEF-2K was first discovered and appropriately named Ca^{2+}-calmodulin mediated kinase III (CaMK-III) as calmodulin binding is a prerequisite for eEF-2K activation and substrate phosphorylation[34,220]. Ca^{2+} under normal conditions is also necessary as it promotes a CaM conformation favorable to eEF-2K binding; Ca^{2+}-independent activity has previously only been seen following Ser-500 phosphorylation[36,135,220]. CaM is bilobal (with each lobe having two calcium-binding EF-hands) and is known to bind eEF-2K with its C-terminal domain (without calcium) and to loosely associate with its N-terminal domain (calcium bound)[33,190,221]. In previous chapters, we have: 1) Demonstrated a novel mechanism for H^+ ion-promoted Ca^{2+}-independent intrinsic activity (both autophosphorylation and substrate phosphorylation) of eEF-2K; and 2) Proposed that the likely mechanism behind this effect is due to a H^+-mediated increased binding of CaM to eEF-2K. It has been also been suggested as an alternate mechanism that the ionizable

imidazole group on histidine residues could have altered pK_as that directly affect eEF-2K under acidic conditions[12].

The initial study by Xie et al. (2015) that looked into the effect of histidine residues on eEF-2K activity identified five conserved histidine residues: three in the CaM binding site (His-80, His-87 and His-94) and two in the ATP binding site (His-227 and His-230) as being critical to the enzyme's activation by acidity. It is important to note that these studies were performed using the GST-tagged form of eEF-2K, which as discussed earlier has minimal activity compared to our human recombinant His^6-tagged enzyme. We decided to expand this list of residues to those that are highly conserved and in the CaM binding domain (CBD) (His-80, His-87, His-94), two in between domains (His-103, His-115), in the kinase domain (His-157, His-201, His-227, His-230, His-268, His-288), and in the Sel1-like helical repeats (SHR) necessary for substrate interaction (His-527, His-534, His-495, His-579, His-580, His-639) (Scheme 5.1). To test which histidine mutants could be contributing to eEF-2K activity under low pH, various eEF-2K histidine to glutamine mutants were screened. The histidine mutations were generated using the G6 eEF-2K construct, which is a fully functional simplified model of full length eEF-2K. It has a truncated N-terminus and partially truncated R-loop that is replaced with a 6-residue glycine linker. All comparisons for the histidine mutants are made against the non-mutated G6 eEF-2K enzyme. The rates under the conditions pH 6.2 (using Bis-Tris) in the absence of calcium and pH 7.5 (using HEPES) in the presence of calcium were measured to look at the ability of the mutant to retain activity under low pH and to verify the mutant had activity under standard conditions, respectively. 2 nM enzyme, 50 nM CaM, 150 μM substrate peptide and either 10 mM EGTA (pH 6.2) or 50 μM free calcium (pH 7.5) were incubated in reaction buffer (Buffer 5.A) before initiating substrate phosphorylation with 1 mM γ-^{32}P-ATP. Phosphate incorporation was measured over time and the corresponding slope for each enzyme is reported above as the

observed rate (k_{obs}). G6-eEF-2K and mutant parameters used 50nM CaM to mitigate against the saturation of CaM binding masking any minor fluctuations in kinetic behavior due to a mutation (originally mutants were tested with 500 nM CaM (not shown) which didn't fully show the difference between the two conditions). Specifically, we were looking for mutants to further characterize that had activity at pH 7.5 in the presence of calcium but had significantly lower activity under pH 6.2 without calcium (opposite of G6-eEF-2K) enzyme. To determine which mutants to further characterize, the ratio between k_{obs} of pH 6.2 in the absence of Ca^{2+} (where a histidine residue could potentially be critical) and pH 7.5 in the presence of Ca^{2+} (where the activity of the enzyme should be optimal) was calculated and compared to the G6-eEF-2K (ratio of 1.1 (Table 5.1). We selected mutants with at least a two-fold difference in ratio (ratio < 0.32) to study further: H103Q, H201Q, H227Q, H230Q and H288Q. Also of note were four consecutive mutants (His-527, His-534, His-495, His-579) in the SHR domain that did not have activity at either pH. This may be due to sub-optimized expression and purification conditions, as the SDS-PAGE and Coomassie-stained gel showed the presence of eEF-2K in the purification (not shown); additional studies are needed to clarify these mutants.

5.4.2. Characterization of CaM dependence of select eEF-2K histidine mutants

Here we are the first to report a quantitative kinetic analysis, namely parameters associated with a CaM dose response curve, of eEF-2K histidine mutants with the goal of identifying potential residues contributing to eEF-2K activity under acidic conditions. The following histidine mutants with a two-fold difference in pH 6.2 – Ca^{2+}: pH 7.5 + Ca^{2+} ratio from G6-eEF-2K were selected for further characterization: H103Q, H201Q, H227Q, H230Q, H288Q. 2nM of each mutant was incubated with various CaM

concentrations (0, 1, 5, 10, 25, 50, 250, 500, 1000 nM), 10 mM EGTA and 150 μM substrate peptide at 27°C in reaction buffer (Buffer 5.A, Bis-Tris) at pH 6.2 before substrate phosphorylation was initiated with 1mM γ-^{32}P-ATP (Figure 5.1). Each CaM dose-response curve was performed in duplicate and k_{obs} for each mutant was plotted against CaM to determine the maximum apparent rate constant (k_{max}^{app}) and the concentration of CaM at half max rate (K_{CaM}^{app}). The k_{max}^{app} and K_{CaM}^{app} for each mutant, respectively, were: H103Q (4.0 ± 0.2 s^{-1}, 14.6 ± 3.8 nM), H201Q (1.1 ± 0.03 $s^{-1,}$ 6.3 ± 1.1 nM), H227Q (1.0 ± 0.2 s^{-1}, 47.7 ± 26.3 nM), H230Q (1.0 ± 0.1 s^{-1}, 26.3 ± 7.9 nM), H288Q (n/a, n/a) compared to G6-eEF-2K (41.8 ± 0.8 s^{-1}, 3.9 ± 0.5 nM). H288Q parameters could not be established because there was no activity. The other mutants had k_{max}^{app} values ranging from 1 - 4 s^{-1}, were 4-5 times less active at pH 6.2 –Ca^{2+} than at pH 7.5 + $Ca^{2+}$and were all 6.5-25 times less active than G6-eEF-2K enzyme under the same conditions (pH 6.2 –Ca^{2+}). H227Q and H230Q likely affect CaM binding as they have a K_{CaM}^{app} 7-12 times higher than G6-eEF-2K (47.7 ± 26.3, 26.3 ± 7.9 and 3.9 ± 0.5 nM respectively). The remaining K_{CaM}^{app} values are comparable or lower than G6-eEF-2K, so loss of activity from mutations are not likely due to an impact on CaM binding. All this taken together supports the model that these histidine residues may contribute to promoting Ca^{2+}-independent activity under acidic conditions, although this is likely in tandem with the H^+ effect on CaM binding described in previous chapters.

5.6. CONCLUSION

eEF-2K has many signaling inputs which primarily involve the interpretation of multisite phosphorylation by the enzyme in order to have various levels of global downregulation of protein synthesis[21,135]. pH is a form of regulation on eEF-2K that does

not rely on phosphorylation to convey its effect; our previous data (Chapters 1-4) has suggested a model in which H^+ and Ca^{2+} affect CaM conformation similarly, promoting its binding to eEF-2K and subsequently autophosphorylation and substrate phosphorylation. In this model acidity is still affecting eEF-2K indirectly through enhanced CaM affinity. To address the question of whether low pH could be directly effecting the enzyme through ionizable histidine residues we looked into 17 conserved histidine to glutamine mutants. We screened for mutants that retained activity under standard conditions (pH 7.5 with calcium) but had significantly lower activity under acidic conditions in the absence of calcium. We further studied five mutants and their CaM dose dependence curve to further characterize how different their behavior was under acidic conditions and compare them to G6-eEF-2K.

Here we predict that the histidine residues: H103Q, H201Q, H227Q, H230Q, H288Q supplement the effect of H^+ promotion of Ca^{2+}-independent eEF-2K activation, activity, and CaM binding to achieve the overall phenomenon of upregulation of eEF-2K under low pH. Further mutation studies could be useful to more concretely identify effect on CaM binding (our data suggests histidine mutations have an effect on activity independent of binding), to study the effect if histidine was replaced with a positively charged amino acid such as lysine, and to determine pK_as of the residues to determine physiological relevance.

Table 5.1. A summary of eEF-2K histidine mutant activities.

Enzyme	pH 6.2 $-Ca^{2+}$	7.5 $+Ca^{2+}$	V_{max} Ratio
	$V_{obs}(s^{-1})$	$V_{obs}(s^{-1})$	
H80Q	2.7 ± 0.1	6.7±0.2	0.40
H94Q	12.1 ± 0.2	23.2±0.4	0.52
H103Q	2.4 ± 0.1	11.1±0.3	0.22
H115Q	0.70 ± 0.06	1.3±0.1	0.54
H201Q	2.0 ± 0.1	6.6±0.02	0.29
H227Q	0.60 ± 0.02	3.1±0.1	0.19
H230Q	1.6 ± 0.1	7.7±0.4	0.21
H87Q	27.3 ± 0.03	38.1±0.4	0.72
H157Q	9.3 ± 0.1	11±0.3	0.85
H268Q	0.6 ± 0.09	1.7±0.1	0.35
H288Q	0.1 ± 0.03	3.1±2.7	0.03
H527Q	0	0	0.00
H534Q	0	0	0.00
H554Q	0	0	0.00
H579Q	0	0	0.00
H580Q	6.9 ± 2.7	17.1±0.6	0.40
H639Q	3.8 ± 0.04	6.4±0.1	0.59
eEF-2K G6	38.4±0.9	35.0 ± 1.4	1.10

To test which histidine mutants could be contributing to eEF-2K activity under low pH, various eEF-2K histidine to glutamine mutants were screened. The rates under the conditions pH 6.2 (using Bis-Tris) in the absence of calcium and pH 7.5 (using HEPES) in the presence of calcium were measured to look at the ability of the mutant to retain activity under low pH and to verify the mutant had activity under standard conditions, respectively. 2 nM enzyme, 50 nM CaM, 150 µM substrate peptide and either 10 mM EGTA (pH 6.2) or 50µM free calcium (pH 7.5) were

incubated in reaction buffer (Buffer 5.A) before initiating substrate phosphorylation with 1mM γ-^{32}P-ATP. Phosphate incorporation was measured over time and the corresponding slope for each enzyme is reported above as the observed rate (V_{obs}). The mutants were expressed using the G6 eEF-2K variant, which is an eEF-2K without a regulatory loop. This non-mutated eEF-2K G6 enzyme was used for comparison observed rates were also determined using 50 nM CaM; lower CaM was used for the mutants to ensure that saturation was not masking any minor fluctuations in kinetic behavior do to a mutation. To determine which mutants to further characterize, the ratio between V_{obs} of pH 6.2 in the absence of Ca^{2+} (where a histidine residue could potentially be critical) and pH 7.5 in the presence of Ca^{2+} (where the activity of the enzyme should be optimal) was calculated and compared to eEF-2K G6 (ratio of 1.10). We selected mutants with greater than a three-fold difference in ratio (ratio < 0.34) to study further (yellow highlighted mutants).

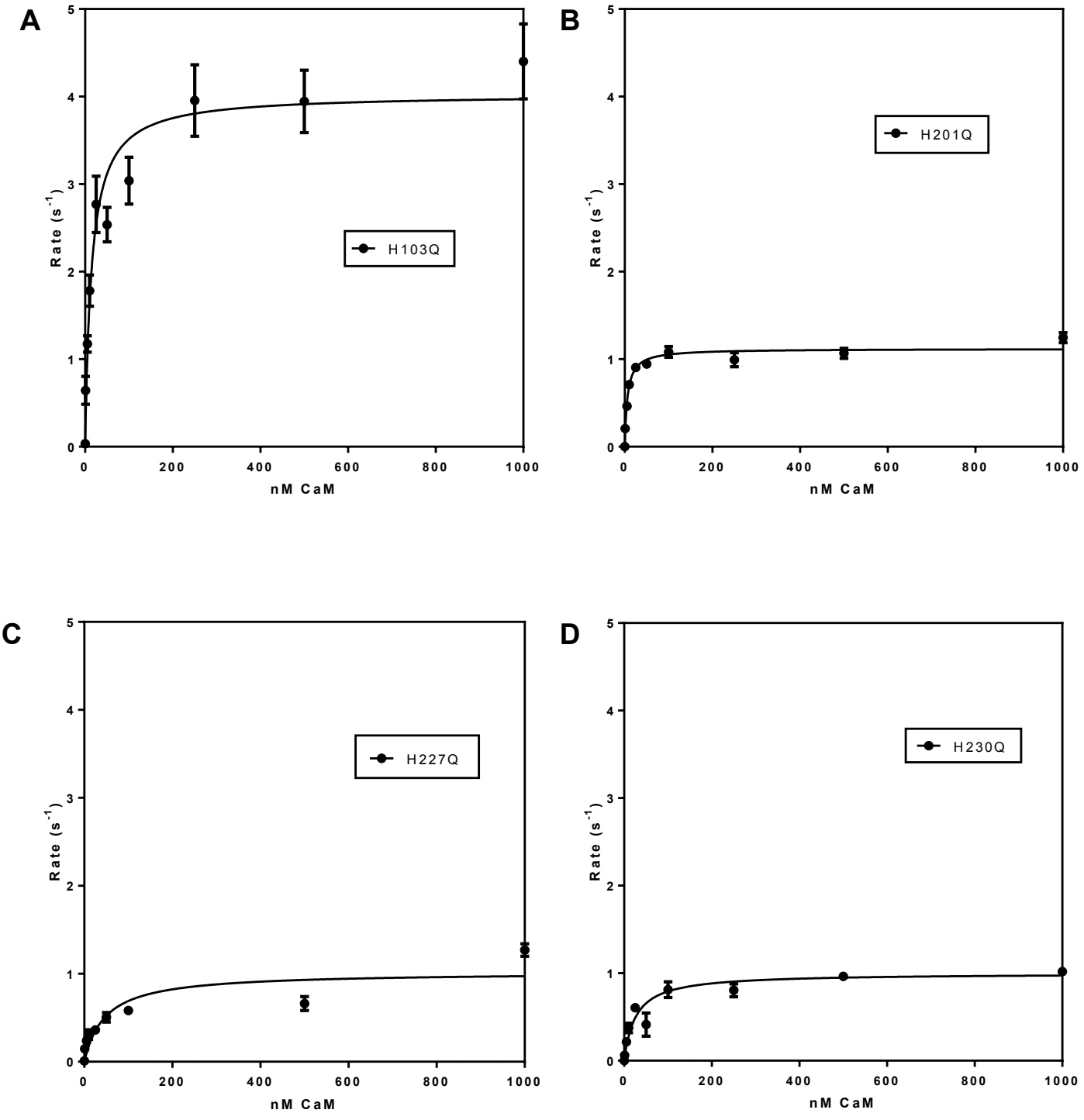
A
B
C
D
H103Q
H201Q
H227Q
H230Q
Rate (s^{-1})
nM CaM
0
1
2
3
4
5
0
200
400
600
800
1000

E

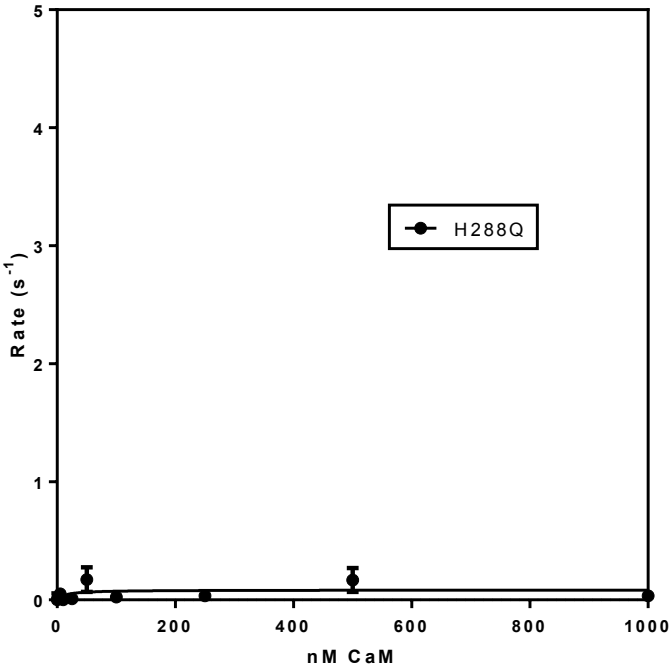

F

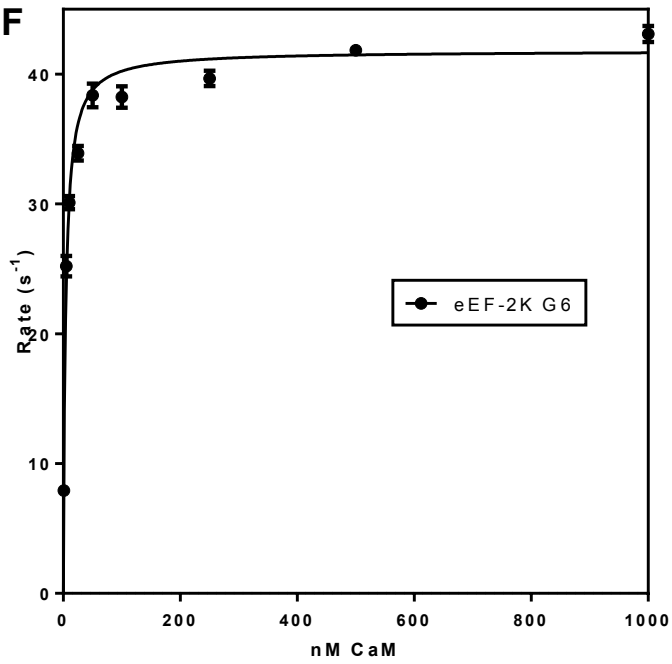

G

Mutant	V_{max}^{app} (s^{-1})	K_{CaM}^{app} (nM)
H103Q	4.0 ± 0.2	14.6 ± 3.8
H201Q	1.1 ±0.03	6.3 ± 1.1
H227Q	1.0 ±0 .2	47.7 ± 26.3
H230Q	1.0 ± 0.1	26.3 ± 7.9
H288Q	n/a	n/a
G6-eEF-2K	41.8 ± 0.8	3.9 ± 0.5

Figure 5.1. Characterization of the CaM dependence of select eEF-2K histidine mutants.

(A-F) The following histidine mutants with a two-fold difference in pH 6.2 – Ca^{2+} : pH 7.5 + Ca^{2+} ratio from G6-eEF-2K were selected for further characterization: H103Q, H201Q, H227Q, H230Q, H288Q. 2 mM of each mutant was incubated with various CaM concentrations (0, 1, 5, 10, 25, 50, 250, 500, 1000 nM), 1 mM EGTA and 150 μM substrate peptide at 27°C in reaction buffer (Buffer 5.A, Bis-Tris) at pH 6.2 before substrate phosphorylation was initiated with 1 mM γ-^{32}P-ATP. Each CaM dose-response curve was performed in duplicate and the average rate (k_{obs}) for each mutant was plotted against CaM concentration to determine maximum rate (k_{max}^{app}) and concentration of CaM at half max rate (K_{CaM}^{app}). **(H)** Depicts a summary table of the obtained kinetic parameters. **(G)** A plot of the CaM dependence curve for G6-eEF-2K eEF-2K at pH 6.2 in the absence of Ca^{2+} for comparison (as determined in Chapter 3).

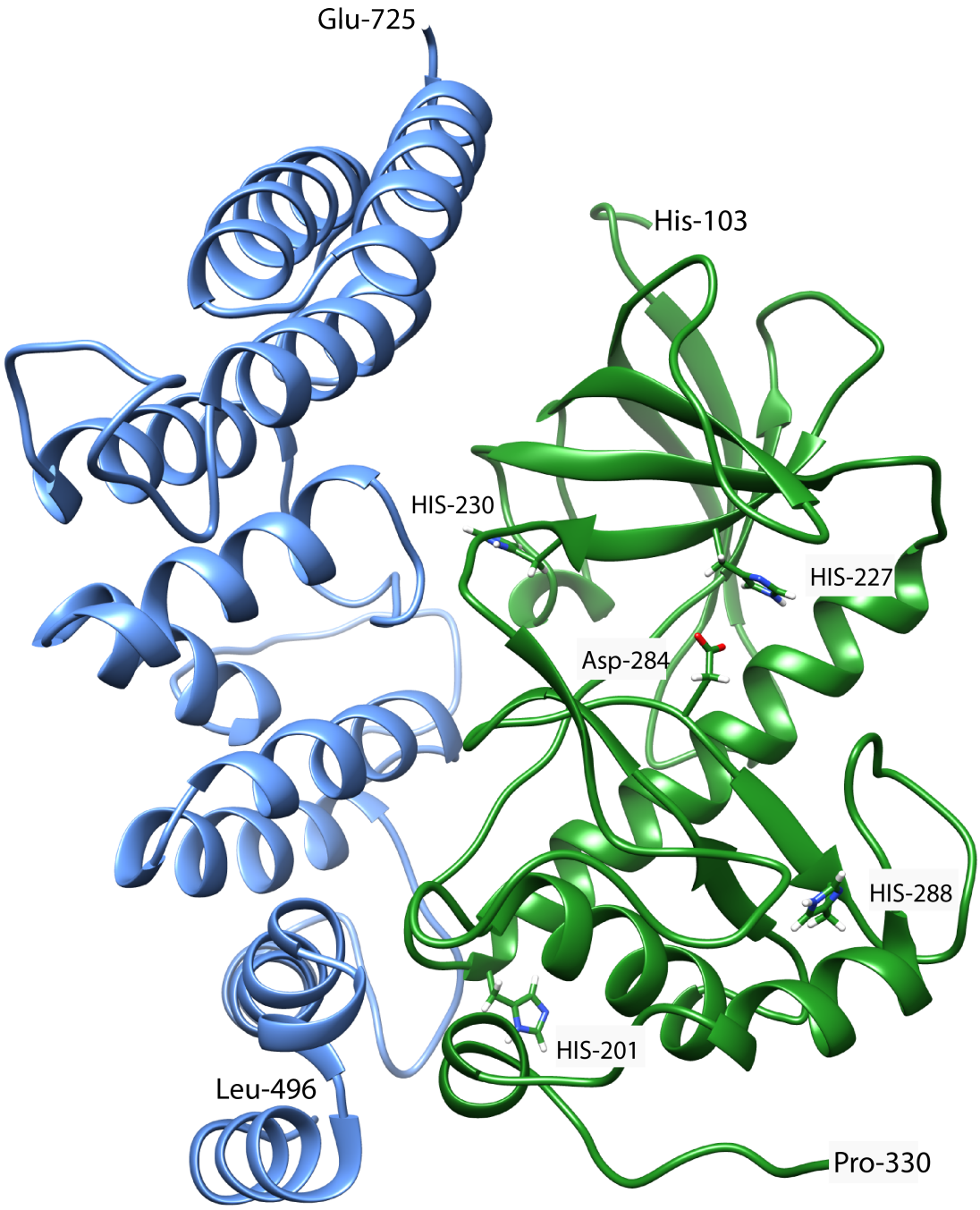

Figure 5.2. (See following page)

Figure 5.2. Model of the three-dimensional structure of eEF-2K.

Model of the three dimensional structure of eEf-2K reported by our laboratory[221]. Green residues 103-330, Blue, residues 496-725.

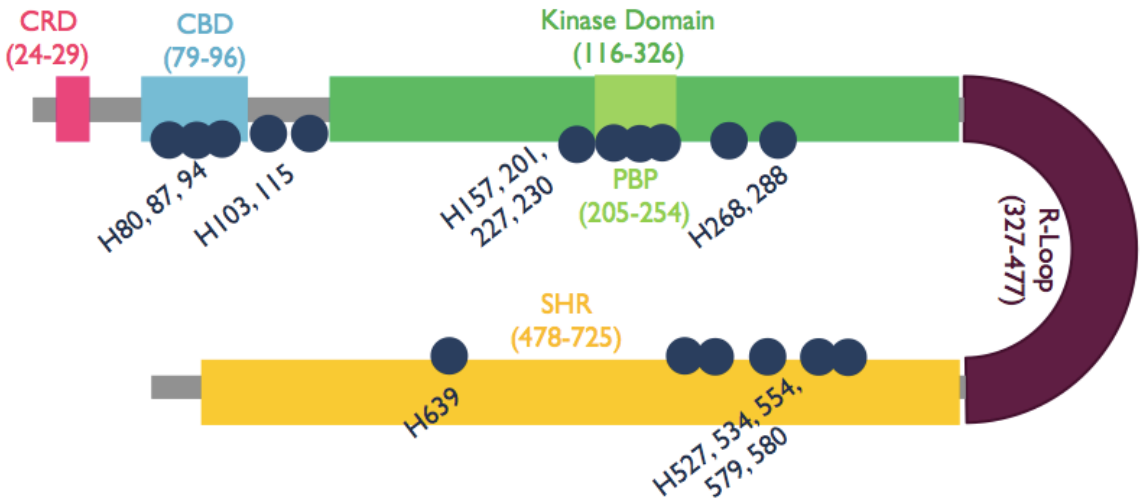

Scheme 5.1. Illustration of histidine mutants on eEF-2K.

Depiction of the structural layout and regulatory sites of eEF-2K based on various truncation studies and homology models[48,53,54,57,58,172,201,202]. The highlighted domains include the proposed DXDXDG Ca^{2+}-binding site (CRD, pink), the CaM-binding region (CBD, blue), the kinase catalytic domain and phosphate binding pocket (PBP) (green), the regulatory loop (R-loop) and associated phosphorylation sites, the degron motif (DM, lavender), and the C-terminal helical domain (SHR, yellow) containing three SEL1-like helical repeats required for eEF-2 binding. The residue numbers assigned are estimates based on previous experimental studies and the prediction software[30,42,48]. Conserved histidine residues chosen for His to Gln mutations and their location in various domains are depicted in navy (17 total).

Chapter 6: Summary

Previously, our laboratory discovered that at pH 7.5, eEF-2K is activated through a two-step mechanism, whereby Ca^{2+}-CaM binding induces a conformational transition in eEF-2K to promote autophosphorylation on Thr-348. These two steps are essential to achieve full activity towards a peptide substrate and continued CaM binding is essential to maintain eEF-2K activity. In this dissertation I investigated the role of pH in the regulation of eEF-2K. I discovered that eEF-2K activation and activity is acutely sensitive to a slight drop in pH and identified mechanisms contributing to this.

I discovered that CaM can rapidly induce the activation of eEF-2K in the absence of Ca^{2+} ions at pH 6.2, whereas at pH 7.5 autophosphorylation is more than 50-fold slower.

I found that in the presence of Ca^{2+} ions the maximal activity of eEF-2K towards a peptide substrate at pH 6.2 and pH 7.5 are comparable, demonstrating that pH has no effect on the intrinsic activity of the kinase. However, I showed that in the absence of Ca^{2+} ions, H^{+} ions promote the binding of CaM to Thr-348-phosphorylated eEF-2K to stimulate its activity. The half-maximal concentration of CaM required to maintain eEF-2K activity at pH 6.2 in the absence of Ca^{2+} ions is 36 nM. I also found that the maximal activity of eEF-2K at pH 6.2 in the absence of Ca^{2+} ions is comparable to the activity in the presence of Ca^{2+} ions, suggesting that CaM can adopt a similar active conformation in complex with eEF-2K in the presence and absence of Ca^{2+} ions. Notably, the pH-dependence of the eEF-2K activity in the absence of Ca^{2+} ions was most consistent with

two independent protonation events occurring to promote the activity, with pKa's around 6.85.

Interestingly, I found that in the presence of Ca^{2+} ions the binding of CaM appeared to be significantly tighter (< 0.5 nM) at pH 6.2 than in the absence of Ca^{2+} ions, suggesting that H^+ and Ca^{2+} ions can promote CaM binding at least in part through distinct, complementary mechanisms.

By following changes in fluorescence lifetime, I monitored CaM binding to eEF2K in the absence of Ca^{2+} ions. I found that CaM binds eEF-2K tightly at pH 6.2, but could not be detected at pH 7.5. The pH dependence of CaM binding was consistent with two independent protonation events occurring with pKa's around 6.85, suggesting that CaM binding is acutely sensitive to a drop in pH. Taken together the data suggest that the pH-dependence of eEF-2K is largely related to the promotion of CaM binding by a decrease in pH.

I examined the possibility that the pH-dependent binding of CaM was mediated, in part, by a histidine residue and looked for histidine residues whose mutation to glutamine more strongly impacted the activity of eEF-2K at pH6.2 in the absence of Ca^{2+}, than at pH 7.5 in the presence of Ca^{2+}. Using a minimalized form of eEF-2K (lacking the N-terminus as well as the Regulatory loop), but which is still pH-sensitive I found three candidate histidines. I found that that mutation of His-227, His-230 or His-288 that are found in the kinase domain, had a larger impact on the activity of eEF-2K at pH 6.2 in the absence of Ca^{2+} ions than at pH 7.5 in the presence of Ca^{2+} ions. Introduction of the H227Q or H230Q mutants resulted in a significant increase in K_m (CaM) at pH 6.2 in the

absence of Ca^{2+}. These data support the notion that protonation of H227 or H230 support the activity at pH6.2. Further studies are needed to examine the pH dependence of the structure and activity of these mutants.

In summary, the studies in this dissertation lay the foundation for future structure/activity studies to reveal the molecular basis for how low pH regulates the activity of eEF-2K. My studies support the notion that eEF-2K is acutely activated by slight drops in cellular pH, potentially providing a fast and reversible control mechanism for regulating the rates of protein synthesis.

Appendix

A.1. List of Abbreviations

ADP	Adenosine diphosphate
AMPK	AMP-activated protein kinase
Apo-CaM	Calcium -free form of calmodulin
ATP	Adenosine triphosphate
APK	Atypical protein kinase
Ca^{2+}	Calcium
$[Ca^{2+}]_{free}$	Free calcium concentration
CaM	Calmodulin
$CaM(C75)_{IAE}$	Calmodulin where the IAEDANS label is attached to Cys-75
CaMK	Calcium/calmodulin-dependent protein kinase
cAMP	Cyclic adenosine monophosphate
CDK1	Cyclin-dependent kinase 1
CDK2	Cyclin-dependent kinase 2
DTT	Dithiothreitol
EDTA	Ethylenediaminetetraacetic acid
eEF-1a	Elongation factor-1 alpha
eEF-2	Eukaryotic elongation factor 2
eEF-2K	Eukaryotic elongation factor 2 kinase
eEF-3	Elongation factor-3
EGTA	Ethylene glycol tetraacetic acid
ERK	Extracellular-signal-regulated kinases
FPLC	Fast performance liquid chromatography
(*G-D-I*)-eEF-2K	Recombinant human eEF-2K preceded by three residues (Gly-Asp-Ile) – a remnant of the Trx-His_6-tag after cleavage

GTP	Guanosine triphosphate
HAK	Heart alpha-kinase
HEPES	*4*-(*2*-hydroxyethyl)-*1*-piperazineethanesulfonic acid
HPLC	High-performance liquid chromatography
i-CaM	Calmodulin where the IAEDANS label is attached to Cys-75
IPTG	Isopropyl *β*-*D*-*1*-thiogalactopyranoside
IRES	Internal ribosome entry site
k_{cat}^{app}	Apparent catalytic constant
k_{obs}^{app}	Apparent rate constant
K_{M}^{app}	Apparent substrate concentration required to achieve half maximal activity
K_{a}^{app}	Apparent MgATP concentration required to achieve half maximal activity
K_{c}^{app}	Apparent co-activator concentration required to achieve half maximal activity
K_{d}	Dissociation constant
k_{off}	Dissociation rate
k_{on}	Association rate
KAcO	Potassium acetate
K-type effect	Effect due to a change in affinity
MAK	Muscle alpha-kinase
MAPK	Mitogen-activated protein kinase
MAPKAP-K	Mitogen-activated protein kinase-activated protein kinase
MEK	MAPK/ERK kinase
Mg^{2+}	Magnesium
MgATP	Magnesium-bound ATP
MHCK A	Myosin II heavy chain kinase A

MLCK	Myosin light-chain kinase
mTOR	Mammalian target of rapamycin
Ni-NTA	Nickel-nitrilotriacetic acid
PCR	Polymerase chain reaction
p-eEF-2K$^{Thr-348}$	eEF-2K autophosphorylated at Thr-348
PKA	cAMP-dependent protein kinase
PP1	Protein phosphatase 1
PP2A	Protein phosphatase 2A
PVDF	Polyvinylidene fluoride
p-WT$^{Thr-348}$	eEF-2K wild type autophosphorylated at Thr-348
SCF	Skp, Cullin, F-box containing complex
SDS-PAGE	Sodium dodecyl sulfate polyacrylamide gel electrophoresis
TCSPC	Time-correlated single photon counting
TBS	Tris-buffered saline
TBST	Tris-buffered saline/Tween 20
TEV	Tobacco etch virus
TPCK	Tosyl phenylalanyl chloromethyl ketone
TRPM6	Transient receptor potential cation channel, subfamily M, member 6
TRPM7	Transient receptor potential cation channel, subfamily M, member 7
Trx-His_6-tag	Thioredoxin-6xhistidine-tag
T-type effect	Effect due to a change in affinity by trapping calmodulin
V-type effect	Effect due to a change in catalytic rate
V_{max}^{app}	Apparent maximum velocity
WT	Wild type

A.2. AUTHOR'S NOTE

A.2.1. MATERIALS AND METHODS

Introduction. I recognize this is a nontraditional (nonexistent?) section to write, but it means so much to me that I thought I'd try and shove it at the end, anyway. The journey to earning this degree has been such a tremendous life experience. I've learned many things far beyond the bench and number crunching that it seems unfair to exclude purely on the grounds of professionalism. You've seen all the data and metrics and scientific findings that I've had to offer, and now I'd like to present my additional observations and hypotheses for the general pursuit of PhDs everywhere. I retained the "materials and methods" title of this section in the spirit of science, though I would like to add a disclaimer that these observations by no means follow the scientific method. For starters, I only have official records for n=1 (party of me).

Pursuit of benefitting society. I initially wanted to pursue a PhD with an emphasis in cancer research because of the disease history of my family. There are few feelings worse than the one of being helpless. I knew on some level that I would probably be a cog in a machine, but in all of my naivety I was still set on making some sort of contribution regardless of how small. I wanted to learn about niche and novel research, contribute ideas. Unfortunately within my first year I was firmly disillusioned by bureaucracy, a trend that I saw among my classmates and senior students. Exactly how much research is noise in the void of a system that encourages sub-par work for the cycle of publishing and earning grants? What would a better system even look like?

Pursuit of meaning. Another painfully common phenomenon among graduate students is imposter syndrome, which describes the potent sense of being inadequate and

out of depth. I have spoken to handfuls of people who have severely struggled with the sink-or-swim nature of starting grad school, which seems inefficient and unnecessary. Having this be a rite-of-passage, vetting or "well I did it too" occurrence seems a waste of resources, time and potential.

Between the disillusionment of potential societal impact to my nearly debilitating imposter syndrome, I sought out another avenue to put my expertise to use. I found a fellowship that allowed me to visit primary school classrooms and explain their science topics in terms of active research. This was the most fulfilling experience of my PhD, but it was not easy to find or get into. The PhD was originally meant for people on a primarily academic track, but with supply far outnumbering demand for these positions this is no longer the case. Despite that most graduates go on to non-academic careers, PhD training has been slow to adapt and resistant to accommodating the modern needs of its students.

A.2.2. Results and Discussion

I have only seen the higher education academic system for 6 years (12 including pre-PhD work which I don't). I am painfully aware that I have neither the experience nor reach necessary to truly impact such an old and traditional system. All I know is that there is room for improvement, and what I can do right now is express, debate and alter my observations and ideas with more experienced persons than I. As they are my ideas may be simplistic, but they are a starting point. I will summarize and bullet point four main calls for change.

The first is a stronger initial guidance and requirements.

The second is about the physical and practical limitations of one person. When a university asks their faculty to mentor students, bring in grant funds, teach classes, run a lab and take on administrative or bureaucratic responsibilities, how can performance not be expected to suffer? As an aspiring educator, it is especially frustrating when this is reflected in undergraduate classes when students are turned off of a subject.

The third I bring up because the climate is right. I'll try to be brief. Are you treating male and female scientists equally? Everyone is here because of a passion for learning, a driving curiosity. Everyone made it to this point because they possessed a basic amount of capability that can be nurtured. If a woman starts wearing jeans in the lab instead of a skirt and leggings because she notices she is treated better in pants, that is an issue. If female scientists notice that they get stopped and corrected and questioned and talked over more frequently than their male counterparts, that is a problem. Looks, style, body parts, femininity, masculinity, mannerisms, and personality presentation have no bearing on scientific or intellectual capability. That fact needs to be reflected in the treatment of people.

Lastly, and probably most critically, is the need for PhD programs to have more out-of-academia experiences and skill training. Research grants are currently and primarily meant to fund lab studies, results, and data. We are oversaturated in graduate students and postdoctoral positions. What would it look like if graduate programs paired with companies and agencies so that students spent part of their time in the lab working out a dissertation and part of their time in relevant career training? A few hours a week

teaching in a classroom, helping out in a policy maker's office, interning for technical writers? Is that really too far out of reach?

References

1. Ryazanov, a G., Shestakova, E. a & Natapov, P. G. Phosphorylation of elongation factor 2 by EF-2 kinase affects rate of translation. *Nature* **334,** 170–173 (1988).
2. White-Gilbertson, S., Kurtz, D. T. & Voelkel-Johnson, C. The role of protein synthesis in cell cycling and cancer. *Mol. Oncol.* **3,** 402–408 (2009).
3. Marin, P. *et al.* Glutamate-dependent phosphorylation of elongation factor-2 and inhibition of protein synthesis in neurons. *J. Neurosci.* **17,** 3445–3454 (1997).
4. Gideons, E. S., Kavalali, E. T. & Monteggia, L. M. Mechanisms underlying differential effectiveness of memantine and ketamine in rapid antidepressant responses. *Proc. Natl. Acad. Sci. U. S. A.* **111,** 8649–54 (2014).
5. Li, X., Alafuzoff, I., Soininen, H., Winblad, B. & Pei, J.-J. Levels of mTOR and its downstream targets 4E-BP1, eEF2, and eEF2 kinase in relationships with tau in Alzheimer's disease brain. *FEBS J.* **272,** 4211–20 (2005).
6. Fang, J. S., Gillies, R. D. & Gatenby, R. A. Adaptation to hypoxia and acidosis in carcinogenesis and tumor progression. *Semin. Cancer Biol.* **18,** 330–7 (2008).
7. Neri, D. & Supuran, C. T. Interfering with pH regulation in tumours as a therapeutic strategy. *Nature Reviews Drug Discovery* **10,** 767–777 (2011).
8. Kraut, J. A. & Madias, N. E. Metabolic acidosis: pathophysiology, diagnosis and management. *Nat. Rev. Nephrol.* **6,** 274–85 (2010).
9. Fitts, R. H. Cellular mechanisms of muscle fatigue. *Physiol. Rev.* **74,** 49–94 (1994).
10. Nairn, a. C., Nichols, R. a., Brady, M. J. & Palfrey, H. C. Nerve growth factor treatment or cAMP elevation reduces Ca2+/calmodulin-dependent protein kinase III activity in PC12 cells. *J. Biol. Chem.* **262,** 14265–14272 (1987).
11. Dorovkov, M. V., Pavur, K. S., Petrov, A. N. & Ryazanov, A. G. Regulation of elongation factor-2 kinase by pH. *Biochemistry* **41,** 13444–13450 (2002).
12. Xie, J. *et al.* Molecular mechanism for the control of eukaryotic elongation factor 2 kinase by pH; a role in cancer cell survival. *Mol. Cell. Biol.* **35,** MCB.00012-15 (2015).

13. Manning, G., Whyte, D. B., Martinez, R., Hunter, T. & Sudarsanam, S. The Protein Kinase Complement of the Human Genome. *Science (80-.).* **298,** 1912–1934 (2002).
14. Dhanasekaran, N. & Reddy, E. P. Signaling by dual specificity kinases. *Oncogene* **17,** 1447–1455 (1998).
15. Besant, P. G., Tan, E. & Attwood, P. V. Mammalian protein histidine kinases. *Int. J. Biochem. Cell Biol.* **35,** 297–309 (2003).
16. Drennan, D. & Ryazanov, A. G. Alpha-kinases: Analysis of the family and comparison with conventional protein kinases. *Prog. Biophys. Mol. Biol.* **85,** 1–32 (2004).
17. Ryazanov, a G. *et al.* Identification of a new class of protein kinases represented by eukaryotic elongation factor-2 kinase. *Proc. Natl. Acad. Sci. U. S. A.* **94,** 4884–4889 (1997).
18. Reiterer, V., Eyers, P. A. & Farhan, H. Day of the dead: pseudokinases and pseudophosphatases in physiology and disease. *Trends Cell Biol.* **24,** 489–505 (2014).
19. Pavitt, G. D. & Proud, C. G. Protein synthesis and its control in neuronal cells with a focus on vanishing white matter disease. *Biochem Soc Trans* **37,** 1298–1310 (2009).
20. Mitsui, K., Brady, M., Palfrey, H. C. & Nairn, A. C. Purification and characterization of calmodulin-dependent protein kinase III from rabbit reticulocytes and rat pancreas. *J Biol Chem* **268,** 13422–13433 (1993).
21. Redpath, N. T., Price, N. T., Severinov, K. V & Proud, C. G. Regulation of elongation factor-2 by multisite phosphorylation. *Eur. J. Biochem.* **213,** 689–699 (1993).
22. Bagaglio, D. M. *et al.* Phosphorylation of elongation factor 2 in normal and malignant rat glial cells. *Cancer Res* **53,** 2260–2264 (1993).
23. Hughes, S. J., Smith, H. & Ashcroft, S. J. Characterization of Ca2+/calmodulin-dependent protein kinase in rat pancreatic islets. *Biochem J* **289 (Pt 3,** 795–800

(1993).

24. Palmquist, K., Riis, B., Nilsson, A. & Nygard, O. Interaction of the calcium and calmodulin regulated eEF-2 kinase with heat shock protein 90. *FEBS Lett* **349,** 239–242 (1994).
25. Li, H., Chen, H. C. & Huang, F. L. Identification of a rapidly dephosphorylating 95-kDa protein as elongation factor 2 during 8-Br-cAMP treatment of N1E115 neuroblastoma cells. *Biochem Biophys Res Commun* **217,** 131–137 (1995).
26. Redpath, N. T., Foulstone, E. J. & Proud, C. G. Regulation of translation elongation factor-2 by insulin via a rapamycin-sensitive signalling pathway. *EMBO J* **15,** 2291–2297 (1996).
27. Nygard, O., Nilsson, A., Carlberg, U., Nilsson, L. & Amons, R. Phosphorylation regulates the activity of the eEF-2-specific Ca(2+)- and calmodulin-dependent protein kinase III. *J Biol Chem* **266,** 16425–16430 (1991).
28. Severinov, K. V, Melnikova, E. G. & Ryazanov, A. G. Downregulation of the translation elongation factor 2 kinase in Xenopus laevis oocytes at the final stages of oogenesis. *New Biol* **2,** 887–893 (1990).
29. Redpath, N. T., Price, N. T. & Proud, C. G. Cloning and expression of cDNA encoding protein synthesis elongation factor-2 kinase. *J Biol Chem* **271,** 17547–17554 (1996).
30. Pavur, K. S., Petrov, A. N. & Ryazanov, A. G. Mapping the functional domains of elongation factor-2 kinase. *Biochemistry* **39,** 12216–12224 (2000).
31. Abramczyk, O. *et al.* Purification and characterization of tagless recombinant human elongation factor 2 kinase (eEF-2K) expressed in Escherichia coli. *Protein Expr. Purif.* **79,** 237–244 (2011).
32. Niedziela-Majka, A., Rymarczyk, G., Kochman, M. & Ożyhar, A. GST-Induced Dimerization of DNA-Binding Domains Alters Characteristics of Their Interaction with DNA. *Protein Expr. Purif.* **14,** 208–220 (1998).
33. Pigott, C. R. *et al.* Insights into the regulation of eukaryotic elongation factor 2 kinase and the interplay between its domains. **118,** 105–118 (2012).

34. Nairn, A. C. & Palfrey, H. C. Identification of the major Mr 100,000 substrate for calmodulin-dependent protein kinase III in mammalian cells as elongation factor-2. *J Biol Chem* **262,** 17299–17303 (1987).
35. Redpath, N. T. & Proud, C. G. Purification and phosphorylation of elongation factor-2 kinase from rabbit reticulocytes. *Eur. J. Biochem.* **212,** 511–520 (1993).
36. Tavares, C. D. *et al.* Signal Integration at Elongation Factor 2 Kinase: THE ROLES OF CALCIUM, CALMODULIN, AND SER-500 PHOSPHORYLATION. *J Biol Chem* **292,** 2032–2045 (2017).
37. Manning, B. D. Adaptation to starvation: translating a matter of life or death. *Cancer Cell* **23,** 713–715 (2013).
38. Hanks, S. K. & Hunter, T. Protein kinases 6. The eukaryotic protein kinase superfamily: kinase (catalytic) domain structure and classification. *FASEB J.* **9,** 576–96 (1995).
39. Middelbeek, J., Clark, K., Venselaar, H., Huynen, M. A. & van Leeuwen, F. N. The alpha-kinase family: an exceptional branch on the protein kinase tree. *Cell. Mol. Life Sci.* **67,** 875–890 (2010).
40. Kannan, N., Taylor, S. S., Zhai, Y., Venter, J. C. & Manning, G. Structural and Functional Diversity of the Microbial Kinome. *PLoS Biol.* **5,** e17 (2007).
41. Scheeff, E. D. & Bourne, P. E. Structural Evolution of the Protein Kinase–Like Superfamily. *PLoS Comput. Biol.* **1,** e49 (2005).
42. Ryazanov, A. G. Elongation factor-2 kinase and its newly discovered relatives. *FEBS Lett* **514,** 26–29 (2002).
43. Vaillancourt, J. P., Lyons, C. & Côté, G. P. Identification of two phosphorylated threonines in the tail region of Dictyostelium myosin II. *J. Biol. Chem.* **263,** 10082–7 (1988).
44. Lück-Vielmetter, D., Schleicher, M., Grabatin, B., Wippler, J. & Gerisch, G. Replacement of threonine residues by serine and alanine in a phosphorylatable heavy chain fragment of Dictyostelium myosin II. *FEBS Lett.* **269,** 239–43 (1990).
45. Clark, K. *et al.* The alpha-kinases TRPM6 and TRPM7, but not eEF-2 kinase,

phosphorylate the assembly domain of myosin IIA, IIB and IIC. *FEBS Lett* **582,** 2993–2997 (2008).

46. Adams, J. A. Kinetic and Catalytic Mechanisms of Protein Kinases. *Chem. Rev.* **101,** 2271–2290 (2001).
47. Middelbeek, J., Clark, K., Venselaar, H., Huynen, M. A. & Van Leeuwen, F. N. The alpha-kinase family: an exceptional branch on the protein kinase tree. doi:10.1007/s00018-009-0215-z
48. Diggle, T. A., Seehra, C. K., Hase, S. & Redpath, N. T. Analysis of the domain structure of elongation factor-2 kinase by mutagenesis. *FEBS Lett* **457,** 189–192 (1999).
49. Rigden, D. J. & Galperin, M. Y. The DxDxDG motif for calcium binding: Multiple structural contexts and implications for evolution. *J. Mol. Biol.* **343,** 971–984 (2004).
50. Chen, Y. *et al.* Mechanisms for increased levels of phosphorylation of elongation factor-2 during hibernation in ground squirrels. *Biochemistry* **40,** 11565–11570 (2001).
51. Yamaguchi, H., Matsushita, M., Nairn, A. C. & Kuriyan, J. Crystal structure of the atypical protein kinase domain of a TRP channel with phosphotransferase activity. *Mol. Cell* **7,** 1047–57 (2001).
52. Pyr Dit Ruys, S. *et al.* Identification of autophosphorylation sites in eukaryotic elongation factor-2 kinase. *Biochem J* **442,** 681–692 (2012).
53. Tavares, C. D. J. *et al.* Calcium/Calmodulin Stimulates the Autophosphorylation of Elongation Factor 2 Kinase on Thr-348 and Ser-500 to Regulate its Activity and Calcium Dependence. **51,** 2232–2245 (2013).
54. Tavares, C. D. J. *et al.* The Molecular Mechanism of Eukaryotic Elongation Factor 2 Kinase Activation. *J. Biol. Chem.* **289,** 0–32 (2014).
55. Kruiswijk, F. *et al.* Coupled Activation and Degradation of eEF2K Regulates Protein Synthesis in Response to Genotoxic Stress. *Sci. Signal.* **5,** ra40-ra40 (2012).

56. Wiseman, S. L., Shimizu, Y., Palfrey, C. & Nairn, A. C. Proteasomal degradation of eukaryotic elongation factor-2 kinase (EF2K) is regulated by cAMP-PKA signaling and the SCF??TRCP ubiquitin E3 ligase. *J. Biol. Chem.* **288,** 17803–17811 (2013).
57. Moore, C. E., Regufe da Mota, S., Mikolajek, H. & Proud, C. G. A conserved loop in the catalytic domain of eukaryotic elongation factor 2 kinase plays a key role in its substrate specificity. *Mol Cell Biol* **34,** 2294–2307 (2014).
58. Will, N. *et al.* Structure of the C-Terminal Helical Repeat Domain of Eukaryotic Elongation Factor 2 Kinase. *Biochemistry* **55,** 5377–5386 (2016).
59. Smith, E. M. & Proud, C. G. cdc2-cyclin B regulates eEF2 kinase activity in a cell cycle- and amino acid-dependent manner. *EMBO J.* **27,** 1005–1016 (2008).
60. Skogerson, L. & Wakatama, E. A ribosome-dependent GTPase from yeast distinct from elongation factor 2. *Proc. Natl. Acad. Sci. U. S. A.* **73,** 73–6 (1976).
61. Kaul, G., Pattan, G. & Rafeequi, T. Eukaryotic elongation factor-2 (eEF2): its regulation and peptide chain elongation. *Cell Biochem. Funct.* **29,** 227–34 (2011).
62. Kamath, A. & Chakraburtty, K. Role of yeast elongation factor 3 in the elongation cycle. *J. Biol. Chem.* **264,** 15423–8 (1989).
63. Proud, C. G. Protein phosphorylation in translational control. *Curr. Top. Cell. Regul.* **32,** 243–369 (1992).
64. Ryazanov, A. G. Ca2+/calmodulin-dependent phosphorylation of elongation factor 2. *FEBS Lett* **214,** 331–334 (1987).
65. Ryazanov, A. G., Natapov, P. G., Shestakova, E. A., Severin, F. F. & Spirin, A. S. Phosphorylation of the elongation factor 2: the fifth Ca2+/calmodulin-dependent system of protein phosphorylation. *Biochimie* **70,** 619–626 (1988).
66. Ryazanov, A. G. & Davydova, E. K. Mechanism of elongation factor 2 (EF-2) inactivation upon phosphorylation. Phosphorylated EF-2 is unable to catalyze translocation. *FEBS Lett.* **251,** 187–90 (1989).
67. Brigotti, M., Sperti, S., Carnicelli, D. & Montanaro, L. Ribosome-bound elongation factor 2 escapes phosphorylation by Ca2+/calmodulin-dependent

protein kinase III. *Ital. J. Biochem.* **41,** 195–9

68. Hizli, A. A. *et al.* Phosphorylation of eukaryotic elongation factor 2 (eEF2) by cyclin A-cyclin-dependent kinase 2 regulates its inhibition by eEF2 kinase. *Mol Cell Biol* **33,** 596–604 (2013).
69. Verpelli, C. *et al.* Synaptic activity controls dendritic spine morphology by modulating eEF2-dependent BDNF synthesis. *J Neurosci* **30,** 5830–5842 (2010).
70. Scheetz, A. J., Nairn, A. C. & Constantine-Paton, M. NMDA receptor-mediated control of protein synthesis at developing synapses. *Nat Neurosci* **3,** 211–216 (2000).
71. Park, S. *et al.* Elongation factor 2 and fragile X mental retardation protein control the dynamic translation of Arc/Arg3.1 essential for mGluR-LTD. *Neuron* **59,** 70–83 (2008).
72. Hayashi, A. A. & Proud, C. G. The rapid activation of protein synthesis by growth hormone requires signaling through mTOR. *Am J Physiol Endocrinol Metab* **292,** E1647-55 (2007).
73. Roberts, N. A., Haworth, R. S. & Avkiran, M. Effects of bisindolylmaleimide PKC inhibitors on p90RSK activity in vitro and in adult ventricular myocytes. *Br J Pharmacol* **145,** 477–489 (2005).
74. Knebel, A., Haydon, C. E., Morrice, N. & Cohen, P. Stress-induced regulation of eukaryotic elongation factor 2 kinase by SB 203580-sensitive and -insensitive pathways. *Biochem J* **367,** 525–532 (2002).
75. Diggle, T. A. *et al.* Phosphorylation of elongation factor-2 kinase on serine 499 by cAMP-dependent protein kinase induces Ca2+/calmodulin-independent activity. *Biochem J* **353,** 621–626 (2001).
76. Nairn, A. C., Nichols, R. A., Brady, M. J. & Palfrey, H. C. Nerve growth factor treatment or cAMP elevation reduces Ca2+/calmodulin-dependent protein kinase III activity in PC12 cells. *J Biol Chem* **262,** 14265–14272 (1987).
77. Devkota, A. K. *et al.* Investigating the kinetic mechanism of inhibition of elongation factor 2 kinase by NH125: evidence of a common in vitro artifact.

Biochemistry **51,** 2100–2112 (2012).

78. Schmitz, C., Brandao, K. & Perraud, A. L. The channel-kinase TRPM7, revealing the untold story of Mg(2+) in cellular signaling. *Magnes Res* **27,** 9–15 (2014).
79. Perraud, A. L., Zhao, X., Ryazanov, A. G. & Schmitz, C. The channel-kinase TRPM7 regulates phosphorylation of the translational factor eEF2 via eEF2-k. *Cell Signal* **23,** 586–593 (2011).
80. Browne, G. J., Finn, S. G. & Proud, C. G. Stimulation of the AMP-activated protein kinase leads to activation of eukaryotic elongation factor 2 kinase and to its phosphorylation at a novel site, serine 398. *J Biol Chem* **279,** 12220–12231 (2004).
81. Hochachka, P. W., Buck, L. T., Doll, C. J. & Land, S. C. Unifying theory of hypoxia tolerance: molecular/metabolic defense and rescue mechanisms for surviving oxygen lack. *Proc. Natl. Acad. Sci. U. S. A.* **93,** 9493–9498 (1996).
82. Cheng, Y. *et al.* Integrated regulation of autophagy and apoptosis by EEF2K controls cellular fate and modulates the efficacy of curcumin and velcade against tumor cells. *Autophagy* **9,** 208–219 (2013).
83. Leprivier, G. *et al.* The eEF2 Kinase Confers Resistance to Nutrient Deprivation by Blocking Translation Elongation. *Cell* **153,** 1064–1079 (2013).
84. Knight, J. R. *et al.* Eukaryotic elongation factor 2 kinase regulates the cold stress response by slowing translation elongation. *Biochem J* **465,** 227–238 (2015).
85. Py, B. F., Boyce, M. & Yuan, J. A critical role of eEF-2K in mediating autophagy in response to multiple cellular stresses. *Autophagy* **5,** 393–396 (2009).
86. Fu, L. L., Xie, T., Zhang, S. Y. & Liu, B. Eukaryotic elongation factor-2 kinase (eEF2K): a potential therapeutic target in cancer. *Apoptosis* **19,** 1527–31 (2014).
87. Cheng, Y. *et al.* Cytoprotective effect of the elongation factor-2 kinase-mediated autophagy in breast cancer cells subjected to growth factor inhibition. *PLoS One* **5,** e9715 (2010).
88. Semenza, G. L. HIF-1 and human disease: one highly involved factor. *Genes Dev.* **14,** 1983–91 (2000).
89. Rose, A. J. *et al.* A Ca(2+)-calmodulin-eEF2K-eEF2 signalling cascade, but not

AMPK, contributes to the suppression of skeletal muscle protein synthesis during contractions. *J Physiol* **587,** 1547–1563 (2009).

90. Browne, G. J., Finn, S. G. & Proud, C. G. Stimulation of the AMP-activated Protein Kinase Leads to Activation of Eukaryotic Elongation Factor 2 Kinase and to Its Phosphorylation at a Novel Site, Serine 398. *J. Biol. Chem.* **279,** 12220–12231 (2004).
91. Proud, C. G. Role of mTOR signalling in the control of translation initiation and elongation by nutrients. *Curr Top Microbiol Immunol* **279,** 215–244 (2004).
92. Connolly, E., Braunstein, S., Formenti, S. & Schneider, R. J. Hypoxia inhibits protein synthesis through a 4E-BP1 and elongation factor 2 kinase pathway controlled by mTOR and uncoupled in breast cancer cells. *Mol Cell Biol* **26,** 3955–3965 (2006).
93. Leprivier, G. *et al.* XThe eEF2 kinase confers resistance to nutrient deprivation by blocking translation elongation. *Cell* **153,** (2013).
94. Leprivier, G., Rotblat, B., Khan, D., Jan, E. & Sorensen, P. H. Stress-mediated translational control in cancer cells. *Biochim Biophys Acta* **1849,** 845–860 (2015).
95. Wang, X. *et al.* Regulation of elongation factor 2 kinase by p90 RSK1 and p70 S6 kinase. *EMBO J.* **20,** (2001).
96. Proud, C. G. Signalling to translation: how signal transduction pathways control the protein synthetic machinery. *Biochem. J.* **403,** 217–234 (2007).
97. Terai, K. *et al.* AMP-activated protein kinase protects cardiomyocytes against hypoxic injury through attenuation of endoplasmic reticulum stress. *Mol Cell Biol* **25,** 9554–9575 (2005).
98. Abelaira, H. M. *et al.* Effects of ketamine administration on mTOR and reticulum stress signaling pathways in the brain after the infusion of rapamycin into prefrontal cortex. *J. Psychiatr. Res.* **87,** 81–87 (2017).
99. Segalés, J., Perdiguero, E. & Muñoz-Cánoves, P. Regulation of Muscle Stem Cell Functions: A Focus on the p38 MAPK Signaling Pathway. *Front. Cell Dev. Biol.* **4,** 91 (2016).

100. Knebel, A., Morrice, N. & Cohen, P. A novel method to identify protein kinase substrates: eEF2 kinase is phosphorylated and inhibited by SAPK4/p38delta. *EMBO J* **20,** 4360–4369 (2001).
101. Wu, H., Yang, J. M., Jin, S., Zhang, H. & Hait, W. N. Elongation factor-2 kinase regulates autophagy in human glioblastoma cells. *Cancer Res* **66,** 3015–3023 (2006).
102. Moore, C. E. *et al.* Elongation factor 2 kinase promotes cell survival by inhibiting protein synthesis without inducing autophagy. *Cell Signal* **28,** 284–293 (2016).
103. Ashour, A. a. *et al.* Elongation factor-2 kinase regulates TG2/β1 integrin/Src/uPAR pathway and epithelial-mesenchymal transition mediating pancreatic cancer cells invasion. *J. Cell. Mol. Med.* **18,** 2235–2251 (2014).
104. Shi, Q. *et al.* MicroRNA-877 acts as a tumor suppressor by directly targeting eEF2K in renal cell carcinoma. *Oncol Lett* **11,** 1474–1480 (2016).
105. Niu, M. *et al.* Comparative proteomic analysis implicates eEF2 as a novel target of PI3Kgamma in the MDA-MB-231 metastatic breast cancer cell line. *Proteome Sci* **11,** 4 (2013).
106. Liu, X.-Y., Zhang, L., Zhang, Y. & Yang, J.-M. Roles of eEF-2 kinase in cancer. *Chin. Med. J. (Engl).* **125,** 2908–13 (2012).
107. Parmer, T. G. *et al.* Activity and regulation by growth factors of calmodulin-dependent protein kinase III (elongation factor 2-kinase) in human breast cancer. *Br J Cancer* **79,** 59–64 (1999).
108. Rosenwald, I. B. *et al.* Transient inhibition of protein synthesis induces expression of proto-oncogenes and stimulates resting cells to enter the cell cycle. *Cell Prolif.* **28,** 631–44 (1995).
109. Meric-Bernstam, F. *et al.* Aberrations in translational regulation are associated with poor prognosis in hormone receptor-positive breast cancer. *Breast Cancer Res* **14,** R138 (2012).
110. Pott, L. L. *et al.* Eukaryotic elongation factor 2 is a prognostic marker and its kinase a potential therapeutic target in HCC. *Oncotarget* **8,** 11950–11962 (2017).

111. Tekedereli, I. *et al.* Targeted silencing of elongation factor 2 kinase suppresses growth and sensitizes tumors to doxorubicin in an orthotopic model of breast cancer. *PLoS One* **7,** (2012).
112. Wibrand, K. *et al.* MicroRNA regulation of the synaptic plasticity-related gene Arc. *PLoS One* **7,** e41688 (2012).
113. Citri, A. & Malenka, R. C. Synaptic plasticity: multiple forms, functions, and mechanisms. *Neuropsychopharmacology* **33,** 18–41 (2008).
114. Heise, C. *et al.* Elongation factor-2 phosphorylation in dendrites and the regulation of dendritic mRNA translation in neurons. *Front Cell Neurosci* **8,** 35 (2014).
115. Taha, E., Gildish, I., Gal-Ben-Ari, S. & Rosenblum, K. The role of eEF2 pathway in learning and synaptic plasticity. *Neurobiol Learn Mem* (2013). doi:10.1016/j.nlm.2013.04.015
116. Sutton, M. A., Taylor, A. M., Ito, H. T., Pham, A. & Schuman, E. M. Postsynaptic decoding of neural activity: eEF2 as a biochemical sensor coupling miniature synaptic transmission to local protein synthesis. *Neuron* **55,** 648–661 (2007).
117. Scheetz, A. J., Nairn, A. C. & Constantine-Paton, M. NMDA receptor-mediated control of protein synthesis at developing synapses. *Nat. Neurosci.* **3,** 211–6 (2000).
118. Reese, A. L. & Kavalali, E. T. Spontaneous neurotransmission signals through store-driven Ca(2+) transients to maintain synaptic homeostasis. *Elife* **4,** (2015).
119. Davidkova, G. & Carroll, R. C. Characterization of the Role of Microtubule-Associated Protein 1B in Metabotropic Glutamate Receptor-Mediated Endocytosis of AMPA Receptors in Hippocampus. *J. Neurosci.* **27,** 13273–13278 (2007).
120. Nosyreva, E. *et al.* Acute suppression of spontaneous neurotransmission drives synaptic potentiation. *J Neurosci* **33,** 6990–7002 (2013).
121. Ronesi, J. A. & Huber, K. M. Homer interactions are necessary for metabotropic glutamate receptor-induced long-term depression and translational activation. *J Neurosci* **28,** 543–547 (2008).
122. Johnson, G. *et al.* Increased phosphorylation of elongation factor 2 in Alzheimer's

disease. *Brain Res Mol Brain Res* **15,** 319–326 (1992).

123. Garcia-Esparcia, P. *et al.* Altered mechanisms of protein synthesis in frontal cortex in Alzheimer disease and a mouse model. *Am J Neurodegener Dis* **6,** 15–25 (2017).
124. Monteggia, L. M., Gideons, E. & Kavalali, E. T. The role of eukaryotic elongation factor 2 kinase in rapid antidepressant action of ketamine. *Biol Psychiatry* **73,** 1199–1203 (2013).
125. Niciu, M. J., Henter, I. D., Luckenbaugh, D. A., Zarate Jr., C. A. & Charney, D. S. Glutamate receptor antagonists as fast-acting therapeutic alternatives for the treatment of depression: ketamine and other compounds. *Annu Rev Pharmacol Toxicol* **54,** 119–139 (2014).
126. Veglia, G. & Li, G. Tunable Liaisons: eEF-2K, CaM, and Calcium. *Structure* **24,** 1438–1439 (2016).
127. Clapham, D. E. Calcium Signaling. *Cell* **131,** 1047–1058 (2007).
128. Chin, D. & Means, A. R. Calmodulin: a prototypical calcium sensor. *Trends Cell Biol.* **10,** 322–8 (2000).
129. Bootman, M. D. *et al.* Calcium Signalling and Regulation of Cell Function. in *eLS* (John Wiley & Sons, Ltd, 2012). doi:10.1002/9780470015902.a0001265.pub3
130. Thomas, A. P., Bird, G. S., Hajnóczky, G., Robb-Gaspers, L. D. & Putney, J. W. Spatial and temporal aspects of cellular calcium signaling. *FASEB J.* **10,** 1505–17 (1996).
131. Allbritton, N. L. & Meyer, T. Localized calcium spikes and propagating calcium waves. *Cell Calcium* **14,** 691–7 (1993).
132. Conigrave, A. D. & Morris, M. B. A 96-well plate assay for the study of calmodulin-activated Ca2+-pumping ATPase from red-cell membranes. *Biochem. Educ.* **26,** 176–181 (1998).
133. Kakiuchi, S. *et al.* Quantitative determinations of calmodulin in the supernatant and particulate fractions of mammalian tissues. *J. Biochem.* **92,** 1041–8 (1982).
134. Black, D. ., Tran, Q.-K. & Persechini, A. Monitoring the total available calmodulin

concentration in intact cells over the physiological range in free Ca2+. *Cell Calcium* **35,** 415–425 (2004).

135. Tavares, C. D. J. *et al.* Calcium/calmodulin stimulates the autophosphorylation of elongation factor 2 kinase on Thr-348 and Ser-500 to regulate its activity and calcium dependence. *Biochemistry* **51,** 2232–2245 (2012).
136. Laitusis, A. L., Brostrom, C. O., Ryazanov, A. G., and Brostrom, M. A. An Examination of the Role of Increased Cytosolic Free Ca2+ Concentrations in the Inhibition of mRNA Translation. *Arch. Biochem. Biophys.* 270–280 (1998).
137. Nairn, A. C. *et al.* Elongation factor-2 phosphorylation and the regulation of protein synthesis by calcium. *Prog Mol Subcell Biol* **27,** 91–129 (2001).
138. Diggle, T. a *et al.* Phosphorylation of elongation factor-2 kinase on serine 499 by cAMP-dependent protein kinase induces Ca2+/calmodulin-independent activity. *Biochem. J.* **353,** 621–626 (2001).
139. Will, N. *et al.* Structural Dynamics of the Activation of Elongation Factor 2 Kinase by Ca 2+ -Calmodulin. *J. Mol. Biol.* (2018). doi:10.1016/j.jmb.2018.05.033
140. Stratton, M. M., Chao, L. H., Schulman, H. & Kuriyan, J. Structural studies on the regulation of Ca2+/calmodulin dependent protein kinase II. *Curr. Opin. Struct. Biol.* **23,** 292–301 (2013).
141. Lee, K. *et al.* Structural Basis for the Recognition of Eukaryotic Elongation Factor 2 Kinase by Calmodulin. *Structure* **24,** 1441–1451 (2016).
142. Pandey, K. *et al.* Low pH overrides the need of calcium ions for the shape-function relationship of calmodulin: Resolving prevailing debates. *J. Phys. Chem. B* **118,** 5059–5074 (2014).
143. Villarroel, A. *et al.* The ever changing moods of calmodulin: How structural plasticity entails transductional adaptability. *J. Mol. Biol.* **426,** 2717–2735 (2014).
144. Putkey, J. A. & Waxham, M. N. A peptide model for calmodulin trapping by calcium/calmodulin-dependent protein kinase II. *J. Biol. Chem.* **271,** 29619–23 (1996).
145. Palfrey, H. C., Nairn, A. C., Muldoon, L. L. & Villereal, M. L. Rapid activation of

calmodulin-dependent protein kinase III in mitogen-stimulated human fibroblasts. Correlation with intracellular Ca2+ transients. *J Biol Chem* **262,** 9785–9792 (1987).

146. Hovland, R. *et al.* cAMP inhibits translation by inducing Ca2+/calmodulin-independent elongation factor 2 kinase activity in IPC-81 cells. *FEBS Lett* **444,** 97–101 (1999).
147. Nosyreva, E. & Kavalali, E. T. Activity-dependent augmentation of spontaneous neurotransmission during endoplasmic reticulum stress. *J Neurosci* **30,** 7358–7368 (2010).
148. Smith, E. M. & Proud, C. G. cdc2-cyclin B regulates eEF2 kinase activity in a cell cycle- and amino acid-dependent manner. *EMBO J* **27,** 1005–1016 (2008).
149. Smith, E. M., Finn, S. G., Tee, A. R., Browne, G. J. & Proud, C. G. The tuberous sclerosis protein TSC2 is not required for the regulation of the mammalian target of rapamycin by amino acids and certain cellular stresses. *J Biol Chem* **280,** 18717–18727 (2005).
150. Wang, Q., Edupuganti, R., Tavares, C. D., Dalby, K. N. & Ren, P. Using docking and alchemical free energy approach to determine the binding mechanism of eEF2K inhibitors and prioritizing the compound synthesis. *Front Mol Biosci* **2,** 9 (2015).
151. Wiseman, S. L., Shimizu, Y., Palfrey, H. C. & Nairn, A. C. Proteasomal degradation of eukaryotic elongation factor-2 kinase (EF2K) is regulated by cAMP-PKA signaling and the SCFbetaTRCP ubiquitin E3 ligase. *J Biol Chem* (2013). doi:10.1074/jbc.M113.477182
152. Arora, S., Yang, J. M. & Hait, W. N. Identification of the ubiquitin-proteasome pathway in the regulation of the stability of eukaryotic elongation factor-2 kinase. *Cancer Res* **65,** 3806–3810 (2005).
153. Wang, X., Xie, J., da Mota, S. R., Moore, C. E. & Proud, C. G. Regulated stability of eukaryotic elongation factor 2 kinase requires intrinsic but not ongoing activity. *Biochem J* **467,** 321–331 (2015).

154. Nairn, A. C., Bhagat, B. & Palfrey, H. C. Identification of calmodulin-dependent protein kinase III and its major Mr 100,000 substrate in mammalian tissues. *Proc Natl Acad Sci U S A* **82,** 7939–7943 (1985).
155. Madshus, I. H. Regulation of intracellular pH in eukaryotic cells. *Biochem. J.* **250,** 1–8 (1988).
156. Busa, W. & Nuccitelli, R. Metabolic regulation via intracellular pH. *Am. J. Physiol.* **246,** 409–438 (1984).
157. Hand, S. C. Quiescence in Artemia franciscana embryos: reversible arrest of metabolism and gene expression at low oxygen levels. *J. Exp. Biol.* **201,** 1233–1242 (1998).
158. Boron, W. *Medical physiology a cellular and molecular approach*. (Elsevier Saunders, 2006).
159. Xie, J. *et al.* Molecular Mechanism for the Control of Eukaryotic Elongation Factor 2 Kinase by pH: Role in Cancer Cell Survival. *Mol. Cell. Biol.* **35,** 1805–1824 (2015).
160. Knebel, A., Haydon, C. E., Morrice, N. & Cohen, P. Stress-induced regulation of eukaryotic elongation factor 2 kinase by SB 203580-sensitive and -insensitive pathways. *Biochem. J.* **367,** 525–32 (2002).
161. Hershey, J. W. B. Translational Control in Mammalian Cells. *Annu. Rev. Biochem.* **60,** 717–755 (1991).
162. Morley, S. J. & Thomas, G. Intracellular messengers and the control of protein synthesis. *Pharmacol. Ther.* **50,** 291–319 (1991).
163. Rhoads, R. E. Signal transduction pathways that regulate eukaryotic protein synthesis. *J. Biol. Chem.* **274,** 30337–40 (1999).
164. Moldave, K. Eukaryotic Protein Synthesis. *Annu. Rev. Biochem.* **54,** 1109–1149 (1985).
165. Moazed, D. & Noller, H. F. Intermediate states in the movement of transfer RNA in the ribosome. *Nature* **342,** 142–148 (1989).
166. Proud, C. G. Peptide-chain elongation in eukaryotes. *Mol Biol Rep* **19,** 161–170

(1994).

167. Carlberg, U., Nilsson, A. & Nygard, O. Functional properties of phosphorylated elongation factor 2. *Eur J Biochem* **191,** 639–645 (1990).

168. Tanaka, M., Iwasaki, K. & Kaziro, Y. Translocation reaction promoted by polypeptide chain elongation factor-2 from pig liver. *J. Biochem.* **82,** 1035–43 (1977).

169. Browne, G. J. & Proud, C. G. A novel mTOR-regulated phosphorylation site in elongation factor 2 kinase modulates the activity of the kinase and its binding to calmodulin. *Mol Cell Biol* **24,** 2986–2997 (2004).

170. Kapust, R. B. *et al.* Tobacco etch virus protease: mechanism of autolysis and rational design of stable mutants with wild-type catalytic proficiency. *Protein Eng.* **14,** 993–1000 (2001).

171. Kristelly, R., Earnest, B. T., Krishnamoorthy, L. & Tesmer, J. J. G. Preliminary structure analysis of the DH/PH domains of leukemia-associated RhoGEF. *Acta Crystallogr. D. Biol. Crystallogr.* **59,** 1859–62 (2003).

172. Gaertner, T. R. *et al.* Comparative Analyses of the Three-dimensional Structures and Enzymatic Properties of α, β, γ, and δ Isoforms of Ca^{2+} -Calmodulin-dependent Protein Kinase II. *J. Biol. Chem.* **279,** 12484–12494 (2004).

173. Forest, A. *et al.* Role of the N- and C-Lobes of Calmodulin in the Activation of Ca^{2+} /Calmodulin-Dependent Protein Kinase II †. *Biochemistry* **47,** 10587–10599 (2008).

174. Weatherill, D. B. *et al.* Compartment-specific, differential regulation of eukaryotic elongation factor 2 and its kinase within Aplysia sensory neurons. *J Neurochem* **117,** 841–855 (2011).

175. De Gassart, A. *et al.* Pharmacological eEF2K activation promotes cell death and inhibits cancer progression. *EMBO Rep* **17,** 1471–1484 (2016).

176. Arora, S. *et al.* Identification and characterization of an inhibitor of eukaryotic elongation factor 2 kinase against human cancer cell lines. *Cancer Res* **63,** 6894–6899 (2003).

177. Liu, R. & Proud, C. G. Eukaryotic elongation factor 2 kinase as a drug target in cancer, and in cardiovascular and neurodegenerative diseases. *Acta Pharmacol Sin* **37,** 285–294 (2016).
178. Rose, A. J., Bisiani, B., Vistisen, B., Kiens, B. & Richter, E. A. Skeletal muscle eEF2 and 4EBP1 phosphorylation during endurance exercise is dependent on intensity and muscle fiber type. *Am J Physiol Regul Integr Comp Physiol* **296,** R326-33 (2009).
179. Bagaglio, D. M. & Hait, W. N. Role of calmodulin-dependent phosphorylation of elongation factor 2 in the proliferation of rat glial cells. *Cell Growth Differ* **5,** 1403–1408 (1994).
180. Zhang, Y. *et al.* Inhibition of eEF-2 kinase sensitizes human glioma cells to TRAIL and down-regulates Bcl-xL expression. *Biochem Biophys Res Commun* **414,** 129–134 (2011).
181. Autry, A. E. *et al.* NMDA receptor blockade at rest triggers rapid behavioural antidepressant responses. *Nature* **475,** 91–95 (2011).
182. Riis, B. *et al.* Elongation factor 2-specific calcium and calmodulin dependent protein kinase III activity in rat livers varies with age and calorie restriction. *Biochem Biophys Res Commun* **192,** 1210–1216 (1993).
183. Riis, B. & Nygard, O. Kinetics of calcium and calmodulin-dependent protein kinase III from embryonic chicken leg muscle cells. *FEBS Lett* **407,** 21–24 (1997).
184. Wang, X. *et al.* Eukaryotic elongation factor 2 kinase activity is controlled by multiple inputs from oncogenic signaling. *Mol Cell Biol* **34,** 4088–4103 (2014).
185. Johanns, M. *et al.* Direct and indirect activation of eukaryotic elongation factor 2 kinase by AMP-activated protein kinase. *Cell Signal* **36,** 212–221 (2017).
186. Hamurcu, Z., Ashour, A., Kahraman, N. & Ozpolat, B. FOXM1 regulates expression of eukaryotic elongation factor 2 kinase and promotes proliferation, invasion and tumorgenesis of human triple negative breast cancer cells. *Oncotarget* **7,** 16619–16635 (2016).
187. Ryazanov, A. G. & Spirin, A. S. Phosphorylation of elongation factor 2: a key

mechanism regulating gene expression in vertebrates. *New Biol* **2,** 843–850 (1990).

188. Lee, K. *et al.* Structural Basis for the Recognition of Eukaryotic Elongation Factor 2 Kinase by Calmodulin. *Structure* **24,** 1441–1451 (2016).
189. Leclerc, E. & Vetter, S. Characterization of a calcium-dependent calmodulin-binding domain in the 135-kD human protein 4.1 isoform. *Eur. J. Biochem.* **258,** 567–571 (1998).
190. Vetter, S. W. & Leclerc, E. Novel aspects of calmodulin target recognition and activation. *Eur. J. Biochem.* **270,** 404–14 (2003).
191. Lakowicz, J. R. & Geddes, C. D. *Topics in fluorescence spectroscopy*. (Plenum Press, 1991).
192. Grabarek, Z. Insights into modulation of calcium signaling by magnesium in calmodulin, troponin C and related EF-hand proteins. *Biochim. Biophys. Acta - Mol. Cell Res.* **1813,** 913–921 (2011).
193. Tsai, M. D., Drakenberg, T., Thulin, E. & Forsén, S. Is the binding of magnesium (II) to calmodulin significant? An investigation by magnesium-25 nuclear magnetic resonance. *Biochemistry* **26,** 3635–43 (1987).
194. Senguen, F. T. & Grabarek, Z. X-ray Structures of Magnesium and Manganese Complexes with the N-Terminal Domain of Calmodulin: Insights into the Mechanism and Specificity of Metal Ion Binding to an EF-Hand. *Biochemistry* **51,** 6182–6194 (2012).
195. Ohashi, W., Hirota, H. & Yamazaki, T. Solution structure and fluctuation of the Mg^{2+} -bound form of calmodulin C-terminal domain. *Protein Sci.* **20,** 690–701 (2011).
196. Usui, T., Okada, M., Hara, Y. & Yamawaki, H. Eukaryotic elongation factor 2 kinase regulates the development of hypertension through oxidative stress-dependent vascular inflammation. *Am J Physiol Hear. Circ Physiol* (2013). doi:10.1152/ajpheart.00373.2013
197. Belelovsky, K., Elkobi, A., Kaphzan, H., Nairn, A. C. & Rosenblum, K. A molecular switch for translational control in taste memory consolidation. *Eur J*

Neurosci **22,** 2560–2568 (2005).

198. Liu, X.-Y., Zhang, L., Zhang, Y. & Yang, J.-M. Roles of eEF-2 kinase in cancer. *Chin. Med. J. (Engl).* **125,** 2908–13 (2012).
199. Serfass, L., Van Herpen, C. & Saghatchian, M. Molecular targets and cancer therapeutics. *Eur J Cancer* **43,** 1494–1495 (2007).
200. Monteggia, L. M., Gideons, E. & Kavalali, E. T. The Role of Eukaryotic Elongation Factor 2 Kinase in Rapid Antidepressant Action of Ketamine. *Biol Psychiatry* (2012). doi:10.1016/j.biopsych.2012.09.006
201. Andersen, C. B. F. *et al.* Structure of eEF3 and the mechanism of transfer RNA release from the E-site. *Nature* **443,** 663–668 (2006).
202. Buchan, D. W. A. *et al.* Protein annotation and modelling servers at University College London. *Nucleic Acids Res.* **38,** W563–W568 (2010).
203. Horman, S. *et al.* Activation of AMP-activated protein kinase leads to the phosphorylation of elongation factor 2 and an inhibition of protein synthesis. *Curr Biol* **12,** 1419–1423 (2002).
204. Alirezaei, M., Marin, P., Nairn, A. C., Glowinski, J. & Premont, J. Inhibition of protein synthesis in cortical neurons during exposure to hydrogen peroxide. *J Neurochem* **76,** 1080–1088 (2001).
205. Kenney, J. W., Moore, C. E., Wang, X. & Proud, C. G. Eukaryotic elongation factor 2 kinase, an unusual enzyme with multiple roles. *Adv. Biol. Regul.* **55,** 15–27 (2014).
206. McCamphill, P. K., Farah, C. A., Anadolu, M. N., Hoque, S. & Sossin, W. S. Bidirectional Regulation of eEF2 Phosphorylation Controls Synaptic Plasticity by Decoding Neuronal Activity Patterns. *J Neurosci* **35,** 4403–4417 (2015).
207. Buss, W. C., Stepanek, J. & Queen, S. A. Association of tissue-specific changes in translation elongation after cyclosporin with changes in elongation factor 2 phosphorylation. *Biochem Pharmacol* **48,** 1459–1469 (1994).
208. Leprivier, G. *et al.* The eEF2 kinase confers resistance to nutrient deprivation by blocking translation elongation. *Cell* **153,** 1064–79 (2013).

209. Thomson, D. M., Fick, C. A. & Gordon, S. E. AMPK activation attenuates S6K1, 4E-BP1, and eEF2 signaling responses to high-frequency electrically stimulated skeletal muscle contractions. *J Appl Physiol* **104,** 625–632 (2008).
210. Chan, A. Y. & Dyck, J. R. Activation of AMP-activated protein kinase (AMPK) inhibits protein synthesis: a potential strategy to prevent the development of cardiac hypertrophy. *Can J Physiol Pharmacol* **83,** 24–28 (2005).
211. McLeod, L. E. & Proud, C. G. ATP depletion increases phosphorylation of elongation factor eEF2 in adult cardiomyocytes independently of inhibition of mTOR signalling. *FEBS Lett* **531,** 448–452 (2002).
212. Hong-Brown, L. Q., Brown, C. R., Huber, D. S. & Lang, C. H. Alcohol and indinavir adversely affect protein synthesis and phosphorylation of MAPK and mTOR signaling pathways in C2C12 myocytes. *Alcohol Clin Exp Res* **30,** 1297–1307 (2006).
213. Wang, L. & Proud, C. G. Regulation of the phosphorylation of elongation factor 2 by MEK-dependent signalling in adult rat cardiomyocytes. *FEBS Lett* **531,** 285–289 (2002).
214. Liu, L. *et al.* Inhibition of eEF-2 kinase sensitizes human nasopharyngeal carcinoma cells to lapatinib-induced apoptosis through the Src and Erk pathways. *BMC Cancer* **16,** 813 (2016).
215. Diggle, T. A., Redpath, N. T., Heesom, K. J. & Denton, R. M. Regulation of protein-synthesis elongation-factor-2 kinase by cAMP in adipocytes. *Biochem J* **336 (Pt 3,** 525–529 (1998).
216. Zhang, C. *et al.* Phosphorylated eEF2 is SUMOylated and induces cardiomyocyte apoptosis during myocardial ischemia reperfusion. *J Cardiol* **69,** 689–698 (2017).
217. Meier, J. J. Beta cell mass in diabetes: a realistic therapeutic target? *Diabetologia* **51,** 703–13 (2008).
218. Chrusch, C. *et al.* Blood pH level modulates organ metabolism of lactate in septic shock in dogs. *J. Crit. Care* **17,** 188–202 (2002).
219. Xie, J. *et al.* Molecular Mechanism for the Control of Eukaryotic Elongation

Factor 2 Kinase by pH: Role in Cancer Cell Survival. *Mol Cell Biol* **35,** 1805–1824 (2015).

220. Tavares, C. D. *et al.* Calcium/calmodulin stimulates the autophosphorylation of elongation factor 2 kinase on Thr-348 and Ser-500 to regulate its activity and calcium dependence. *Biochemistry* **51,** 2232–2245 (2012).

221. Will, N. *et al.* Structural Dynamics of the Activation of Elongation Factor 2 Kinase by Ca 2 + -Calmodulin. (2018). doi:10.1016/j.jmb.2018.05.033